JOURNAL OF MATHEMATICAL SCIENCES AND MODELLING

ISSN: 2636-8692

VOLUME II
ISSUE II

VOLUME II ISSUE II
ISSN 2636-8692

August 2019
http://dergipark.gov.tr/jmsm

JOURNAL OF MATHEMATICAL SCIENCES AND MODELLING

Editors

Editorial Board of Journal of Mathematical Sciences and Modelling

Contents

Journal of Mathematical Sciences and Modelling, 2 (2) (2019) 74-81
Research Article

Journal of Mathematical Sciences and Modelling

Journal Homepage: www.dergipark.gov.tr/jmsm
ISSN 2636-8692
DOI: http://dx.doi.org/10.33187/jmsm.459461

Stochastic Extended Korteweg-De Vries Equation

Anna Karczewska[1*] **and Maciej Szczeciński**[1]

[1] *Faculty of Mathematics, Computer Science and Econometrics, University of Zielona Góra, Poland*
[*] *Corresponding author*

Article Info

Keywords: *Extended KdV, Extended KdV equation, Mild solution, Near identity transformation.*
2010 AMS: *60H15, 35Q53, 35Q35, 76B15, 76B25.*
Received: *12 September 2018*
Accepted: *10 January 2019*
Available online: *30 August 2019*

Abstract

In the paper, we consider stochastic Korteweg-de Vries - type equation. We give sufficient conditions for the existence and uniqueness of the local mild solution to the equation with additive noise. We discuss the possibility of the globalization of mild solution, as well.

1. Introduction

Nonlinear wave equations attracted enormous attention in many fields, e.g. physics (hydrodynamics, plasma physics, optics), technology (electric circuits, light impulses propagation) and biology (neuroscience models, protein, and DNA motion). Usually, such equations are obtained as a kind of approximation and/or simplification of the set of several more fundamental equations governing the system with their boundary and initial conditions. Approximations are usually based on the perturbative approach in which some small parameters, related to particular properties of the considered system, appear. Then the relevant quantities are expanded in power series of these small parameters. The limitation to terms of the first or second order allows deriving approximate nonlinear wave equations describing the evolution of a given system.
In several fields the lowest (first) order equation takes form of the Korteveg-de Vries equation (commonly denoted as KdV) [1]

$$\frac{\partial u}{\partial t}+6u\frac{\partial u}{\partial x}+\frac{\partial^3 u}{\partial x^3}=0. \tag{1.1}$$

It was derived firstly for surface gravity waves on shallow water but later found in many other systems, see, e.g. [2, 3, 4, 5].
Although the KdV equation displays dominant features of weekly dispersive nonlinear waves, it is a valid approximation only for constant water depth and waves with small amplitudes. For waves with a larger amplitudes perturbative approach to Euler equations should be applied up to second order in small parameters. Then linear terms with fifth order derivatives and new nonlinear terms appear in final nonlinear wave equation. This equation was derived by Marchant and Smyth and called the **extended KdV** in [6]. For short we call this equation **KdV2** stressing second order perturbation expansion. Contrary to KdV this equation is non-integrable. Despite this fact, we found three kinds of analytic solutions to KdV2, namely single soliton solutions, periodic cnoidal solutions, and periodic superposition solutions, see. e.g. [7, 8, 9].
Nonlinear dispersive waves attracted the considerable attention of mathematicians. Among many examples of mathematical description of those problems, we point out books of Linares and Ponce [10] and Tao [11].
Surface water waves are subjected to some unpredictable influences of the environment, like winds, bottom fluctuations, etc. These unknown factors can be accounted for by introducing a forcing term of stochastic nature into wave equation.
In the current paper, we study stochastic version of KdV2. We supply sufficient conditions for the existence and uniqueness of a local mild solution to the Korteweg-de Vries type equation of the form (2.1) below. We follow and generalize the approach of de Bouard and Debussche [12] and Kenig, Ponce and Vega [13, 14] to such equation.

***Email addresses and ORCID numbers*: A.Karczewska@wmie.uz.zgora.pl, 0000-0001-7160-7908 (A. Karczewska), M.Szczecinski@wmie.uz.zgora.pl (M. Szczeciński)**

We obtained the existence and uniqueness results on a random interval. The generalization of these results to any time interval with the approach due to de Bouard and Debussche [12] is not possible since they use some properties of classical KdV equation and its invariants. In our case, for extended KdV equation, there exists only one (the lowest) exact invariant, the other ones are only adiabatic (approximate) [15]. In Section 3 we discuss the possibility for some globalization of obtained mild solution to stochastic extended KdV equation studied. We use the near-identity transformation (NIT for short) Kodama [16], Dullin et al. [17] to transform original non-integrable extended KdV equation into the asymptotically equivalent equation which has Hamiltonian form and therefore is integrable. The term *asymptotic equivalence* means that solutions of both equations coincide when physically relevant coefficients of the equations tend to zero (for details, see Section 3).

2. Existence and uniqueness

In this section, we prove the existence and uniqueness of mild solution on a random interval to the stochastic extended KdV-type equation of the form

$$\mathrm{d}u+\left(\frac{\partial^3 u}{\partial x^3}+u\frac{\partial u}{\partial x}+u\frac{\partial^3 u}{\partial x^3}+\frac{\partial u}{\partial x}\frac{\partial^2 u}{\partial x^2}\right)\mathrm{d}t=\Phi\,\mathrm{d}W,\quad x\in\mathbb{R},\quad t\geq 0. \tag{2.1}$$

Motivation for studying the equation (2.1) is given in Section 3. In (2.1), W is a cylindrical Wiener process defined on the stochastic basis $(\Omega,\mathscr{F},(\mathscr{F}_t)_{t\geq 0},\mathbb{P})$ with values on $L^2(\mathbb{R})$ adapted to the filtration $(\mathscr{F}_t)_{t\geq 0}$. The operator Φ belongs to L_2^0, where $L_2^0:=L_2^0(L^2(\mathbb{R});H^\sigma(\mathbb{R}))$ is the space of Hilbert-Schmidt operators acting from $L^2(\mathbb{R})$ into $H^\sigma(\mathbb{R})$ and $H^\sigma(\mathbb{R})$ is the Sobolev space (see, e.g., Adams [18]), $\sigma>0$. The equation (2.1) is supplemented with an initial condition

$$u(x,0)=u_0(x),\quad x\in\mathbb{R},\quad t\geq 0. \tag{2.2}$$

Definition 2.1. *A stochastic process $u(t)$, $t\geq 0$, defined on the basis $(\Omega,\mathscr{F},(\mathscr{F}_t)_{t\geq 0},\mathbb{P})$ is said to be a mild solution to (2.1)-(2.2), if*

$$u(t)=V(t)u_0+\int_0^t V(t-s)\left(u\frac{\partial u}{\partial x}+u\frac{\partial^3 u}{\partial x^3}+\frac{\partial u}{\partial x}\frac{\partial^2 u}{\partial x^2}\right)\mathrm{d}s+\int_0^t V(t-s)\Phi\,\mathrm{d}W(s). \tag{2.3}$$

In (2.3), $V(t),t\geq 0$, is a unitary group generated by the linear part of the KdV equation (1.1).
To simplify notation we will use the following abbreviation for stochastic convolution

$$W_V(t):=\int_0^t V(t-s)\Phi\,dW(s),\quad t\geq 0. \tag{2.4}$$

Definition 2.2. *For a given set A by ${}_nA$ we shall denote the biggest subset of A defined as* ${}_nA:=\left\{u\in A:\frac{\partial^{kn}u}{\partial x^{kn}}\in A,k\in\mathbb{N}\right\}$.

In the paper we shall use the following notation

$$X_\sigma(T):=\left\{u\in L^\infty(0,T;H^\sigma(\mathbb{R}))\cap L^2(\mathbb{R};L^\infty([0,T])),D^\sigma\partial_x u\in L^\infty(\mathbb{R},L^2([0,T])),\partial_x u\in L^4([0,T];L^\infty(\mathbb{R}))\right\}.$$

Lemma 2.3. *If $(u_0)_{2x}\in H^\sigma(\mathbb{R})$, then $V(t)(u_0)_{2x}\in X_\sigma(T)$, $\sigma>\frac{3}{4}$.*

Proof. Proof comes from Proposition 3.5 in de Bouard and Debussche [12]. □

Now, we can formulate first result.

Theorem 2.4. *Assume that $\Phi\in L_2^0(L^2(\mathbb{R});H^\sigma(\mathbb{R}))$ with $\alpha>\frac{3}{4}$ and*

$$\frac{\partial^2}{\partial x^2}\left[\int_0^t V(t-s)\Phi\,\mathrm{d}W(s)\right]\in L^2\left(\Omega;L_x^2(L_t^\infty)\right). \tag{2.5}$$

Then $\frac{\partial^2}{\partial x^2}W_V\in\widehat{X}_\sigma(T)$, $\mathbb{P}$-almost surely, where $\widehat{X}_\sigma(T):=\left\{u:L^2(\mathbb{R};L^\infty([0,T])),D^\sigma\partial_x u\in L^\infty(\mathbb{R},L^2([0,T])),\partial_x u\in L^4([0,T];L^\infty(\mathbb{R}))\right\}$, for any $T>0$ and all σ, such that $\frac{3}{4}<\sigma<1$.

Proof. For reader's convenience the proof of Theorem 2.4 is postponed to the section 4. □

Corollary 2.5. *Assume that $\Phi\in L_2^0(L^2(\mathbb{R});H^\sigma(\mathbb{R}))$ and for $\sigma>\frac{3}{4}$ holds*

$$\frac{\partial^2}{\partial x^2}W_V\in L^2\left(\Omega;L_t^\infty\left(H_x^\sigma\right)\right).$$

Then $\frac{\partial^2}{\partial x^2}W_V\in X_\sigma(T)$, $\mathbb{P}$-almost surely for any $T>0$, and σ such that $\frac{3}{4}<\sigma<1$.

Now, we are able to formulate the existence and uniqueness result.

Theorem 2.6. *Assume that $u_0\in{}_2L^2\left(\Omega;H^1(\mathbb{R})\right)\cap{}_2L^4\left(\Omega;L^2(\mathbb{R})\right)$ and it is $\mathscr{F}_0$-measurable and $\Phi\in L_2^0\left(L^2(\mathbb{R});H^1(\mathbb{R})\right)$. If (2.5) holds then there exists a unique mild solution to the equation (2.1) with initial condition (2.2), such that $u\in{}_2X_\sigma(T)$ almost surely for some $T>0$ and for any $\sigma\in\left(\frac{3}{4},1\right)$.*

Proof. As we have already written, in the proof we follow the method used in de Bouard and Debussche [12].
We introduce the mapping $\mathscr{T}$ defined as follows

$$\mathscr{T}(u) := V(t)u_0 + \int_0^t V(t-\tau)(u\frac{\partial u}{\partial x} + u\frac{\partial^3 u}{\partial x^3} + \frac{\partial u}{\partial x}\frac{\partial^2 u}{\partial x^2})\,\mathrm{d}\tau + W_V(t), \quad t \geq 0. \tag{2.6}$$

Then

$$\begin{aligned} \mathscr{T}(u) &= V(t)u_0 + \int_0^t V(t-\tau)(u\partial_x u + u\partial_x u_{2x} + u_{2x}\partial_x u)\,\mathrm{d}\tau + W_V(t)) = \\ &= V(t)u_0 + \int_0^t V(t-\tau)(u\partial_x u)\,\mathrm{d}\tau + \int_0^t V(t-\tau)(u\partial_x u_{2x})\,\mathrm{d}\tau + \int_0^t V(t-\tau)(u_{2x}\partial_x u)\,\mathrm{d}\tau + W_V(t), \quad t \geq 0. \end{aligned} \tag{2.7}$$

We want to obtain the following condition

$$[\, u \in \{u : u \in X_\sigma(T), u_{2x} \in X_\sigma(T)\}\,] \Longrightarrow [\, \mathscr{T}(u) \in \{u : u \in X_\sigma(T), u_{2x} \in X_\sigma(T)\}\,]. \tag{2.8}$$

From Theorem 3.2 and Proposition 3.5 in de Bouard and Debussche [12] and because $u, u_{2x} \in X_\sigma(T)$, the mapping $\mathscr{T}$ maps $X_\sigma(T)$ into itself if $u_0 \in H^\sigma(\mathbb{R})$. We will check when $\frac{\partial^2}{\partial x^2}\mathscr{T}(u) \in X_\sigma(T)$. We have

$$\begin{aligned} \frac{\partial^2}{\partial x^2}\mathscr{T}(u) &= \frac{\partial^2}{\partial x^2}V(t)u_0 + \frac{\partial^2}{\partial x^2}\int_0^t V(t-\tau)(uu_x)\,\mathrm{d}\tau + \frac{\partial^2}{\partial x^2}\int_0^t V(t-\tau)(uu_{3x})\,\mathrm{d}\tau + \frac{\partial^2}{\partial x^2}\int_0^t V(t-\tau)(u_x u_{2x})\,\mathrm{d}\tau + \frac{\partial^2}{\partial x^2}\int_0^t V(t-\tau)\Phi\, dW(\tau) \\ &= V(t)(u_0)_{2x} + \int_0^t V(t-\tau)(uu_{3x} + 3u_x u_{2x})\,\mathrm{d}\tau + \int_0^t V(t-\tau)(u_{2x}u_{3x} + 2u_x u_{4x} + uu_{5x})\,\mathrm{d}\tau \\ &\quad + \int_0^t V(t-\tau)(3u_{2x}u_{3x} + u_x u_{4x})\,\mathrm{d}\tau + \frac{\partial^2}{\partial x^2}\int_0^t V(t-\tau)\Phi\, dW(\tau). \end{aligned}$$

Let $u \in {}_2X_\sigma(T)$. Then $v = u_{2x} \in {}_2X_\sigma(T)$ and $v_{2x} \in {}_2X_\sigma(T)$. We have

$$\int_0^t V(t-\tau)(uu_{3x} + 3u_x u_{2x})\,\mathrm{d}\tau = \int_0^t V(t-\tau)u\partial_x u_{2x}\,\mathrm{d}\tau + 3\int_0^t V(t-\tau)u_{2x}\partial_x u\,\mathrm{d}\tau = \int_0^t V(t-\tau)u\partial_x v\,\mathrm{d}\tau + 3\int_0^t V(t-\tau)v\partial_x u\,\mathrm{d}\tau; \tag{2.9}$$

$$\begin{aligned} \int_0^t V(t-\tau)(u_{2x}u_{3x} + 2u_x u_{4x} + uu_{5x})\,\mathrm{d}\tau &= \int_0^t V(t-\tau)u_{2x}\partial_x u_{2x}\,\mathrm{d}\tau + 2\int_0^t V(t-\tau)u_{4x}\partial_x u\,\mathrm{d}\tau + \int_0^t V(t-\tau)u\partial_x u_{4x}\,\mathrm{d}\tau \\ &= \int_0^t V(t-\tau)v\partial_x v\,\mathrm{d}\tau + 2\int_0^t V(t-\tau)v_{2x}\partial_x u\,\mathrm{d}\tau + \int_0^t V(t-\tau)u\partial_x v_{2x}\,\mathrm{d}\tau; \end{aligned} \tag{2.10}$$

$$\int_0^t V(t-\tau)(3u_{2x}u_{3x} + u_x u_{4x})\,\mathrm{d}\tau = 3\int_0^t V(t-\tau)u_{2x}\partial_x u_{2x}\,\mathrm{d}\tau + \int_0^t V(t-\tau)u_{4x}\partial_x u\,\mathrm{d}\tau \tag{2.11}$$

$$= 3\int_0^t V(t-\tau)v\partial_x v\,\mathrm{d}\tau + \int_0^t V(t-\tau)v_{2x}\partial_x u\,\mathrm{d}\tau. \tag{2.12}$$

From Theorem 3.2, Proposition 3.5 de Bouard and Debussche [12], Lemma 2.3 and Theorem 2.4 above, and equations (2.9)-(2.11) we obtain that the mapping $\mathscr{T}$ maps the set ${}_2X_\sigma(T)$ into itself if $u_0 \in {}_2H^\sigma(\mathbb{R})$ and $\Phi \in {}_2\mathscr{L}_2\left(L^2(\mathbb{R}, H^\sigma(\mathbb{R}))\right)$. We want to find a ball $\mathscr{B}$ in ${}_2X_\sigma(T)$ centered at point 0 and radius $2R$ such that the mapping $\mathscr{T}\big|_{\mathscr{B}}$ is contraction. More precisely, we want to have the following conditions

$$\text{(i) } |u|_{X_\sigma(T)} < 2R \Longrightarrow |\mathscr{T}(u)|_{X_\sigma(T)} < 2R; \quad \text{(ii) } |\mathscr{T}(u) - \mathscr{T}(v)|_{X_\sigma(T)} < |u-v|_{X_\sigma(T)}, \quad |u|_{X_\sigma(T)}, |v|_{X_\sigma(T)} < 2R. \tag{2.13}$$

First, let us note that for any $u \in X_\sigma(T)$ there exists $M_u > 0$ such that $|u_{2x}|_{X_\sigma(T)} = M_u\,|u|_{X_\sigma(T)}$. Denote $M := \sup\{M_u : u \in X_\sigma(T)\}$. Then

$$|u_{2x}|_{X_\sigma(T)} \leq M\,|u|_{X_\sigma(T)}. \tag{2.14}$$

From (2.14) and Proposition 3.5. de Bouard and Debussche [12] we obtain the following estimate

$$\begin{aligned} |\mathscr{T}(u)|_{X_\sigma(T)} &\leq C_1(\sigma,T)|u_0|_{H^\sigma(\mathbb{R})} + C_2(\sigma,T)T^{\frac{1}{2}}|u|^2_{X_\sigma(T)} + C_3(\sigma,T)T^{\frac{1}{2}}|u|_{X_\sigma(T)}|u_{2x}|_{X_\sigma(T)} + C_4(\sigma,T)T^{\frac{1}{2}}|u_{2x}|_{X_\sigma(T)}|u|_{X_\sigma(T)} + |W_V|_{X_\sigma(T)} \\ &\leq C_1(\sigma,T)|u_0|_{H^\sigma(\mathbb{R})} + C_2(\sigma,T)T^{\frac{1}{2}}|u|^2_{X_\sigma(T)} + C_3(\sigma,T)T^{\frac{1}{2}}M|u|^2_{X_\sigma(T)} + C_4(\sigma,T)T^{\frac{1}{2}}M|u|^2_{X_\sigma(T)} + |W_V|_{X_\sigma(T)}. \end{aligned}$$

Here and below we write for shortening W_V instead of $W_V(t)$, $t \geq 0$.
Since $C_i(\sigma,T)$, $i = 1,2,3,4$, are nondecreasing with respect to T, we can use $C(\sigma,T) := \max\limits_T\{C_1(\sigma,T), C_2(\sigma,T), C_3(\sigma,T), C_4(\sigma,T)\}$, which is nondecreasing with respect to T to our estimate. We obtain

$$\begin{aligned} |\mathscr{T}(u)|_{X_\sigma(T)} &\leq C(\sigma,T)|u_0|_{H^\sigma(\mathbb{R})} + C(\sigma,T)T^{\frac{1}{2}}|u|^2_{X_\sigma(T)} + C(\sigma,T)T^{\frac{1}{2}}M|u|^2_{X_\sigma(T)} + C(\sigma,T)T^{\frac{1}{2}}M|u|^2_{X_\sigma(T)} + |W_V|_{X_\sigma(T)} \\ &= C(\sigma,T)|u_0|_{H^\sigma(\mathbb{R})} + C(\sigma,T)T^{\frac{1}{2}}|u|^2_{X_\sigma(T)}(1+2M) + |W_V|_{X_\sigma(T)}. \end{aligned}$$

Now, we shall find R fulfilling condition (2.13)(i). Assume that $|u|_{X_\sigma(T)} < 2R$. Then we have

$$|\mathscr{T}(u)|_{X_\sigma(T)} \leq C(\sigma,T)|u_0|_{H^\sigma(\mathbb{R})} + C(\sigma,T)T^{\frac{1}{2}}4R^2(1+2M) + |W_V|_{X_\sigma(T)}.$$

We want to receive $C(\sigma,T)|u_0|_{H^\sigma(\mathbb{R})}+C(\sigma,T)T^{\frac{1}{2}}4R^2(1+2M)+|W_V|_{X_\sigma(T)}\le 2R$. This is equivalent to $C(\sigma,T)|u_0|_{H^\sigma(\mathbb{R})}+|W_V|_{X_\sigma(T)}\le 2R-C(\sigma,T)T^{\frac{1}{2}}4R^2(1+2M)$. Let us note that it is enough to have such R that

$$C(\sigma,T)|u_0|_{H^\sigma(\mathbb{R})}+|W_V|_{X_\sigma(T)}\ \le\ R\ \le\ 2R-C(\sigma,T)T^{\frac{1}{2}}4R^2(1+2M).$$

From the second inequality we obtain $R\le 2R-C(\sigma,T)T^{\frac{1}{2}}4R^2(1+2M)$, then $0\le R-C(\sigma,T)T^{\frac{1}{2}}4R^2(1+2M)$ and $0\le R[1-4RC(\sigma,T)T^{\frac{1}{2}}(1+2M)]$, so $0\le 1-4RC(\sigma,T)T^{\frac{1}{2}}(1+2M)$, and finally $1\ge 4RC(\sigma,T)T^{\frac{1}{2}}(1+2M)$.
Hence, in order to obtain (2.13) (i), the following inequalities must hold

$$C(\sigma,T)|u_0|_{H^\sigma(\mathbb{R})}+|W_V|_{X_\sigma(T)}\le R\qquad\text{and}\qquad 4RC(\sigma,T)T^{\frac{1}{2}}(1+2M)\le 1. \tag{2.15}$$

Let us note that the second condition in (2.15) will hold too, if

$$\kappa 4RC(\sigma,T)T^{\frac{1}{2}}(1+2M)\le 1\quad\text{for any fixed constant }\kappa>1. \tag{2.16}$$

Now, we will check when the condition (2.13)(ii) holds. First, we shall estimate the norm $|\mathscr{T}(u)-\mathscr{T}(v)|_{X_\sigma(T)}$. We can write

$$\begin{aligned}
|\mathscr{T}(u)-\mathscr{T}(v)|_{X_\sigma(T)} &= \left|\int_0^t V(t-\tau)(u\partial_x u-v\partial_x v)\,\mathrm{d}\tau+\int_0^t V(t-\tau)(u\partial_x u_{2x}-v\partial_x v_{2x})\,\mathrm{d}\tau+\int_0^t V(t-\tau)(u_{2x}\partial_x u-v_{2x}\partial_x v)\,\mathrm{d}\tau\right|_{X_\sigma(T)}\\
&= \frac{1}{2}\left|\int_0^t V(t-\tau)\left[u\partial_x(u-v)+(u-v)\partial_x u+v\partial_x(u-v)+(u-v)\partial_x v\right]\mathrm{d}\tau\right.\\
&\quad+\int_0^t V(t-\tau)\left[u\partial_x(u-v)_{2x}+(u-v)\partial_x u_{2x}+v\partial_x(u-v)_{2x}+(u-v)\partial_x v_{2x}\right]\mathrm{d}\tau\\
&\quad\left.+\int_0^t V(t-\tau)\left[u_{2x}\partial_x(u-v)+(u-v)_{2x}\partial_x u+v_{2x}\partial_x(u-v)+(u-v)_{2x}\partial_x v\right]\mathrm{d}\tau\right|_{X_\sigma(T)}\\
&\le \frac{1}{2}\left|\int_0^t V(t-\tau)\left[u\partial_x(u-v)+(u-v)\partial_x u+v\partial_x(u-v)+(u-v)\partial_x v\right]\mathrm{d}\tau\right|_{X_\sigma(T)}\\
&\quad+\frac{1}{2}\left|\int_0^t V(t-\tau)\left[u\partial_x(u-v)_{2x}+(u-v)\partial_x u_{2x}+v\partial_x(u-v)_{2x}+(u-v)\partial_x v_{2x}\right]\mathrm{d}\tau\right|_{X_\sigma(T)}\\
&\quad+\frac{1}{2}\left|\int_0^t V(t-\tau)\left[u_{2x}\partial_x(u-v)+(u-v)_{2x}\partial_x u+v_{2x}\partial_x(u-v)+(u-v)_{2x}\partial_x v\right]\mathrm{d}\tau\right|_{X_\sigma(T)}.
\end{aligned}$$

Then

$$\begin{aligned}
|\mathscr{T}(u)-\mathscr{T}(v)|_{X_\sigma(T)} &\le \frac{1}{2}C(\sigma,T)T^{\frac{1}{2}}|u|_{X_\sigma(T)}|u-v|_{X_\sigma(T)}+\frac{1}{2}C(\sigma,T)T^{\frac{1}{2}}|u-v|_{X_\sigma(T)}|u|_{X_\sigma(T)}\\
&\quad+\frac{1}{2}C(\sigma,T)T^{\frac{1}{2}}|v|_{X_\sigma(T)}|u-v|_{X_\sigma(T)}+\frac{1}{2}C(\sigma,T)T^{\frac{1}{2}}|u-v|_{X_\sigma(T)}|v|_{X_\sigma(T)}\\
&\quad+\frac{1}{2}C(\sigma,T)T^{\frac{1}{2}}|u|_{X_\sigma(T)}|(u-v)_{2x}|_{X_\sigma(T)}+\frac{1}{2}C(\sigma,T)T^{\frac{1}{2}}|u-v|_{X_\sigma(T)}|u_{2x}|_{X_\sigma(T)}\\
&\quad+\frac{1}{2}C(\sigma,T)T^{\frac{1}{2}}|v|_{X_\sigma(T)}|(u-v)_{2x}|_{X_\sigma(T)}+\frac{1}{2}C(\sigma,T)T^{\frac{1}{2}}|u-v|_{X_\sigma(T)}|v_{2x}|_{X_\sigma(T)}\\
&\quad+\frac{1}{2}C(\sigma,T)T^{\frac{1}{2}}|u_{2x}|_{X_\sigma(T)}|u-v|_{X_\sigma(T)}+\frac{1}{2}C(\sigma,T)T^{\frac{1}{2}}|(u-v)_{2x}|_{X_\sigma(T)}|u|_{X_\sigma(T)}\\
&\quad+\frac{1}{2}C(\sigma,T)T^{\frac{1}{2}}|v_{2x}|_{X_\sigma(T)}|u-v|_{X_\sigma(T)}+\frac{1}{2}C(\sigma,T)T^{\frac{1}{2}}|(u-v)_{2x}|_{X_\sigma(T)}|v|_{X_\sigma(T)}\\
&= \frac{1}{2}C(\sigma,T)T^{\frac{1}{2}}|u-v|_{X_\sigma(T)}\left[2|u|_{X_\sigma(T)}+2|v|_{X_\sigma(T)}+2|u_{2x}|_{X_\sigma(T)}+2|v_{2x}|_{X_\sigma(T)}\right]\\
&\quad+\frac{1}{2}C(\sigma,T)T^{\frac{1}{2}}|(u-v)_{2x}|_{X_\sigma(T)}\left[2|u|_{X_\sigma(T)}+2|v|_{X_\sigma(T)}\right]\\
&\le C(\sigma,T)T^{\frac{1}{2}}|u-v|_{X_\sigma(T)}\left[|u|_{X_\sigma(T)}+|v|_{X_\sigma(T)}+M|u|_{X_\sigma(T)}+M|v|_{X_\sigma(T)}\right]+C(\sigma,T)T^{\frac{1}{2}}M|u-v|_{X_\sigma(T)}\left[|u|_{X_\sigma(T)}+|v|_{X_\sigma(T)}\right].
\end{aligned}$$

Finally we have

$$\begin{aligned}
|\mathscr{T}(u)-\mathscr{T}(v)|_{X_\sigma(T)} &\le C(\sigma,T)T^{\frac{1}{2}}|u-v|_{X_\sigma(T)}\left[|u|_{X_\sigma(T)}+|v|_{X_\sigma(T)}+M|u|_{X_\sigma(T)}+M|v|_{X_\sigma(T)}\right]+C(\sigma,T)T^{\frac{1}{2}}|u-v|_{X_\sigma(T)}\left[M|u|_{X_\sigma(T)}+M|v|_{X_\sigma(T)}\right]\\
&= C(\sigma,T)T^{\frac{1}{2}}|u-v|_{X_\sigma(T)}\left[|u|_{X_\sigma(T)}(2M+1)+|v|_{X_\sigma(T)}(2M+1)\right]=C(\sigma,T)T^{\frac{1}{2}}|u-v|_{X_\sigma(T)}\left(|u|_{X_\sigma(T)}+|v|_{X_\sigma(T)}\right)(2M+1).
\end{aligned}$$

Since $|u|_{X_\sigma(T)}\le 2R$ and $|v|_{X_\sigma(T)}\le 2R$, we have

$$|\mathscr{T}(u)-\mathscr{T}(v)|_{X_\sigma(T)}\le 4RC(\sigma,T)T^{\frac{1}{2}}|u-v|_{X_\sigma(T)}(2M+1). \tag{2.17}$$

From (2.16) we know that $4RC(\sigma,T)T^{\frac{1}{2}}(2M+1)\le\frac{1}{\kappa}$, so, putting this into (2.17), we can write $|\mathscr{T}(u)-\mathscr{T}(v)|_{X_\sigma(T)}\le\frac{1}{\kappa}|u-v|_{X_\sigma(T)}$. Hence, the mapping $\mathscr{T}\big|_{\mathscr{B}}$ is contraction if $\frac{1}{\kappa}|u-v|_{X_\sigma(T)}<|u-v|_{X_\sigma(T)}$, what is satisfied for any $\kappa>1$. So, we have to choose R_0 and T such that

$$C(\sigma,T)|u_0|_{H^\sigma(\mathbb{R})}+|W_V|_{X_\sigma(T)}\le R_0\quad\text{and}\quad\kappa 4R_0C(\sigma,T)T^{\frac{1}{2}}(1+2M)\le 1\quad\text{for some constant}\quad\kappa>1. \tag{2.18}$$

Remark 2.7. *In order to do this it is enough to take* $M := \sup\{M_u : u \in X_\sigma(T), |u|_{X_\sigma(T)} \le 4R\}$.

Proof. We estimated by M only terms $|u|_{X_\sigma(T)}$, $|v|_{X_\sigma(T)}$ and $|u-v|_{X_\sigma(T)}$. Since $|u|_{X_\sigma(T)} \le 2R$ and $|v|_{X_\sigma(T)} \le 2R$, so $|u-v|_{X_\sigma(T)} \le 4R$. □

Hence, the mapping $\mathscr{T}$ maps the ball $\mathscr{B}$ in ${}_2X_\sigma(T)$ centered at 0 with radius $2R$ into itself and, restricted to this ball, the mapping $\mathscr{T}$ is contraction. By Banach contraction theorem, the mapping $\mathscr{T}$ has fixed point in the set ${}_2X_\sigma(T)$, which is a unique solution to the equation (2.1) with initial condition (2.2). □

3. Near-identity transformation for KdV2

The famous Korteweg-de Vries equation [1] was first obtained in consideration of shallow water wave problem with the ideal fluid model. It is assumed that the fluid is inviscid and its motion is irrotational. Then the set of hydrodynamic (Euler's) equations with appropriate boundary conditions at the flat bottom and unknown surface is obtained. Scaling transformation to dimensionless variables introduces small parameters that allow us to apply perturbation approach. First order perturbation approach leads to KdV equation (below written in a fixed reference frame)

$$\eta_t + \eta_x + \frac{3}{2}\alpha\,\eta\,\eta_x + \frac{1}{6}\beta\,\eta_{3x} = 0. \tag{3.1}$$

More exact, second order perturbation approach gives the extended KdV equation [6] called by us KdV2 which has the following form

$$\eta_t + \eta_x + \frac{3}{2}\alpha\,\eta\,\eta_x + \frac{1}{6}\beta\,\eta_{3x} - \frac{3}{8}\alpha^2\eta^2\eta_x + \alpha\beta\left(\frac{23}{24}\eta_x\eta_{2x} + \frac{5}{12}\eta\,\eta_{3x}\right) + \frac{19}{360}\beta^2\eta_{5x} = 0. \tag{3.2}$$

In both equations (3.1) and (3.2) there appear parameters α, β, which should be small. Parameter $\alpha := \frac{A}{h}$ is the ratio of wave amplitude A to water depth h and determines nonlinear terms. Parameter $\beta := (\frac{h}{l})^2$, where l is an average wavelength describes the dispersion properties. When $\alpha \approx \beta \ll 1$ we have a classical shallow water problem. However, our recent paper [7] showed that exact solutions of KdV2 (3.2) occur when β is much less than α. Therefore for further considerations we can safely neglect in (3.2) the last term with fifth derivative. Transformation to a moving reference frame $x' = x - t$ and $t' = t$ yields KdV2 equation in the form

$$\eta_{t'} + \frac{3}{2}\alpha\,\eta\,\eta_{x'} + \frac{1}{6}\beta\,\eta_{3x'} - \frac{3}{8}\alpha^2\eta^2\eta_{x'} + \alpha\beta\left(\frac{23}{24}\eta_{x'}\eta_{2x'} + \frac{5}{12}\eta\,\eta_{3x'}\right) = 0. \tag{3.3}$$

In next steps we drop signs $'$ at x' and t', having in mind that (3.3) represents the KdV2 in a moving frame.
Kodama [16] showed that several nonlinear partial differential equations are *asymptotically equivalent*. This term means that solutions to these equations converge to the same solution when parameters $\alpha, \beta \to 0$. Kodama and several other authors [17, 19, 20] have shown that asymptotically equivalent equations are related to each other by near-identity transformation (NIT).
Let us introduce Near Identity Transformation (NIT for short) in the form used in Dullin et al. [17]

$$\eta = \eta' \pm \alpha a\eta'^2 \pm \beta b\eta'_{xx} + \cdots \tag{3.4}$$

[In the sequel we set the sign $+$. Then the inverse transformation, up to $O(\alpha^2)$ is $\eta' = \eta - \alpha a\eta^2 - \beta b\eta_{xx} + \cdots$]
NIT preserves the structure of the equation (3.3), at most altering some coefficients. Insertion (3.4) into (3.3) gives (up to 2nd order in α, β)

$$\begin{aligned} \eta'_t + \eta'_x \;&+\; \alpha\left[\left(\frac{3}{2}+2a\right)\eta'\eta'_x + 2a\eta'\eta'_t\right] + \beta\left[\left(\frac{1}{6}+b\right)\eta'_{3x} + b\eta'_{xxt}\right] \\ &+\; \alpha^2\left(-\frac{3}{8}+\frac{9}{2}a\right)\eta'^2\eta'_x + \alpha\beta\left\{\left[\left(\frac{23}{24}+a+\frac{3}{2}b\right)\eta'_x\eta'_{2x}\right] + \left[\left(\frac{5}{12}+\frac{1}{3}a+\frac{3}{2}b\right)\eta'\eta'_{3x}\right]\right\} + \beta^2\frac{1}{6}b\eta'_{5x} = 0. \end{aligned} \tag{3.5}$$

Since terms with derivatives with respect to t appear with coefficients α and β, we can replace them by appropriate expressions obtained from (3.2) limited to first order (that is from KdV)

$$\eta'_t = -\eta'_x - \frac{3}{2}\alpha\eta'\eta'_x - \frac{1}{6}\beta\eta'_{3x} \tag{3.6}$$

and

$$\eta'_{xxt} = \partial_{xx}\left(-\eta'_x - \frac{3}{2}\alpha\eta'\eta'_x - \frac{1}{6}\beta\eta'_{3x}\right) = -\eta'_{3x} - \frac{3}{2}\alpha(3\eta'_x\eta'_{2x} + \eta'\eta'_{3x}) - \frac{1}{6}\beta\eta'_{5x}. \tag{3.7}$$

Then terms (3.6) and (3.7) cause the following changes

$$\begin{aligned} \alpha\,2a\eta'\eta'_t + \beta\,b\eta'_{xxt} &= -2\alpha a\eta'\left(\eta'_x + \frac{3}{2}\alpha\eta'\eta'_x + \frac{1}{6}\beta\eta'_{3x}\right) - \beta b\left[\eta'_{3x} + \frac{3}{2}\alpha(3\eta'_x\eta'_{2x} + \eta'\eta'_{3x}) + \frac{1}{6}\beta\eta'_{5x}\right] \\ &= -2\alpha a\,\eta'\eta'_x - 3\alpha^2 a\eta'^2\eta'_x - \beta b\eta'_{3x} - \alpha\beta\left[\frac{1}{2}b\,\eta'_x\eta'_{2x} + \left(\frac{1}{3}a+\frac{3}{2}b\right)\eta'\eta'_{3x}\right] - \frac{1}{6}\beta^2 b\eta'_{5x}. \end{aligned} \tag{3.8}$$

Insertion of (3.8) into (3.5) yields

$$\eta'_t + \eta'_x + \frac{3}{2}\alpha\eta'\eta'_x + \frac{1}{6}\beta\eta'_{3x} + \alpha^2\left(-\frac{3}{8}+\frac{3}{2}a\right)\eta'^2\eta'_x + \alpha\beta\left[\left(\frac{23}{24}+a-3b\right)\eta'_x\eta'_{2x} + \frac{5}{12}\eta'\eta'_{3x}\right] = 0. \tag{3.9}$$

Comparison of (3.9) with (3.3) shows that only two coefficients are altered, that at the term containing α^2, where $-\frac{3}{8} \to -\frac{3}{8}+\frac{3}{2}a$ and that with $\alpha\beta\eta'_x\eta'_{2x}$, where $\frac{23}{24} \to \frac{23}{24}+a-3b$.
Equation (3.9) is asymptotically equivalent to (3.3). NIT gives us some freadom in choosing coefficients a,b. They can be chosen such that the most nonlinear term (with 3-rd order nonlinearity) is canceled and the final equations is integrable. The first goal is obtained if

$$-\frac{3}{8}+\frac{3}{2}a=0 \qquad \Longrightarrow \qquad a=\frac{1}{4}.$$

Integrability is achieved when coefficient in front of the term with $\eta_x\eta_{2x}$ is twice the coefficient in front of the term with $\eta\eta_{3x}$. So, we can choose b such that

$$\frac{23}{24}+a-3b=2\frac{5}{12} \qquad \Longrightarrow \qquad b=\frac{1}{8}.$$

Then, applying to (3.3) NIT (3.4) with parameters $a=\frac{1}{4}$ and $b=\frac{1}{8}$ we obtain asymptotically equivalent integrable equation in the form

$$\eta'_t+\frac{3}{2}\alpha\,\eta'\eta'_x+\frac{1}{6}\beta\,\eta'_{3x}+\frac{5}{12}\alpha\beta\,\left(2\eta'_x\eta'_{2x}+\eta'\eta'_{3x}\right)=0. \tag{3.10}$$

We will show that for (3.10) there exists Hamiltonian form

$$\eta'_t=\frac{\partial}{\partial x}\left(\frac{\delta\mathscr{H}}{\delta\eta'}\right), \tag{3.11}$$

where Hamiltonian $H=\int_{-\infty}^{\infty}\mathscr{H}\,dx$ has the density

$$\mathscr{H}=-\frac{1}{4}\alpha\eta'^3+\frac{1}{12}\beta\eta'^2_x+\frac{5}{24}\alpha\beta\eta'\eta'^2_x.$$

Since $\mathscr{H}=\mathscr{H}(\eta',\eta'_x)$, then functional derivative is given by

$$\frac{\delta\mathscr{H}}{\delta\eta'}=\frac{\partial\mathscr{H}}{\partial\eta'}-\frac{\partial}{\partial x}\frac{\partial\mathscr{H}}{\partial\eta'_x}=-\frac{3}{4}\alpha\eta'^2-\frac{1}{6}\beta\eta'_{2x}-\frac{5}{24}\alpha\beta\eta'^2_x-\frac{5}{12}\alpha\beta\eta'\eta'_{2x}. \tag{3.12}$$

Insertion of (3.12) into (3.11) gives

$$\eta'_t=-\frac{3}{2}\alpha\eta'\eta'_x-\frac{1}{6}\beta\eta'_{3x}-\frac{5}{12}\alpha\beta\left(2\eta'_x\eta'_{xx}+\eta'\eta'_{xxx}\right). \tag{3.13}$$

what coincides with (3.10).
It is worth to notice, that application of inverse NIT to (3.10) brings back the equation (3.3) (up to second order in α,β).
The existence of the Hamiltonian implies that there exist invariants of the equation (3.10). This is the first step towards obtaining a global mild solution according to approach due to de Bouard and Debussche [12].

Remark 3.1. *Equations (3.10) or (3.13), up to numerical coefficients, are the same as left hand side of stochastic equation (2.1). Then study of stochastic equation (2.1) is justified.*

4. Proof of Theorem 2.4

To make the paper self-contained, we recall the following results.

Theorem 4.1. *([12], Proposition A.1) Let $A=L^q_\omega(L^2_t)$ or $A=L^q(\Omega)$, with $1<q<\infty$, and let u be an A-valued function of $x\in\mathbb{R}$. Assume that for some p, with $1<p<\infty$ and some $\sigma>0$*

$$u\in L^p_x(A), \quad D^\sigma u\in L^\infty_x(A);$$

then for any $\alpha\in[0,\sigma]$ $D^\alpha u\in L^{p_\alpha}_x$, with p_α defined by $\frac{1}{p_\alpha}=\frac{1}{p}\left(1-\frac{\alpha}{\sigma}\right)$. Furthermore, there is a constant C such that

$$|D^\alpha|_{L^{p_\alpha}_x(A)}\le C\,|u|^{1-\frac{\alpha}{\sigma}}_{L^{p_\alpha}_x(A)}\,|D^\sigma u|^{\frac{\alpha}{\sigma}}_{L^\infty_x(A)}.$$

Theorem 4.2. *([13], Lemma 2.1) Let $v_0\in L^2(\mathbb{R})$.Then*

$$\int_{-\infty}^{\infty}\left|D^{\frac{\alpha}{2}}V^\alpha(t)v_0(x)\right|^2\,\mathrm{d}t=c_\alpha||v_0||^2_2 \quad \textit{for any} \quad x\in\mathbb{R}.$$

Theorem 4.3. *([13], Theorem 2.4) For any $(\theta,\beta)\in[0,1]\times\left[0,\frac{\alpha-1}{2}\right]$*

$$\left(\int_{-\infty}^{\infty}\left\|D^{\theta\frac{\beta}{2}}U^\alpha(t)v_0\right\|^q_p\,\mathrm{d}t\right)^{\frac{1}{q}}\le c\,\|v_0\|_2$$

and

$$\left(\int_{-\infty}^{\infty}\left\|\int D^{\theta\frac{\beta}{2}}U^\alpha(t-s)f(\cdot,s)\,\mathrm{d}s\right\|^q_p\,\mathrm{d}t\right)^{\frac{1}{q}}\le c\left(\int_{-\infty}^{\infty}\|f(\cdot,s)\|^{q'}_{p'}\,\mathrm{d}t\right)^{\frac{1}{q'}},$$

where $(q,p)=(2(\alpha+1)/(\theta(\beta+1)),2/(1-\theta))$, $\frac{1}{p}+\frac{1}{p'}=\frac{1}{q}+\frac{1}{q'}=1$.

Lemma 4.4. *Asume that* $\widetilde{\sigma} > \sigma > \frac{3}{4}$ *and* $0 < \varepsilon < \inf\{\widetilde{\sigma}, 2\}$. *Then*

$$D^{\widetilde{\sigma}-\varepsilon}\partial_x\left(\frac{\partial^2}{\partial x^2}W_V\right) \in L^2\left(\Omega; L_x^\infty(L_t^2)\right).$$

Proof. Let, as usually, $W_V := \int_0^t V(t-s)\Phi\, \mathrm{d}W(s)$ and let $q = \frac{6}{\varepsilon}$. Estimate the expression $\left|D^{3+\widetilde{\sigma}}W_V\right|_{L_x^\infty(L_\omega^q(L_t^2))}$. We have

$$\begin{aligned}\left|D^{3+\widetilde{\sigma}}W_V\right|_{L_x^\infty(L_\omega^q(L_t^2))} &= \sup_{x\in\mathbb{R}}\mathbb{E}\left(\left(\int_0^T\left|\int_0^t D^{3+\widetilde{\sigma}}V(t-s)\Phi\, \mathrm{d}W(s)\right|^2 \mathrm{d}t\right)^{\frac{q}{2}}\right) \le C\sup_{x\in\mathbb{R}}\int_0^T \mathbb{E}\left(\left|\int_0^t D^{3+\widetilde{\sigma}}V(t-s)\Phi\, \mathrm{d}W(s)\right|^2\right)^{\frac{q}{2}}\mathrm{d}t \\ &\le C\sup_{x\in\mathbb{R}}\int_0^T\left(\int_0^t\sum_{i\in\mathbb{N}}\left|D^{3+\widetilde{\sigma}}V(t-s)\Phi e_i(s)\right|^2 \mathrm{d}s\right)^{\frac{q}{2}}\mathrm{d}t \le C\int_0^T\left(\sum_{i\in\mathbb{N}}\sup_{x\in\mathbb{R}}\int_0^t\left|D^{3+\widetilde{\sigma}}V(t-s)\Phi e_i(s)\right|^2 \mathrm{d}s\right)^{\frac{q}{2}}\mathrm{d}t.\end{aligned} \tag{4.1}$$

Let us substitute in Theorem 4.2 $v_0 = D^{\widehat{\sigma}+\frac{5}{2}}\Phi e_i$ and $\alpha = 1$. Then we obtain

$$C\left|D^{\widehat{\sigma}+\frac{5}{2}}\Phi e_i\right|_{L^2}^2 = \int_{-\infty}^{\infty}|D^{\frac{1}{2}}V(s)D^{\widehat{\sigma}+\frac{5}{2}}\Phi e_i|^2\,\mathrm{d}s = \int_{-\infty}^{\infty}|D^{3+\widehat{\sigma}}V(s)\Phi e_i|^2\,\mathrm{d}s \ge \int_0^t|D^{3+\widehat{\sigma}}V(t-s)\Phi e_i|^2\,\mathrm{d}s.$$

Since Theorem 4.2 holds for all $x\in\mathbb{R}$ and $\left|D^{\widehat{\sigma}+\frac{5}{2}}\Phi e_i\right|_{L^2} \le |\Phi e_i|_{H^{\widehat{\sigma}+\frac{5}{2}}}$, then

$$\sup_{x\in\mathbb{R}}\int_0^t|D^{3+\widehat{\sigma}}V(t-s)\Phi e_i|^2\,\mathrm{d}s \le C\,|\Phi e_i|^2_{H^{\widehat{\sigma}+\frac{5}{2}}}. \tag{4.2}$$

Insertion of (4.2) into (4.1), gives

$$\left|D^{3+\widetilde{\sigma}}W_V\right|^q_{L_x^\infty(L_\omega^q(L_t^2))} \le C\int_0^T\left(\sum_{i\in\mathbb{N}}|\Phi e_i|^2_{H^{\widetilde{\sigma}+\frac{5}{2}}}\right)^{\frac{q}{2}}\mathrm{d}t \le C(T)\,|\Phi|_2^{0,\widehat{\sigma}+\frac{5}{2}} \le C(T)|\Phi|^q_{L_2^{0,\widetilde{\sigma}+\frac{5}{2}}}.$$

Let us estimate $\left|D^{\widetilde{\sigma}}W_V\right|^2_{L_x^2(L_\omega^q(L_t^2))}$. Basing on proof of Proposition 3.3 in de Bouard and Debussche [12] we have that

$$\left|D^{\widetilde{\sigma}}W_V\right|^2_{L_x^2(L_\omega^q(L_t^2))} \le C|\Phi|^2_{L_2^{0,\widetilde{\sigma}}} \le C|\Phi|^q_{L_2^{0,\widetilde{\sigma}+\frac{5}{2}}}.$$

Now, set in Theorem 4.1 $A = L_\omega^q(L_t^2)$, $p=2$, $u = D^{\widetilde{\sigma}}W_V$ $\sigma = 3$ and $\alpha = 3-\varepsilon$ for some $3 > \varepsilon > 0$. Then $D^{3-\varepsilon}D^{\widetilde{\sigma}}W_V = D^{3+\widetilde{\sigma}-\varepsilon}W_V \in L_x^{p_\alpha}(L_\omega^q(L_t^2))$ and there exists a constant C, such that

$$\left|D^{3+\widetilde{\sigma}-\varepsilon}W_V\right|_{L_x^{p_\alpha}(L_\omega^q(L_t^2))} \le C\left|D^{\widetilde{\sigma}}W_V\right|^{1-\frac{3-\varepsilon}{3}}_{L^2(L_\omega^q(L_t^2))}\left|D^{3+\widetilde{\sigma}}W_V\right|^{\frac{3-\varepsilon}{3}}_{L_x^\infty(L_\omega^q(L_t^2))} = C\left|D^{\widetilde{\sigma}}W_V\right|^{\frac{\varepsilon}{3}}_{L^2(L_\omega^q(L_t^2))}\left|D^{3+\widetilde{\sigma}}W_V\right|^{1-\frac{\varepsilon}{3}}_{L_x^\infty(L_\omega^q(L_t^2))},$$

where

$$p_\alpha = \left(\frac{1}{2}\left(1-\frac{3-\varepsilon}{3}\right)\right)^{-1} = \left(\frac{\frac{\varepsilon}{3}}{2}\right)^{-1} = \frac{6}{\varepsilon} = q.$$

Then we have

$$\left|D^{3+\widetilde{\sigma}-\varepsilon}W_V\right|_{L_x^q(L_\omega^q(L_t^2))} \le C\left|D^{\widetilde{\sigma}}W_V\right|^{\frac{2}{q}}_{L^2(L_\omega^q(L_t^2))}\left|D^{3+\widetilde{\sigma}}W_V\right|^{1-\frac{2}{q}}_{L_x^\infty(L_\omega^q(L_t^2))} \le C\,|\Phi|_{L_2^{0,\widetilde{\sigma}+\frac{5}{2}}}. \tag{4.3}$$

Moreover, basing on the proof of Proposition 3.3 in de Bouard and Debussche [12],

$$|W_V|_{L_\omega^q(L_x^q(L_t^2))} \le C\,|\Phi|_{L_2^{0,\widetilde{\sigma}}} \le C\,|\Phi|_{L_2^{0,\widetilde{\sigma}+\frac{5}{2}}}. \tag{4.4}$$

Since $\left|D^{3+\widetilde{\sigma}-\varepsilon}W_V\right|_{L_\omega^q(L_x^q(L_t^2))} = \left|D^{3+\widetilde{\sigma}-\varepsilon}W_V\right|_{L_x^q(L_\omega^q(L_t^2))}$, then from (4.3) oraz (4.4) we obtain

$$|W_V|_{L_\omega^q(W_x^{3+\widetilde{\sigma}-\varepsilon,q}(L_t^2))} \le C\,|\Phi|_{L_2^{0,\widetilde{\sigma}+\frac{5}{2}}}.$$

Because $q\varepsilon > 1$, then $W_x^{\varepsilon,q}(L_t^2) \subset L_x^\infty(L_t^2)$, therefore $D^{3+\widetilde{\sigma}-\varepsilon}W_V \in L_\omega^q(L_x^\infty(T_t^2))$. Moreover

$$\left|D^{3+\widetilde{\sigma}-\varepsilon}W_V\right|_{L_\omega^q(L_x^\infty(L_t^2))} \le C\,|\Phi|_{L_2^{0,\widetilde{\sigma}+\frac{5}{2}}}.$$

Finally

$$D^{\widetilde{\sigma}-\varepsilon}\partial_x\left(\frac{\partial^2}{\partial x^2}W_V\right) = D^{\widetilde{\sigma}-\varepsilon}\partial_{3x}W_V = \int_0^t D^{\widetilde{\sigma}-\varepsilon}\partial_{3x}V(t-s)\Phi\,\mathrm{d}W(s) = \int_0^t D^{3+\widetilde{\sigma}-\varepsilon}V(t-s)\mathscr{H}\Phi\,\mathrm{d}W(s),$$

where $\mathscr{H}$ is the Hilbert transform, what finishes the proof. □

Lemma 4.5.

$$\partial_x\left(\frac{\partial^2}{\partial x^2}W_V\right)\in L^2\left(\Omega;L_t^4\left(L_x^\infty\right)\right).$$

Proof. Let $\varepsilon=\widetilde{\sigma}-\frac{3}{4}$ and $q=4+\frac{12}{\varepsilon}$. Estimate $\left|D^{3+\varepsilon}W_V\right|_{L_t^4(L_x^\infty(L_\omega^q))}$.
We have

$$\left|D^{3+\varepsilon}W_V\right|^4_{L_t^4(L_x^\infty(L_\omega^q))}=\int_0^T\sup_{x\in\mathbb{R}}\mathbb{E}\left(\left|\int_0^t D^{\widetilde{\sigma}+\frac{9}{4}}V(t-s)\Phi\,\mathrm{d}W(s)\right|^q\right)^{\frac{4}{q}}\mathrm{d}t\le C\int_0^T\sup_{x\in\mathbb{R}}\left(\sum_{i\in\mathbb{N}}\int_0^t\left|D^{\widetilde{\sigma}+\frac{9}{4}}V(t-s)\Phi e_i\right|^2\mathrm{d}s\right)^2\mathrm{d}t$$
$$\le C(T)\left(\sum_{i\in\mathbb{N}}\left(\int_0^T\sup_{x\in\mathbb{R}}\left|D^{\widetilde{\sigma}+\frac{9}{4}}V(t-s)\Phi e_i\right|^4\mathrm{d}s\right)^{\frac{1}{2}}\right)^2.$$

Substitute in Theorem 4.3 $\alpha=2$, $\theta=1$, $\beta=\frac{1}{2}$ (like in de Bouard and Debussche [12]). The result is $\int_0^T\sup_{x\in\mathbb{R}}\left|D^{\widetilde{\sigma}+\frac{9}{4}}V(t)\Phi e_i\right|^4\mathrm{d}t\le C\left|D^{\widetilde{\sigma}+2}\Phi e_i\right|^4_{L_x^2}\le C\left|\Phi\right|_{L_2^{0,\widetilde{\sigma}+2}}$, where $L_2^{0,\widetilde{\sigma}+2}=L_2^0(L^2(\mathbb{R});H^{\widetilde{\sigma}+2}(\mathbb{R}))$. This implies $\left|D^{3+\varepsilon}W_V\right|^4_{L_t^4(L_x^\infty(L_\omega^q))}\le C\left|\Phi\right|_{L_2^{0,\widetilde{\sigma}+2}}$, Moreover from the proof of Proposition 3.4 in de Bouard and Debussche [12] we know that $\left|W_V\right|_{L_t^4(L_x^2(L_\omega^q))}\le C\left|\Phi\right|_{L_2^{0,0}}\le C\left|\Phi\right|_{L_2^{0,\widetilde{\sigma}}}\le C\left|\Phi\right|_{L_2^{0,\widetilde{\sigma}+2}}$.

Now substitute in Theorem 4.1 $\sigma=3+\varepsilon$, $A=L_\omega^q=L_q(\Omega)$, $p=2$, $u=W_V$, $\alpha=3+\frac{\varepsilon}{2}$. Then $p\alpha=\left(\frac{1}{2}\left(1-\frac{3+\frac{\varepsilon}{2}}{3+\varepsilon}\right)\right)^{-1}=4+\frac{12}{\varepsilon}=q$ and

$$\left|D^{3+\frac{\varepsilon}{2}}W_V\right|_{L_x^{p\alpha}(L_\omega^q)}\le C\left|W_V\right|^{1-\frac{3+\frac{\varepsilon}{2}}{3+\varepsilon}}_{L_x^{p\alpha}(L_\omega^q)}\left|D^{3+\varepsilon}W_V\right|^{\frac{3+\frac{\varepsilon}{2}}{3+\varepsilon}}_{L_x^\infty(L_\omega^q)}=C\left|W_V\right|^{\frac{\frac{\varepsilon}{2}}{3+\varepsilon}}_{L_x^{p\alpha}(L_\omega^q)}\left|D^{3+\varepsilon}W_V\right|^{\frac{3+\frac{\varepsilon}{2}}{3+\varepsilon}}_{L_x^\infty(L_\omega^q)}=C\left|W_V\right|^{\frac{2}{q}}_{L_x^q(L_\omega^q)}\left|D^{3+\varepsilon}W_V\right|^{1-\frac{2}{q}}_{L_x^\infty(L_\omega^q)}.$$

Since $q=4+\frac{12}{\varepsilon}\ge 4$, then

$$\left|D^{3+\frac{\varepsilon}{2}}W_V\right|_{L_\omega^4(L_t^4(L_x^q))}\le\left|D^{3+\frac{\varepsilon}{2}}W_V\right|_{L_t^4(L_x^q(L_\omega^q))}\le C\left|W_V\right|^{\frac{2}{q}}_{L_x^q(L_\omega^q)}\left|D^{3+\varepsilon}W_V\right|^{1-\frac{2}{q}}_{L_x^\infty(L_\omega^q)}\le C\left|\Phi\right|_{L_2^{0,\widetilde{\sigma}}}\le C\left|\Phi\right|_{L_2^{0,\widetilde{\sigma}+2}}.$$

The proof of Proposition 3.4 in de Bouard and Debussche [12] implies that $\left|W_V\right|\le C(T)\left|\Phi\right|_{L_2^{0,\widetilde{\sigma}}}\le C(T)\left|\Phi\right|_{L_2^{0,\widetilde{\sigma}+2}}$, therefore $\left|W_V\right|_{L_\omega^4\left(L_t^4\left(W_x^{3+\frac{\varepsilon}{2},q}\right)\right)}\le C\left|\Phi\right|_{L_2^{0,\widetilde{\sigma}+2}}$ and, since $q\varepsilon/2>1$, $\left|\partial_{3x}W_V\right|_{L_\omega^4(L_t^4(L_x^\infty))}\le C\left|W_V\right|_{L_\omega^4\left(L_t^4\left(W_x^{3+\frac{\varepsilon}{2},q}\right)\right)}\le C\left|\Phi\right|_{L_2^{0,\widetilde{\sigma}+2}}$. □

References

[1] D.J. Korteweg, H. de Vries, *On the change of form of long waves advancing in a rectangular canal, and on a new type of long stationary waves*, Philosophical Magazine, **39** (1895), 422-443.
[2] P.G. Drazin, R.S. Johnson, . *Solitons: An introduction*, Cambridge University Press, 1989.
[3] E. Infeld, G. Rowlands, *Nonlinear Waves, Solitons and Chaos*, 2nd ed., Cambridge University Press, 2000.
[4] A. Jeffrey, *Role of the Korteweg-de Vries equation in plasma physics*, Q. Jl R. Astr. Soc., **14** (1973), 183-189.
[5] M. Remoissenet, *Waves called solitons*, Springer, 1994.
[6] T.R. Marchant, N.F. Smyth, *The extended Korteweg-de Vries equation and the resonant flow of a fluid over topography*. J. Fluid Mech.,S **221** (1990), 263-288.
[7] E. Infeld, E., Karczewska, A., Rowlands, G. and Rozmej, P.: *Exact cnoidal solutions of the extended KdV equation*, Acta Phys. Pol. A, **133** (2018), 1191-1199. DOI: 10.12693/APhysPolA.133.1191
[8] P. Rozmej, A. Karczewska, *New Exact Superposition Solutions to KdV2 Equation*, Advances in Mathematical Physics, **2018** Article ID 5095482, 1-9. DOI: 10.1155/2018/5095482
[9] P. Rozmej, A. Karczewska, E. Infeld, *Superposition solutions to the extended KdV equation for water surface waves*, Nonlinear Dynamics **91** (2018), 1085-1093. DOI: 10.1007/s11071-017-3931-1
[10] F. Linares, G. Ponce, *Introduction to Nonlinear Dispersive Equations*. Universitext, Springer, 2009.
[11] T. Tao, *Nonlinear Dispersive Equations, Local and Global Analysis*, CBMS Regional Conference Series, 106, American Mathematical Society, 2006.
[12] A. de Bouard, A. Debussche, *On the stochastic Korteweg-de Vries equation*, J. Funct. Anal. **154** (1998), 215-251.
[13] C.E. Kenig, G. Ponce, L. Vega, *Well-posedness of the initial value problem for the Korteweg-de Vries equation*, J. Amer. Math. Soc., **4** (1991), 323-347.
[14] C.E. Kenig, G. Ponce, L. Vega, *Well-posedness for the generalized Korteweg-de Vries equation via contraction principle* Comm. Pure Appl. Math., **46** (1993), 527-620.
[15] A. Karczewska, P. Rozmej, E. Infeld, G. Rowlands, *Adiabatic invariants of the extended KdV equation*, Phys. Lett. A, **381** (2017), 270-275.
[16] Y. Kodama, *On integrable systems with higher order corrections*, Phys. Lett. A., **107** (1985), 245-249.
[17] H.R. Dullin, G.A. Gottwald, D.D. Holm, *An integrable shallow water equation with linear and nonlinear dispersion*, Phys. Rev. Lett. **87** (2001), 194501.
[18] R.A. Adams, *Sobolev Spaces*, Academic Press, 1975.
[19] R. Grimshaw, *Internal Solitary Waves*, Presented at the international conference "Progress in Nonlinear Science", held in Nizhni Novgorod in July 2001, and dedicated to the 100-th Anniversary of Alexander A. Andronov.
[20] G. Grimshaw, G. El, K. Khusnutdinova, *Nonlinear Waves, Lecture 12: Higher-order KdV equations* 2010.

Journal of Mathematical Sciences and Modelling, 2 (2) (2019) 82-98
Research Article

Journal of Mathematical Sciences and Modelling

Journal Homepage: www.dergipark.gov.tr/jmsm
ISSN 2636-8692
DOI: http://dx.doi.org/10.33187/jmsm.488921

Rayleigh-Quotient Representation of the Real Parts, Imaginary Parts, and Moduli of the Eigenvalues of Diagonalizable Matrices

Ludwig Kohaupt[1]

[1]*Department of Mathematics, Beuth University of Technology Berlin, Berlin, Germany*

Article Info

Keywords: *Asymptotic stability of dynamical systems, Circular damped eigenfrequencies, Moduli of eigenvalues, Rayleigh quotient, Real and imaginary parts of eigenvalues, Weighted norm.*
2010 AMS: *11E39, 15A18, 15B57, 15B99, 65F35, 65J05.*
Received: *28 November 2018*
Accepted: *17 January 2019*
Available online: *30 August 2019*

Abstract

In the present paper, formulas for the Rayleigh-quotient representation of the real parts, imaginary parts, and moduli of the eigenvalues of diagonalizable matrices are obtained that resemble corresponding formulas for the eigenvalues of self-adjoint matrices. These formulas are new and of interest in Linear Algebra and in the theory of linear dynamical systems. Since the style of paper is expository, it could also be of interest in graduate/undergraduate teaching or research at college level. The key point is that a weighted scalar product is used that is defined by means of a special positive definite matrix. As applications, one obtains convexity properties of newly-defined numerical ranges of a matrix. A numerical example underpins the theoretical findings.

1. Introduction

For self-adjoint matrices, there are formulas for the eigenvalues in the form of Rayleigh quotients; more precisely, max-, min-, minmax-, and maxmin-formulas are known; for this, see, e.g., the book [12, Section 5.4].
In the present paper, we obtain corresponding formulas for the real and imaginary parts as well as for the moduli of the eigenvalues of a diagonalizable matrix. First, these formulas are of interest on their own in Linear Algebra. Second, these are also of potential interest, for example, in the theory of linear dynamical systems. The reason for this is as follows. The real parts of the eigenvalues multiplied by the time are equal to the arguments of the exponential functions that describe the decay behavior of the solution (see, e.g., [4, Section 7.1, p.2011, Formulas (89), (90)]). Further, the system is asymptotically stable if the real parts of all eigenvalues are negative. Moreover, when the eigenvalues are pairwise conjugate-complex, then the moduli of the imaginary parts are the circular damped eigenfrequencies of the system (see, e.g., [4, Section 7.1, p. 2011, (89)]).
The paper is structured as follows.
In Section 2, preliminary materials are assembled on biorthogonality relations for the eigenvectors of a diagonalizable matrix A and the eigenvectors of A^* that will be useful in the sequel. Moreover, the construction of positive semi-definite matrices R_j and of the positive definite matrix $R = \sum_{j=1}^{n} R_j$ is reviewed where the last one is employed to define a weighted scalar product $(\cdot,\cdot)_R$ that plays a key role in deriving the new results. In Sections 3, 4, and 5, formulas for the Rayleigh-quotient representation of the real parts, imaginary parts, and moduli of the eigenvalues of a diagonalizable matrix are given, as the case may be. In Section 6, a connection between the matrices $R^{-1}\frac{A^*R+RA}{2}$,$R^{-1}\frac{RA-A^*R}{2i}$, and $R^{-1}A^*RA$ is established that play a key role in the study of the real parts, imaginary parts, and moduli of the eigenvalues of A, respectively. Section 7 describes the applications and Section 8 a numerical example. Finally, Section 9 contains the conclusions and an outlook on to future work. The non-cited references [1], [7], [8], [9], [10], and [11] are given because they may be useful to the reader in the context of the present paper.

2. Preliminaries

As a preparation to Theorem 2.1, we formulate the following conditions $(C1)$ - $(C4)$:

Email addresses and ORCID numbers: kohaupt@bht-berlin.de, 0000-0003-1781-0600 (L. Kohaupt)

(C1) $A \in \mathbb{C}^{n\times n}$
(C2) A is diagonalizable, and $\lambda_i, i = 1,\cdots,n$ are the eigenvalues of A as well as $p_i, i = 1,\cdots,n$ the associated eigenvectors
(C3) $u_i^*, i = 1,\cdots,n$ are the eigenvectors of A^* corresponding to the eigenvalues $\overline{\lambda_i}, i = 1,\cdots,n$ of A^*
(C4) $\lambda_i \neq \lambda_j, i \neq j, i, j = 1,\cdots,n$

Based on Theorem 2.1, in Theorem 2.2 the positive semi-definite matrices R_j and the positive definite matrix $R = \sum_{j=1}^{n} R_j$ are constructed; they play a key role in the subsequent sections.
We mention that, even though condition $(C4)$ may be omitted, it is nevertheless useful here since it will turn out to be fulfilled in the numerical example in Section 8 and since the biorthogonal system in Theorem 2.1 can be constructed more easily than without this condition. As a consequence, also the matrices R_j and R can be computed more easily than without condition $(C4)$.
The material in this section is known, i.e. this is a review section. Therefore, the compiled results are given without proofs. But, it is indicated where the proofs can be found. Now, two theorems follow.

Theorem 2.1. *(Biorthogonality relations with $\lambda_i \neq \lambda_j, i \neq j, i, j = 1,\cdots,n$)*
Let the conditions $(C1)$ - $(C4)$ be fulfilled. Then, after appropriate normalization of the eigenvectors $p_i, i = 1,\cdots,n$ and $u_i^*, i = 1,\cdots,n$, one has the biorthogonality relations

$$(p_i, u_j^*) = \delta_{ij},\ i, j = 1,\cdots,n, \tag{2.1}$$

where $(\cdot,\cdot)$ is the usual scalar product on $\mathbb{C}^n$.

Proof. See [2, Theorem 1]. □

Theorem 2.2. *(Construction of positive definite matrix R)*
Let the conditions $(C1)$ - $(C4)$ be fulfilled. Let $\alpha_j = \lambda_j(A)$ be the eigenvalues and u_j be the associated left eigenvectors of A for $j = 1,\cdots,n$; further, let $A^* \in \mathbb{C}^{n\times n}$ be the adjoint matrix of A so that u_j^* are the right eigenvectors of A^* corresponding to the eigenvalues $\overline{\alpha_j}$ of A^* for $j = 1,\cdots,n$, i.e.,

$$u_j A = \alpha_j u_j,\ j = 1,\cdots,n$$

and

$$A^* u_j^* = \overline{\alpha_j} u_j^*,\ j = 1,\cdots,n.$$

Let

$$\rho_j = \overline{\alpha_j} + \alpha_j = 2\,Re\,\alpha_j = 2\,Re\,\overline{\alpha_j},\ j = 1,\cdots,n, \tag{2.2}$$

$$\sigma_j = \alpha_j - \overline{\alpha_j} = 2\,i\,Im\,\alpha_j,\ j = 1,\cdots,n,$$

and

$$R_j = u_j^* u_j,\ j = 1,\cdots,n. \tag{2.3}$$

Then,

$$A^* R_j + R_j A = \rho_j R_j,\ j = 1,\cdots,n, \tag{2.4}$$

$$R_j A - A^* R_j = \sigma_j R_j,\ j = 1,\cdots,n. \tag{2.5}$$

In other words: The matrix eigenvalue problem

$$A^* V + V A = \mu V$$

has the n solution pairs

$$(\mu, V) = (\rho_j, R_j)$$

with real ρ_j, and the matrix eigenvalue problem

$$V A - A^* V = \mu V$$

has the n solution pairs

$$(\mu, V) = (\sigma_j, R_j)$$

with purely imaginary σ_j.
The matrices $R_j \in \mathbb{C}^{n\times n}$ are positive semi-definite for $j = 1,\cdots,n$. Further,

$$R := \sum_{j=1}^{n} R_j \tag{2.6}$$

is positive definite.

Proof. The assertions on (2.4) and on R_j and R follow from [5, Theorems 4 - 6]. The proof of (2.5) is derived in a similar way as for (2.4). □

Remark 2.3. *Since R in (2.6) is positive definite, by*

$$(u,v)_R := (Ru,v),\ u,\ v \in \mathbf{C}^n,$$

a weighted scalar product $(\cdot,\cdot)_R$ *is defined and by*

$$\|u\|_R := (Ru,u)^{\frac{1}{2}},\ u \in \mathbf{C}^n,$$

a weighted norm $\|\cdot\|_R$.

Remark 2.4. *For definiteness, one can assume condition $(C4)$ for Theorem 2.2. But, as [3, Theorem 4] shows, Theorem 2.2 is valid without this condition.*

3. Formulas for the representation of the real parts of the eigenvalues of a diagonalizable matrix

In this section, we want to derive formulas for the representation of the real parts of the eigenvalues of a diagonalizable matrix A by Rayleigh quotients. More precisely, max-, min-, minmax-, and maxmin-representations are obtained corresponding to associated formulas for the eigenvalues of self-adjoint matrices, assembled, for instance, in the book [12, Section 5.4].
First, we want to derive a relation corresponding to that of [12, Section 5.4(18)]. This is done in the following Formula (3.2).

Lemma 3.1. Let the conditions $(C1)$ - $(C4)$ be fulfilled. Then, with the denotations of Theorem 2.2,

$$(Au,u)_R = \sum_{j=1}^{n} \lambda_j(A)\,(u,u)_{R_j},\ u \in \mathbf{C}^n \tag{3.1}$$

leading to

$$Re\,(Au,u)_R = \sum_{j=1}^{n} Re\,\lambda_j(A)\,(u,u)_{R_j},\ u \in \mathbf{C}^n. \tag{3.2}$$

If matrix A is, beyond this, asymptotically stable, i.e., if

$$Re\,\lambda_j(A) < 0,\ j = 1,\cdots,n, \tag{3.3}$$

then

$$Re\,(Au,u)_R = -\sum_{j=1}^{n} |Re\,\lambda_j(A)|\,(u,u)_{R_j},\ u \in \mathbf{C}^n, \tag{3.4}$$

so that, in this case,

$$Re\,(Au,u)_R < 0,\ 0 \neq u \in \mathbf{C}^n \tag{3.5}$$

and

$$|Re\,(Au,u)_R| = \sum_{j=1}^{n} |Re\,\lambda_j(A)|\,(u,u)_{R_j},\ u \in \mathbf{C}^n. \tag{3.6}$$

Proof. Let $u \in \mathbf{C}^n$. Then from Theorem 2.1,

$$u = \sum_{j=1}^{n} (u,u_j^*)p_j \tag{3.7}$$

implying

$$\begin{aligned}
(Au,u)_R &= (RAu,u) = (Au,Ru) \\
&= \sum_{j,k=1}^{n} (u,u_j^*)\overline{(u,u_k^*)}(Ap_j,Rp_k) \\
&= \sum_{j,k=1}^{n} (u,u_j^*)\overline{(u,u_k^*)}\lambda_j(p_j,Rp_k) \\
&= \sum_{j,k=1}^{n} (u,u_j^*)\overline{(u,u_k^*)}\lambda_j(p_j,u_k^*) \\
&= \sum_{j=1}^{n} \lambda_j|(u,u_j^*)|^2 \\
&= \sum_{j=1}^{n} \lambda_j(u,u)_{R_j}
\end{aligned} \tag{3.8}$$

since

$$(u,u)_{R_j} = (R_j u,u) = (u_j^* u_j u,u) = (u_j u,u_j u) = |u_j u|^2 = |(u,u_j^*)|^2. \tag{3.9}$$

So, (3.1) is proven. The rest is clear. □

Next, we have

Lemma 3.2. Let the conditions $(C1)$ - $(C4)$ be fulfilled. Further, let matrix A be asymptotically stable. Then, A^*R+RA is negative definite.

Proof. From (2.4) and (2.2), we obtain

$$\begin{aligned}(-[A^*R+RA]u,u) &= \sum_{j=1}^{n}(-\rho_j)\,(u,u)_{R_j} = 2\sum_{j=1}^{n} Re\,(-\lambda_j(A))\,(u,u)_{R_j}\\ &= 2\sum_{j=1}^{n}|Re\,\lambda_j(A)|\,(u,u)_{R_j}\\ &\geq 2\min_{j=1,\cdots,n}|Re\,\lambda_j(A)|\sum_{j=1}^{n}(u,u)_{R_j}\\ &= c_0(Ru,u) > 0,\ 0\neq u\in \mathbb{C}^n\end{aligned} \tag{3.10}$$

with $c_0 = 2\min\limits_{j=1,\cdots,n}|Re\,\lambda_j(A)| > 0$. □

Next, we want to define vector spaces similar to those in [12, Section 5.4,(23)].
Comparing the formulas in [12, Section 5.4,(17)] and (3.2), one is led to define here the following vector spaces.

$$M_1 := \mathbb{C}^n,\ M_k := \{u\in\mathbb{C}^n\,|\,(u,u)_{R_i} = 0,\ i = 1,2,\cdots,k-1\},\ k = 2,\cdots,n. \tag{3.11}$$

The next lemma characterizes these spaces.

Lemma 3.3. Let the conditions $(C1)$ - $(C4)$ be fulfilled as well as $\{p_1,\cdots,p_n\}$ and $\{u_1^*,\cdots,u_n^*\}$ be a biorthogonal set of eigenvectors of A and A^*, i.e., such that

$$(p_j,u_k^*) = \delta_{jk},\ j,k = 1,\cdots,n.$$

Then,

$$M_k = [p_k,p_{k+1},\cdots,p_n],\ k = 1,\cdots,n. \tag{3.12}$$

Proof. The proof is done for $k = 3$. The general case can be made by induction. So, we have to prove

$$M_3 = \{u\in\mathbb{C}^n\,|\,(u,u)_{R_1} = 0,\,(u,u)_{R_2} = 0\} = [p_3,p_4,\cdots,p_n]. \tag{3.13}$$

(i) $\underline{[p_3,p_4,\cdots,p_n]\subset M_3}$:
Let $u\in[p_3,p_4,\cdots,p_n]$. Then, $u = \sum_{j=3}^{n}\beta_j p_j$ with elements $\beta_j\in\mathbb{C}$, $j = 3,\cdots,n$. Let $s\in\{1,2\}$. This entails, due to Theorem 2.1,

$$\begin{aligned}(u,u)_{R_s} &= \sum_{j,k=3}^{n}\beta_j\overline{\beta_k}(p_j,p_k)_{R_s} = \sum_{j,k=3}^{n}\beta_j\overline{\beta_k}(u_s^*u_s p_j,p_k)\\ &= \sum_{j,k=3}^{n}\beta_j\overline{\beta_k}(u_s^*(u_s p_j),p_k) = \sum_{j,k=3}^{n}\beta_j\overline{\beta_k}(u_s^*(p_j,u_s^*),p_k)\\ &= \sum_{j,k=3}^{n}\beta_j\overline{\beta_k}\delta_{sj}(u_s^*,p_k) = \sum_{j,k=3}^{n}\beta_j\overline{\beta_k}\delta_{sj}\delta_{sk} = 0.\end{aligned}$$

Therefore, $(u,u)_{R_s} = 0$, $s = 1,2$ and thus $u\in M_3$ so that $[p_3,p_4,\cdots,p_n]\subset M_3$ is proven.
(ii) $\underline{M_3\subset[p_3,p_4,\cdots,p_n]}$:
Let $u\in M_3$. This implies $(u,u)_{R_s} = 0$, $s = 1,2$ or $(R_s u,u) = (u_s^*u_s u,u) = (u_s^*(u,u_s^*),u) = (u,u_s^*)(u_s^*,u) = (u,u_s^*)\overline{(u,u_s^*)} = |(u,u_s^*)|^2 = 0$, $s = 1,2$, that is,

$$(u,u_s^*) = 0,\ s = 1,2.$$

Thus,

$$u\in[u_1^*,u_2^*]^{\perp}. \tag{3.14}$$

Now,

$$[u_1^*,u_2^*]\oplus[u_1^*,u_2^*]^{\perp} = \mathbb{C}^n.$$

Since also

$$[u_1^*,u_2^*]\oplus[u_3^*,u_4^*,\cdots,u_n^*] = \mathbb{C}^n,$$

we deduce

$$[u_1^*, u_2^*]^\perp = [u_3^*, u_4^*, \cdots, u_n^*]. \tag{3.15}$$

So, according to (3.14) and (3.15),

$$u \in [u_3^*, u_4^*, \cdots, u_n^*].$$

Thus, there exist elements $\gamma_3, \cdots, \gamma_n \in \boldsymbol{C}$ such that

$$u = \sum_{j=3}^{n} \gamma_j u_j^* \in [p_1, p_2]^\perp = [p_3, p_4, \cdots, p_n].$$

This completes the proof of the assertion. □

Similarly to [12, Section 5.4,(22)], we suppose that the eigenvalues $\lambda_1(A), \cdots, \lambda_n(A)$ of matrix A are arranged such that

$$Re\,\lambda_1(A) \geq Re\,\lambda_2(A) \geq \cdots \geq Re\,\lambda_n(A). \tag{3.16}$$

If A is asymptotically stable, (3.16) is replaced by

$$|Re\,\lambda_1(A)| \geq |Re\,\lambda_2(A)| \geq \cdots \geq |Re\,\lambda_n(A)|. \tag{3.17}$$

One has

Theorem 3.4. Let the conditions $(C1)$ - $(C4)$ be fulfilled. Further, let the eigenvalues of A be arranged according to (3.16). Moreover, let the vector spaces M_k, $k = 1, \cdots, n$ be defined by (3.11) or (3.12).
Then,

$$Re\,\lambda_k(A) = \max_{0 \neq u \in M_k} \frac{Re(Au,u)_R}{(u,u)_R},\ k = 1, 2, \cdots, n. \tag{3.18}$$

If matrix A is, beyond this, asymptotically stable, i.e., if (3.2) is valid and if the eigenvalues are arranged according to (3.17), then also

$$|Re\,\lambda_k(A)| = \max_{0 \neq u \in M_k} \frac{|Re(Au,u)_R|}{(u,u)_R},\ k = 1, 2, \cdots, n. \tag{3.19}$$

The maximum is attained for $u = p_k$.

Proof. There are two methods to derive this theorem.
Method 1: One uses equation (3.2) as starting point, i.e.,

$$Re(Au,u)_R = \sum_{j=1}^{n} Re\,\lambda_j(A)(R_j u, u),\ u \in \boldsymbol{C}^n.$$

Choosing $k \in \{1, \cdots, n\}$ fixed and $u \in M_k$, using (3.11), one obtains

$$\begin{aligned} Re(Au,u)_R &= \sum_{j=k}^{n} Re\,\lambda_j(A)(R_j u, u) \leq \max_{j=k,\cdots,n} Re\,\lambda_j(A) \sum_{j=k}^{n} (R_j u, u) \\ &= Re\,\lambda_k(A) \sum_{j=1}^{n} (R_j u, u) = Re\,\lambda_k(A)\,(u,u)_R, \end{aligned}$$

that is,

$$\frac{Re(Au,u)_R}{(u,u)_R} \leq Re\,\lambda_k(A),\ 0 \neq u \in M_k$$

and thus

$$\max_{0 \neq u \in M_k} \frac{Re(Au,u)_R}{(u,u)_R} \leq Re\,\lambda_k(A). \tag{3.20}$$

Now, the maximum is attained for $u = p_k \in M_k$, that is,

$$Re\,\lambda_k(A) = \frac{Re(Ap_k, p_k)_R}{(p_k, p_k)_R} \leq \max_{0 \neq u \in M_k} \frac{Re(Au,u)_R}{(u,u)_R} \leq Re\,\lambda_k(A)$$

so that the assertion (3.18) is proven.
Relation (3.19) is proven in the same way as (3.18), but based on (3.6) instead of (3.2) and (3.17) instead of (3.16).
Method 2: Let $\lambda_j(R^{-1}\frac{A^*R+RA}{2})$ be the eigenvalues of $R^{-1}\frac{A^*R+RA}{2}$ and $v_j = v_j(R^{-1}\frac{A^*R+RA}{2})$ be the corresponding eigenvectors for $j = 1, 2, \cdots, n$. Define

$$M_1^{(R)} := \boldsymbol{C}^n,\ M_k^{(R)} := \{u \in \boldsymbol{C}^n \,|\, (u, v_j)_R = 0,\ j = 1, \cdots, k-1\},\ k = 2, \cdots, n.$$

From [12, Section 5.4(24)], it follows that

$$\lambda_k(R^{-1}\frac{A^*R+RA}{2}) = \max_{0\neq u\in M_k^{(R)}} \frac{(R^{-1}\frac{A^*R+RA}{2}u,u)_R}{(u,u)_R}$$

as $R^{-1}\frac{A^*R+RA}{2}$ is self-adjoint in the scalar product $(\cdot,\cdot)_R$. Since from [6, Theorem 6, (25)]

$$\lambda_k(R^{-1}\frac{A^*R+RA}{2}) = Re\lambda_k(A)$$

and further

$$(R^{-1}\frac{A^*R+RA}{2}u,u)_R = Re\,(Au,u)_R,\ u\in C^n,$$

we obtain

$$Re\,\lambda_k(A) = \max_{0\neq u\in M_k^{(R)}} \frac{Re\,(Au,u)_R}{(u,u)_R}.$$

Now, also due to [6, Theorem 6, (26)],

$$v_j = v_j(R^{-1}\frac{A^*R+RA}{2}) = p_j = p_j(A),\ j=1,2,\cdots,n.$$

Therefore,

$$\begin{aligned}(u,v_j)_R &= \Sigma_{l=1}^n(u,R_lv_j) = \Sigma_{l=1}^n(u,u_l^*u_lp_j)\\ &= \Sigma_{l=1}^n(u,u_l^*(p_j,u_l^*)) = \Sigma_{l=1}^n(u,u_l^*\delta_{jl})\\ &= (u,u_j^*),\ j=1,2,\cdots,k-1\end{aligned}$$

so that

$$\begin{aligned}M_k^{(R)} &= \{u\in C^n\,|\,(u,v_j)_R=0,\ j=1,\cdots,k-1\}\\ &= \{u\in C^n\,|\,(u,u_j^*)=0,\ j=1,\cdots,k-1\}\\ &= [p_k,p_{k+1},\cdots,p_n] = M_k,\ k=1,2,\cdots,n.\end{aligned}$$

Thus, Formula (3.18) is proven.
Summarizing, in the first method, one follows a similar way as in the case of self-adjoint matrices A, and in the second method, one reduces the case of diagonalizable matrices to the case of self-adjoint matrices by using a self-adjoint matrix that has the eigenvalues $Re\lambda_k(A)$. □

From the two proofs of Theorem 3.4, it is clear that one can carry over many results from the self-adjoint case to the case of diagonalizable matrices. In the sequel, we shall do so essentially without giving proofs.
So, we have the following further Rayleigh-quotient representations corresponding to [12, Subsection 5.4, (25)] in the case of self-adjoint matrices.
One has the following theorem.

Theorem 3.5. Let the conditions $(C1)$ - $(C4)$ be fulfilled. Further, let the eigenvalues of A be arranged according to (3.16). Then, for every $j=1,\cdots,n$ and every subspace $M\subset C^n$ with $dimM = m = n+1-j$, the following inequalities are valid:

$$Re\,\lambda_j(A) \leq \max_{0\neq u\in M}\frac{Re(Au,u)_R}{(u,u)_R} \leq Re\,\lambda_1(A), \tag{3.21}$$

and the following representation formulas hold:

$$Re\,\lambda_j(A) = \min_{dimM=m}\max_{0\neq u\in M}\frac{Re(Au,u)_R}{(u,u)_R}. \tag{3.22}$$

If matrix A is, beyond this, asymptotically stable and the eigenvalues are arranged according to (3.17), then also

$$|Re\,\lambda_j(A)| = \min_{dimM=m}\max_{0\neq u\in M}\frac{|Re(Au,u)_R|}{(u,u)_R}. \tag{3.23}$$

Remark 3.6. *From (3.21), it follows*

$$\frac{Re\,(Au,u)_R}{(u,u)_R} \leq \nu[A] = \max_{j=1,\cdots,n} Re\,\lambda_j(A),\ 0\neq u\in C^n.$$

For the following theorem, we need the vector spaces N_k defined by

$$N_k := [p_1,p_2,\cdots,p_k],\ k=1,2,\cdots,n. \tag{3.24}$$

Then, we have a result similar to that of Theorem 3.4.

Theorem 3.7. Let the conditions $(C1)$ - $(C4)$ be fulfilled. Further, let the eigenvalues of A be arranged according to (3.16). Moreover, let the vector spaces N_k, $k = 1, \cdots, n$ be defined by (3.24).
Then,

$$Re\,\lambda_k(A) = \min_{0 \neq u \in N_k} \frac{Re(Au,u)_R}{(u,u)_R},\ k = 1,2,\cdots,n. \tag{3.25}$$

If matrix A is, beyond this, asymptotically stable, i.e., if (3.3) is valid and if the eigenvalues are arranged according to (3.17), then also

$$|Re\,\lambda_k(A)| = \min_{0 \neq u \in N_k} \frac{|Re(Au,u)_R|}{(u,u)_R},\ k = 1,2,\cdots,n. \tag{3.26}$$

The minimum is attained for $u = p_k$.

Next, we want to state a maxmin characterization for the real parts of eigenvalues similar to results for the eigenvalues in [12, Subsection 5.4, (26)].
One has the following theorem.

Theorem 3.8. Let the conditions $(C1)$ - $(C4)$ be fulfilled. Further, let the eigenvalues of A be arranged according to (3.16).
Then, for every $j = 1, \cdots, n$ and every subspace $N \subset \mathbf{C}^n$ with $dim N = j$, the following inequalities are valid:

$$Re\,\lambda_n(A) \leq \min_{0 \neq u \in N} \frac{Re(Au,u)_R}{(u,u)_R} \leq Re\,\lambda_j(A), \tag{3.27}$$

and the following representation formulas hold:

$$Re\,\lambda_j(A) = \max_{dim N = j} \min_{0 \neq u \in N} \frac{Re(Au,u)_R}{(u,u)_R}. \tag{3.28}$$

If matrix A is, beyond this, asymptotically stable and the eigenvalues are arranged according to (3.17), then also

$$|Re\,\lambda_j(A)| = \max_{dim N = j} \min_{0 \neq u \in N} \frac{|Re(Au,u)_R|}{(u,u)_R}. \tag{3.29}$$

Remark 3.9. *From (3.27), it follows*

$$\frac{Re\,(Au,u)_R}{(u,u)_R} \geq -\nu[-A] = \min_{j=1,\cdots,n} Re\,\lambda_j(A),\ 0 \neq u \in \mathbf{C}^n.$$

4. Formulas for the representation of the imaginary parts of the eigenvalues of a diagonalizable matrix

In this section, we want to state formulas for the representation of the imaginary parts of the eigenvalues of a diagonalizable matrix A by Rayleigh quotients. More precisely, max-, min-, minmax-, and maxmin-representations are obtained corresponding to associated formulas for the eigenvalues of self-adjoint matrices, assembled, for instance, in the textbook [12, Section 5.4] resp. corresponding to those for the real parts of diagonalizable matrices in Section 3.
First, we want to state a relation corresponding to that of [12, Section 5.4(18)]. This is done in the following Formula (4.1).

Lemma 4.1. Let the conditions $(C1)$ - $(C4)$ be fulfilled. Then, with the denotations of Theorem 2.1,

$$Im\,(Au,u)_R = \sum_{j=1}^{n} Im\,\lambda_j(A)\,(u,u)_{R_j},\ u \in \mathbf{C}^n. \tag{4.1}$$

Proof. Equation (4.1) follows directly from Lemma 3.1, Formula (3.1). □

Similarly to [12, Section 5.4,(22)] or (3.16), we suppose that the eigenvalues $\lambda_1(A), \cdots, \lambda_n(A)$ of matrix A are arranged such that

$$Im\,\lambda_1(A) \geq Im\,\lambda_2(A) \geq \cdots \geq Im\,\lambda_n(A). \tag{4.2}$$

Then, one has a series of theorems for the imaginary parts of the eigenvalues corresponding to those of Theorems 3.4 - 3.8.

Theorem 4.2. Let the conditions $(C1)$ - $(C4)$ be fulfilled. Further, let the eigenvalues of A be arranged according to to (4.2). Moreover, let the vector spaces M_k, $k = 1, \cdots, n$ be defined by (3.11) or (3.12).
Then,

$$Im\,\lambda_k(A) = \max_{0 \neq u \in M_k} \frac{Im(Au,u)_R}{(u,u)_R},\ k = 1,2,\cdots,n. \tag{4.3}$$

The maximum is attained for $u = p_k$.

Proof. As for Theorem 3.4, there are two methods to derive this theorem.
Method 1: One uses equation (4.1) as starting point and proceeds as in Method 1 for the proof of Theorem 3.4.
Method 2: Let $\lambda_j(R^{-1}\frac{RA-A^*R}{2i})$ be the eigenvalues of $R^{-1}\frac{RA-A^*R}{2i}$ and $v_j = v_j(R^{-1}\frac{RA-A^*R}{2i})$ be the corresponding eigenvectors for $j = 1, \cdots, n$.
Then, with [6, Theorem 6], the assertion follows in a similar way as in Method 2 for the proof of Theorem 3.4. □

Next, we state a minmax characterization for the imaginary parts of eigenvalues similar to results for the eigenvalues in [12, Section 5.4, (25)] or for the real parts of the eigenvalues in Theorem 3.5.
One has the following theorem.

Theorem 4.3. Let the conditions $(C1)$ - $(C4)$ be fulfilled. Further, let the eigenvalues of A be arranged according to (4.2).
Then, for every $j = 1, \cdots, n$ and every subspace $M \subset \boldsymbol{C}^n$ with $dim M = m = n+1-j$, the following inequalities are valid:

$$Im\,\lambda_j(A) \leq \max_{0 \neq u \in M} \frac{Im(Au,u)_R}{(u,u)_R} \leq Im\,\lambda_1(A), \tag{4.4}$$

and the following representation formulas hold:

$$Im\,\lambda_j(A) = \min_{dim M = m} \max_{0 \neq u \in M} \frac{Im(Au,u)_R}{(u,u)_R}. \tag{4.5}$$

Remark 4.4. *From (4.4), it follows*

$$\frac{Im\,(Au,u)_R}{(u,u)_R} \leq \max_{j=1,\cdots,n} Im\,\lambda_j(A),\ 0 \neq u \in \boldsymbol{C}^n.$$

Next, we have a result similar to that of Theorem 4.2.

Theorem 4.5. Let the conditions $(C1)$ - $(C4)$ be fulfilled. Further, let the eigenvalues of A be arranged according to (4.2). Moreover, let the vector spaces N_k, $k = 1, \cdots, n$ be defined by (3.24).
Then,

$$Im\,\lambda_k(A) = \min_{0 \neq u \in N_k} \frac{Im(Au,u)_R}{(u,u)_R},\ k = 1, 2, \cdots, n. \tag{4.6}$$

The minimum is attained for $u = p_k$.

Next, we state a maxmin characterization for the imaginary parts of eigenvalues similar to results for the eigenvalues in [12, Subsection 5.4, (26)] for self-adjoint matrices or for the real parts in Theorem 3.8.
One has the following theorem.

Theorem 4.6. Let the conditions $(C1)$ - $(C4)$ be fulfilled. Further, let the eigenvalues of A be arranged according to (4.2).
Then, for every $j = 1, \cdots, n$ and every subspace $N \subset \boldsymbol{C}^n$ with $dim N = j$, the following inequalities are valid:

$$Im\,\lambda_n(A) \leq \min_{0 \neq u \in N} \frac{Im(Au,u)_R}{(u,u)_R} \leq Im\,\lambda_j(A), \tag{4.7}$$

and the following representation formulas hold:

$$Im\,\lambda_j(A) = \max_{dim N = j} \min_{0 \neq u \in N} \frac{Im(Au,u)_R}{(u,u)_R}. \tag{4.8}$$

5. Formulas for the representation of the moduli of the eigenvalues of a diagonalizable matrix

In this section, we want to state formulas for the representation of the moduli of the eigenvalues of a diagonalizable matrix A by Rayleigh quotients. More precisely, max-, min-, minmax-, and maxmin-representations are obtained corresponding to associated formulas for the eigenvalues of self-adjoint matrices, assembled, for instance, in the textbook [12, Section 5.4] resp. corresponding to those for the real parts in Section 3 and for the imaginary parts in Section 4.
First, we want to give a relation corresponding to that of [12, Section 5.4(18)]. This is done in the following Formula (5.1).

Lemma 5.1. Let the conditions $(C1)$ - $(C4)$ be fulfilled. Then, with the denotations of Theorem 2.2,

$$\|A\,u\|_R^2 = \sum_{j=1}^{n} |\lambda_j(A)|^2\, \|u\|_{R_j}^2,\ u \in \boldsymbol{C}^n. \tag{5.1}$$

Proof. Let $u \in \boldsymbol{C}^n$. From (3.7),

$$u = \sum_{k=1}^{n} (u, u_k^*) p_k \tag{5.2}$$

and thus,

$$Au = \sum_{k=1}^{n} (u, u_k^*) \lambda_k p_k. \tag{5.3}$$

This entails

$$\|Au\|_R^2 = (RAu, Au) = \sum_{j=1}^{n} (Au, Au)_{R_j} = \sum_{j,k,i=1}^{n} (u, u_k^*) \lambda_k\, \overline{(u, u_i^*)\lambda_i}\, (p_k, p_i)_{R_j}. \tag{5.4}$$

Now, due to (2.1),

$$\begin{aligned}(p_k,p_i)_{R_j} &= (u_j^* u_j p_k, p_i) = (u_j^*(p_k,u_j^*),p_i)\\ &= (p_k,u_j^*)\,(u_j^*,p_i) = (p_k,u_j^*)\,\overline{(p_i,u_j^*)} = \delta_{kj}\,\delta_{ij}.\end{aligned} \tag{5.5}$$

Therefore, from (5.4) and (5.5),

$$\|Au\|_R^2 = \sum_{k=1}^{n} |\lambda_k|^2 |(u,u_k^*)|^2.$$

Taking into account (3.9), leads to the assertion. □

Similarly to [12, Section 5.4,(22)] or (3.16) resp. (4.2), we suppose in this section that the moduli of the eigenvalues $\lambda_1(A),\cdots,\lambda_n(A)$ of matrix A are arranged such that

$$|\lambda_1(A)| \geq |\lambda_2(A)| \geq \cdots \geq |\lambda_n(A)|. \tag{5.6}$$

Then, one has a series of theorems for the moduli of the eigenvalues corresponding to Theorems 3.4 - 3.8 and Theorems 4.2 -4.6.

Theorem 5.2. Let the conditions $(C1)$ - $(C4)$ be fulfilled. Further, let the moduli of the eigenvalues of A be arranged according to (5.6). Moreover, let the vector spaces $M_k, k = 1,\cdots,n$ be defined by (3.11) or (3.12).
Then,

$$|\lambda_k(A)| = \max_{0\neq u\in M_k} \frac{\|Au\|_R}{\|u\|_R},\ k = 1,2,\cdots,n. \tag{5.7}$$

Proof. As in Theorems 3.4 and 4.2, there are two methods to derive this theorem.
Method 1: According to (5.1), one has

$$\|A\,u\|_R^2 = \sum_{j=1}^{n} |\lambda_j(A)|^2\,\|u\|_{R_j}^2,\ u\in \boldsymbol{C}^n.$$

Choosing $k\in\{1,\cdots,n\}$ fixed and $u\in M_k$, one obtains

$$\begin{aligned}\|A\,u\|_R^2 &= \sum_{j=k}^{n} |\lambda_j(A)|^2\,\|u\|_{R_j}^2 \leq \max_{j=k,\cdots,n} |\lambda_j(A)|^2 \sum_{j=k}^{n} \|u\|_{R_j}^2\\ &= |\lambda_k(A)|^2 \sum_{j=1}^{n} \|u\|_{R_j}^2 = |\lambda_k(A)|^2\,\|u\|_R^2,\end{aligned}$$

that is,

$$\frac{\|A\,u\|_R^2}{\|u\|_R^2} \leq |\lambda_k(A)|^2,\ 0\neq u\in M_k$$

and thus

$$\max_{0\neq u\in M_k} \frac{\|A\,u\|_R}{\|u\|_R} \leq |\lambda_k(A)|. \tag{5.8}$$

Now, the maximum is attained for $u = p_k \in M_k$, that is,

$$|\lambda_k(A)| = \frac{\|A\,p_k\|_R}{\|p_k\|_R} \leq \max_{0\neq u\in M_k} \frac{\|A\,u\|_R}{\|u\|_R} \leq |\lambda_k(A)|.$$

so that the assertion (5.7) is proven.
Method 2:
Let $\lambda_j(R^{-1}A^*RA)$ be the eigenvalues of $R^{-1}A^*RA$ and $v_j = v_j(R^{-1}A^*RA)$ be the corresponding eigenvectors for $j = 1,2,\cdots,n$. With the spaces $M_k^{(R)}$ defined in the proof of Theorem 3.4, from [12, Section 5.4(24)], it follows that

$$\lambda_k(R^{-1}A^*RA) = \max_{0\neq u\in M_k^{(R)}} \frac{(R^{-1}A^*RA\,u,u)_R}{(u,u)_R}$$

as $R^{-1}A^*RA$ is self-adjoint in the scalar product $(\cdot,\cdot)_R$. Since from [6, Theorem 7, (29)],

$$\lambda_k(R^{-1}A^*RA) = |\lambda_k(A)|^2$$

and further

$$(R^{-1}A^*RA\,u,u)_R = (Au,Au)_R = \|Au\|_R^2,\ u\in\boldsymbol{C}^n,$$

we obtain

$$|\lambda_k(A)|^2 = \max_{0\neq u\in M_k^{(R)}} \frac{\|Au\|_R^2}{\|u\|_R^2}$$

and thus

$$|\lambda_k(A)| = \max_{0\neq u\in M_k^{(R)}} \frac{\|Au\|_R}{\|u\|_R}.$$

Now, also due to [6, Theorem 7,(30)],

$$v_j = v_j(R^{-1}A^*RA) = p_j = p_j(A),\ j = 1,2,\cdots,n.$$

Therefore, as in Section 3,

$$(u,v_j)_R = (u,u_j^*),\ j = 1,2,\cdots,k-1$$

and

$$M_k^{(R)} = [p_k, p_{k+1},\cdots,p_n] = M_k,\ k = 1,2,\cdots,n.$$

Thus, Formula (5.7) is proven. □

Next, we want to state a minmax characterization for the moduli of eigenvalues similar to results for the eigenvalues in [12, Subsection 5.4, (25)].
One has the following theorem whose proof is conducted along the lines of Method 1 or Method 2 in the proof of Theorem 5.2.

Theorem 5.3. Let the conditions $(C1)$ - $(C4)$ be fulfilled. Further, let the eigenvalues of A be arranged according to (5.6).
Then, for every $j = 1,\cdots,n$ and every subspace $M \subset \mathbf{C}^n$ with $dim M = m = n+1-j$, the following inequalities are valid:

$$|\lambda_j(A)| \leq \max_{0\neq u\in M} \frac{\|Au\|_R}{\|u\|_R} \leq |\lambda_1(A)|, \tag{5.9}$$

and the following representation formulas hold:

$$|\lambda_j(A)| = \min_{dim M=m=n+1-j} \max_{0\neq u\in M} \frac{\|Au\|_R}{\|u\|_R}. \tag{5.10}$$

Remark 5.4. *From (5.9), it follows*

$$\frac{\|Au\|_R}{\|u\|_R} \leq \rho(A) = \max_{j=1,\cdots,n} |\lambda_j(A)|,\ 0 \neq u \in \mathbf{C}^n.$$

The next theorems correspond to Theorems 3.7 and 3.8 resp. Theorems 4.5 and 4.6.

Theorem 5.5. Let the conditions $(C1)$ - $(C4)$ be fulfilled. Further, let the moduli of the eigenvalues of A be arranged according to (5.6). Moreover, let the vector spaces N_k, $k = 1,\cdots,n$ be defined by (3.24).
Then,

$$|\lambda_k(A)| = \min_{0\neq u\in N_k} \frac{\|Au\|_R}{\|u\|_R},\ k = 1,2,\cdots,n. \tag{5.11}$$

Finally, one has the following theorem.

Theorem 5.6. Let the conditions $(C1)$ - $(C4)$ be fulfilled. Further, let the moduli of the eigenvalues of A be arranged according to (5.6).
Then, for every $j = 1,\cdots,n$ and every subspace $N \subset \mathbf{C}^n$ with $dim N = j$, the following inequalities are valid:

$$|\lambda_n(A)| \leq \min_{0\neq u\in N} \frac{\|Au\|_R}{\|u\|_R} \leq |\lambda_j(A)|, \tag{5.12}$$

and the following representation formulas hold:

$$|\lambda_j(A)| = \max_{dim N=j} \min_{0\neq u\in N} \frac{\|Au\|_R}{\|u\|_R}. \tag{5.13}$$

Remark 5.7. *From (5.12), it follows*

$$\frac{\|Au\|_R}{\|u\|_R} \geq \min_{j=1,\cdots,n} |\lambda_j(A)| = [\rho(A^{-1})]^{-1},\ 0 \neq u \in \mathbf{C}^n, \tag{5.14}$$

where the last equal sign holds if A is nonsingular. If A is singular, then $[\rho(A^{-1})]^{-1}$ has to be interpreted as zero.

6. Connection between the matrices $\mathbf{R^{-1}\frac{A^*R+RA}{2}}$, $\mathbf{R^{-1}\frac{RA-A^*R}{2i}}$, and $\mathbf{R^{-1}A^*RA}$

The equation

$$(Re\,z)^2+(Im\,z)^2=|z|^2 \tag{6.1}$$

is valid for all $z\in C$.
Now, let $A\in C^{n\times n}$, $n\in N$, $j\in\{1,\ldots,n\}$, and $\lambda_j(A)$ be an eigenvalue of A. Set $z=\lambda_j(A)$. Then,

$$|\lambda_j(A)|^2=(Re\,\lambda_j(A))^2+(Im\,\lambda_j(A))^2. \tag{6.2}$$

According to [6, Theorems 6 and 7],

$$Re\,\lambda_j(A)=\lambda_j(R^{-1}\tfrac{A^*R+RA}{2}), \tag{6.3}$$

$$Im\,\lambda_j(A)=\lambda_j(R^{-1}\tfrac{RA-A^*R}{2i}), \tag{6.4}$$

and

$$|\lambda_j(A)|^2=\lambda_j(R^{-1}A^*RA) \tag{6.5}$$

leading to

$$(\lambda_j(R^{-1}\tfrac{A^*R+RA}{2}))^2+(\lambda_j(R^{-1}\tfrac{RA-A^*R}{2i}))^2=\lambda_j(R^{-1}A^*RA)$$

or

$$\lambda_j((R^{-1}\tfrac{A^*R+RA}{2})^2)+\lambda_j((R^{-1}\tfrac{RA-A^*R}{2i})^2)=\lambda_j(R^{-1}A^*RA) \tag{6.6}$$

From this relation, the question arises as to whether a similar relation also holds for the pertinent matrices. This turns out to be indeed true. Namely, we have

Theorem 6.1. Let the conditions $(C1)$ - $(C4)$ be fulfilled. Then,

$$\left(R^{-1}\tfrac{A^*R+RA}{2}\right)^2+\left(R^{-1}\tfrac{RA-A^*R}{2i}\right)^2=R^{-1}A^*RA. \tag{6.7}$$

Proof. The proof is based on [6, Theorems 6 and 7]. One has

$$\begin{aligned}
&\left[\left(R^{-1}\tfrac{A^*R+RA}{2}\right)^2+\left(R^{-1}\tfrac{RA-A^*R}{2i}\right)^2\right]p_j\\
=\;&\left(R^{-1}\tfrac{A^*R+RA}{2}\right)^2p_j+\left(R^{-1}\tfrac{RA-A^*R}{2i}\right)^2p_j\\
=\;&[Re\lambda_j(A)]^2p_j+[Im\lambda_j(A)]^2p_j\\
=\;&|\lambda_j(A)|^2p_j=\lambda_j(R^{-1}A^*RA)p_j=R^{-1}A^*RAp_j,
\end{aligned} \tag{6.8}$$

$j=1,\cdots,n$ so that

$$\left[\left(R^{-1}\tfrac{A^*R+RA}{2}\right)^2+\left(R^{-1}\tfrac{RA-A^*R}{2i}\right)^2\right]u=R^{-1}A^*RAu,\ u\in C^n$$

which is equivalent to (6.7). □

7. Applications

In this section, we apply the results of Sections 3, 4, and 5 to obtain the convexity of newly-defined numerical ranges of a diagonalizable matrix A.

7.1. Applications pertinent to Section 3

In this subsection, we first generalize the notion of the *numerical range* of a matrix A with respect to the ordinary scalar product $(\cdot,\cdot)$ on C^n, denoted by $W_{(\cdot,\cdot)}(A)$, to the corresponding notion with weighted scalar product $W_{(\cdot,\cdot)_R}(A)$.
As the next step, the real part of the numerical range $W_{(\cdot,\cdot)_R}(A)$ will be defined, denoted by $Re[W_{(\cdot,\cdot)_R}(A)]$.
Further, the real part of the spectrum $Re[\sigma(A)]$ is introduced.
Based on these notions, some applications of the derived results are obtained.
For example, the alternative form

$$Re[W_{(\cdot,\cdot)_R}(A)]=W_{(\cdot,\cdot)_R}(R^{-1}\tfrac{A^*R+RA}{2})$$

is derived where the matrix $R^{-1}\frac{A^*R+RA}{2}$ is regular if A is asymptotically stable.

Let the conditions $(C1)$ - $(C4)$ be fulfilled and the matrices R_j and R be given by (2.3) and (2.6).
The *numerical range of A with respect to the scalar product* $(\cdot,\cdot)$ is defined by

$$W_{(\cdot,\cdot)}(A) = \left\{ z \in \boldsymbol{C} \mid z = \frac{(Au,u)}{(u,u)},\ 0 \neq u \in \boldsymbol{C}^n \right\},$$

cf. [12, Section 5.4]. Accordingly, we define

$$W_{(\cdot,\cdot)_R}(A) = \left\{ z \in \boldsymbol{C} \mid z = \frac{(Au,u)_R}{(u,u)_R},\ 0 \neq u \in \boldsymbol{C}^n \right\}.$$

Further, let

$$Re[W_{(\cdot,\cdot)_R}(A)] := \left\{ x \in \boldsymbol{R} \mid x = \frac{Re(Au,u)_R}{(u,u)_R},\ 0 \neq u \in \boldsymbol{C}^n \right\};$$

we call it *real part of the numerical range* $W_{(\cdot,\cdot)_R}(A)$.
Let $\sigma(A) = \{\lambda_j(A),\ j = 1,\cdots,n\}$ be the *spectrum of A*, i.e., the set of all eigenvalues of A.
Similarly as before, we define

$$Re[\sigma(A)] := \{Re\,\lambda_j(A),\ j = 1,\cdots,n\}$$

and call it the *real part of the spectrum of A*.
Finally, let $co\{Re[\sigma(A)]\}$ be the *convex hull of* $Re[\sigma(A)]$.
Next, we show the following corollary as an application of Theorem 3.5, Formula (3.21), and Theorem 3.8, Formula (3.27).

Corollary 7.1. *(Application 1)*
Let the conditions $(C1)$ - $(C4)$ be fulfilled. Then, the set $Re[W_{(\cdot,\cdot)_R}(A)]$ is convex, and one has the chain of equations

$$\begin{aligned} Re[W_{(\cdot,\cdot)_R}(A)] &= \left\{ x \in \boldsymbol{R} \mid x = \frac{Re(Au,u)_R}{(u,u)_R},\ 0 \neq u \in \boldsymbol{C}^n \right\} \\ &= \left\{ x \in \boldsymbol{R} \mid x = \frac{(R^{-1}\frac{A^*R+RA}{2}u,u)_R}{(u,u)_R},\ 0 \neq u \in \boldsymbol{C}^n \right\} \\ &= W_{(\cdot,\cdot)_R}(R^{-1}\tfrac{A^*R+RA}{2}) \\ &= co\{Re\,[\sigma(A)]\}. \end{aligned}$$

If the eigenvalues of A are arranged according to (3.16), then

$$Re[W_{(\cdot,\cdot)_R}(A)] = [Re\,\lambda_n(A), Re\,\lambda_1(A)].$$

Proof. Let $0 \neq u \in \boldsymbol{C}^n$. Then,

$$2\,\frac{Re(Au,u)_R}{(u,u)_R} = \frac{([A^*R+RA]u,u)}{(u,u)_R} = \frac{(R^{-1}[A^*R+RA]u,u)_R}{(u,u)_R}.$$

The convexity follows from the last form with $R^{-1}[A^*R+RA]$ and the scalar product $(\cdot,\cdot)_R$, see the convexity of the numerical range of a matrix due to Hausdorff in [12, Section 5.4]. Since, with (3.16), one has

$$co\{Re\,[\sigma(A)]\} = [Re\,\lambda_n(A), Re\,\lambda_1(A)],$$

it remains to show that

$$Re[W_{(\cdot,\cdot)_R}(A)] = [Re\,\lambda_n(A), Re\,\lambda_1(A)].$$

The proof of this relation is as follows.
(i) $Re[W_{(\cdot,\cdot)_R}(A)] \subset [Re\,\lambda_n(A), Re\,\lambda_1(A)]$
This inclusion can be deduced from (3.21) with $dim\,M = m = n - j + 1$ for $j = 1$ and (3.27) with $dim\,N = n$. Namely, from (3.21), for $j = 1$ and $dim\,M = n$, i.e., $M = \boldsymbol{C}^n$, one has

$$\max_{0 \neq u \in \boldsymbol{C}^n} \frac{Re(Au,u)_R}{(u,u)_R} \leq Re\,\lambda_1(A)$$

and from (3.27), for $j = n$ and $dim\,N = n$, i.e., $N = \boldsymbol{C}^n$,

$$\min_{0 \neq u \in \boldsymbol{C}^n} \frac{Re(Au,u)_R}{(u,u)_R} \geq Re\,\lambda_n(A).$$

(ii) $[Re\,\lambda_n(A), Re\,\lambda_1(A)] \subset Re[W_{(\cdot,\cdot)_R}(A)]$
Let $\beta \in [Re\,\lambda_n(A), Re\,\lambda_1(A)]$. Then, there exists an α in $0 \leq \alpha \leq 1$ with

$$\beta = \alpha\, Re\lambda_n(A) + (1-\alpha)\, Re\lambda_1(A).$$

Now, with the eigenvectors p_n and p_1,

$$Re\lambda_n(A) = \frac{Re(Ap_n, p_n)_R}{(p_n, p_n)_R} \in Re[W_{(\cdot,\cdot)_R}(A)]$$

and

$$Re\lambda_1(A) = \frac{Re(Ap_1, p_1)_R}{(p_1, p_1)_R} \in Re[W_{(\cdot,\cdot)_R}(A)].$$

Thus, due to the convexity of $Re[W_{(\cdot,\cdot)_R}(A)]$, it follows that $\beta \in Re[W_{(\cdot,\cdot)_R}(A)]$. □

Corollary 7.2. *(Application 2)*
Let the conditions $(C1)$ - $(C4)$ be fulfilled. Further, let A be asymptotically stable. Then,

$$Re[W_{(\cdot,\cdot)_R}(A)] \subset \boldsymbol{R}^- = \{x \in \boldsymbol{R} \,|\, x < 0\}.$$

If A is only stable, then

$$Re[W_{(\cdot,\cdot)_R}(A)] \subset \boldsymbol{R}_0^- = \{x \in \boldsymbol{R} \,|\, x \leq 0\}.$$

Proof. The first assertion follows from (3.5). The second assertion follows in a similar way. □

7.2. Applications pertinent to Section 4

In this section, we proceed in a similar way as in 7.1. So, let

$$Im[W_{(\cdot,\cdot)_R}(A)] = \left\{ x \in \boldsymbol{R} \,|\, x = \frac{Im(Au,u)_R}{(u,u)_R}, 0 \neq u \in \boldsymbol{C}^n \right\};$$

we call it the *imaginary part of the numerical range* $W_{(\cdot,\cdot)_R}(A)$.
Further, we define

$$Im[\sigma(A)] := \{Im\,\lambda_j(A),\ j = 1, \cdots, n\}$$

and call it the *imaginary part of the spectrum of A*.
Finally, let $co\{Im[\sigma(A)]\}$ be the *convex hull of* $Im[\sigma(A)]$.
Herewith, we obtain

Corollary 7.3. *(Application 3)*
Let the conditions $(C1)$ - $(C4)$ be fulfilled. Then, the set $Im[W_{(\cdot,\cdot)_R}(A)]$ is convex, and one has the chain of equations

$$\begin{aligned} Im[W_{(\cdot,\cdot)_R}(A)] &= \left\{ x \in \boldsymbol{R} \,|\, x = \frac{Im(Au,u)_R}{(u,u)_R}, 0 \neq u \in \boldsymbol{C}^n \right\} \\ &= \left\{ x \in \boldsymbol{R} \,|\, x = \frac{(R^{-1}\frac{RA-A^*R}{2i}u,u)_R}{(u,u)_R}, 0 \neq u \in \boldsymbol{C}^n. \right\} \\ &= W_{(\cdot,\cdot)_R}(R^{-1}\tfrac{RA-A^*R}{2i}) \\ &= co\{Im\,[\sigma(A)]\}. \end{aligned}$$

If the eigenvalues of A are arranged according to (4.2), then

$$Im[W_{(\cdot,\cdot)_R}(A)] = [Im\,\lambda_n(A), Im\,\lambda_1(A)].$$

Proof. The proof is similar to that of Corollary 7.1 and therefore omitted. □

7.3 Applications pertinent to Section 5

In this subsection, we continue along the same lines as in 7.1 and 7.2.
Thus, let

$$W_{\|\cdot\|_R}(A) := \left\{ x \in \boldsymbol{R}_0^+ \,|\, x = \frac{\|Au\|_R}{\|u\|_R},\ 0 \neq u \in \boldsymbol{C}^n \right\};$$

and call it *the numerical range of A with respect to the norm* $\|\cdot\|_R$.
Further, we define

$$|\sigma(A)| := \{|\lambda_j(A)|,\ j = 1, \cdots, n\}$$

and call it the *modulus of the spectrum of A*.
Moreover, let $co\{|\sigma(A)|\}$ be the *convex hull of* $|\sigma(A)|$.
Finally, let $S \subset \boldsymbol{R}_0^+$ be any set. We define

$$S^2 := \{y \,|\, y = s^2,\ s \in S\}.$$

Next, we show the following corollary.

Corollary 7.4. *(Application 4)*
Let the conditions $(C1)$ - $(C4)$ be fulfilled. Then, the set $[W_{\|\cdot\|_R}(A)]^2$ is convex, and one has the chain of equations

$$\begin{aligned}
[W_{\|\cdot\|_R}(A)]^2 &= \left\{ x \in \boldsymbol{R}_0^+ \,|\, x = \left[\frac{\|Au\|_R}{\|u\|_R}\right]^2 = \frac{\|Au\|_R^2}{\|u\|_R^2}, 0 \neq u \in \boldsymbol{C}^n \right\} \\
&= \left\{ x \in \boldsymbol{R}_0^+ \,|\, x = \frac{([R^{-1}A^*RA]\,u,u)_R}{(u,u)_R}, 0 \neq u \in \boldsymbol{C}^n. \right\} \\
&= W_{(\cdot,\cdot)_R}(R^{-1}A^*RA) \\
&= co\{|\sigma(A)|^2\},
\end{aligned}$$

and $R^{-1}A^*RA$ is self-adjoint and positive semi-definite in the weighted scalar product $(\cdot,\cdot)_R$. If A is regular, then $R^{-1}A^*RA$ is apparently positive definite.
Further, if the moduli of the eigenvalues of A are arranged according to (5.6), then

$$[W_{\|\cdot\|_R}(A)]^2 = [|\lambda_n(A)|^2, |\lambda_1(A)|^2].$$

Proof. The proof is done by using Theorem 5.3, Formula (5.9) and Theorem 5.5, Formula (5.12). □

Next, for $S \subset \boldsymbol{R}_0^+$, we define

$$\sqrt{S} := \{y \,|\, y = \sqrt{s},\ s \in S\}.$$

Herewith, one can rewrite Corollary 7.4 in the following form.

Corollary 7.5. *(Application 5)*
Let the conditions $(C1)$ - $(C4)$ be fulfilled. Then, the set $W_{\|\cdot\|_R}(A)$ is convex, and one has the chain of equations

$$\begin{aligned}
W_{\|\cdot\|_R}(A) &= \left\{ x \in \boldsymbol{R}_0^+ \,|\, x = \frac{\|Au\|_R}{\|u\|_R}, 0 \neq u \in \boldsymbol{C}^n \right\} \\
&= \left\{ x \in \boldsymbol{R}_0^+ \,|\, x = \sqrt{\frac{([R^{-1}A^*RA]\,u,u)_R}{(u,u)_R}}, 0 \neq u \in \boldsymbol{C}^n. \right\} \\
&= \sqrt{W_{(\cdot,\cdot)_R}(R^{-1}A^*RA)} \\
&= \sqrt{co\{|\sigma(A)|^2\}}.
\end{aligned}$$

If the moduli of the eigenvalues of A are arranged according to (5.6), then

$$W_{\|\cdot\|_R}(A) = [|\lambda_n(A)|, |\lambda_1(A)|].$$

Proof. For any subset $S \subset \boldsymbol{R}_0^+$, one has

$$\sqrt{S^2} = (\sqrt{S})^2 = S.$$

Thus, from Corollary 7.4, the equations of Corollary 7.5 follow. Since, for the arrangement (5.6), $W_{\|\cdot\|_R}(A) = [|\lambda_n(A)|, |\lambda_1(A)|]$ and since the interval $[|\lambda_n(A)|, |\lambda_1(A)|]$ is convex, so is $W_{\|\cdot\|_R}(A)$. □

8. Numerical example

In this section, we check the results of Subsection 7.1 as well as of Theorem 6.1, Formula (6.7) numerically. The numerical check of the results of Subsections 7.2 and 7.3 is left to the reader.

8.1. A multi-mass vibration model

We take up the multi-mass vibration model of [2], shown in *Fig.1*.

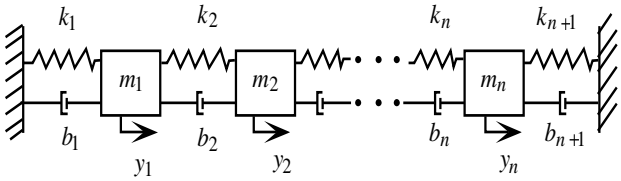

Fig.1: Multi-mass vibration model

The associated initial value problem is given by

$$M\ddot{y}+B\dot{y}+Ky=0,\ y(0)=y_0,\dot{y}(0)=\dot{y}_0,$$

where $y=[y_1,\cdots,y_n]^T$ and

$$M=\begin{bmatrix} m_1 & & & & \\ & m_2 & & & \\ & & m_3 & & \\ & & & \ddots & \\ & & & & m_n \end{bmatrix},$$

$$B=\begin{bmatrix} b_1+b_2 & -b_2 & & & & \\ -b_2 & b_2+b_3 & -b_3 & & & \\ & -b_3 & b_3+b_4 & -b_4 & & \\ & & \ddots & \ddots & \ddots & \\ & & & -b_{n-1} & b_{n-1}+b_n & -b_n \\ & & & & -b_n & b_n+b_{n+1} \end{bmatrix},$$

$$K=\begin{bmatrix} k_1+k_2 & -k_2 & & & & \\ -k_2 & k_2+k_3 & -k_3 & & & \\ & -k_3 & k_3+k_4 & -k_4 & & \\ & & \ddots & \ddots & \ddots & \\ & & & -k_{n-1} & k_{n-1}+k_n & -k_n \\ & & & & -k_n & k_n+k_{n+1} \end{bmatrix}$$

with the *mass, damping,* and *stiffness matrices* M, B, and K, as the case may be, and the *displacement vector* y as in [2]. In *state-space description*, this problem takes the form

$$\dot{x}=Ax, t\geq 0, x(0)=x_0,$$

where $x=[y^T,z^T]^T$, $z=\dot{y}$, and where the *system matrix* A is given by

$$A=\left[\begin{array}{c|c} 0 & E \\ \hline -M^{-1}K & -M^{-1}B \end{array}\right].$$

8.2. Data

The values m_j, $j=1,\cdots,n$ and b_j, k_j, $j=1,\cdots,n+1$ are also specified as in [2], namely as

$$\begin{aligned} m_j &= 1,\ j=1,\cdots,n \\ k_j &= 1,\ j=1,\cdots,n+1 \end{aligned}$$

and

$$b_j = \begin{cases} 1/2,\ j\ even \\ 1/4,\ j\ odd. \end{cases}$$

Then,

$$M = E,$$

$$B=\begin{bmatrix} \frac{3}{4} & -\frac{1}{2} & & & & \\ -\frac{1}{2} & \frac{3}{4} & -\frac{1}{4} & & & \\ & -\frac{1}{4} & \frac{3}{4} & -\frac{1}{2} & & \\ & & \ddots & \ddots & \ddots & \\ & & -\frac{1}{4} & \frac{3}{4} & -\frac{1}{2} & \\ & & & -\frac{1}{2} & \frac{3}{4} & \end{bmatrix}$$

(if n is even), and

$$K=\begin{bmatrix} 2 & -1 & & & & \\ -1 & 2 & -1 & & & \\ & -1 & 2 & -1 & & \\ & & \ddots & \ddots & \ddots & \\ & & -1 & 2 & -1 & \\ & & & -1 & 2 & \end{bmatrix}.$$

We add the details from [2] in order to make the paper more readable on its own. Further, we choose $n = 5$ in this paper so that the state-space vector has dimension $m = 2n = 10$. For the initial time, we take

$$t_0 = 0.$$

Finally, the initial conditions for $y(t)$ and $\dot{y}(t)$ can be chosen as

$$y_0 = [-1, 1, -1, 1, -1]^T$$

as well as

$$\dot{y}_0 = [-1, -1, -1, -1, -1]^T$$

(which corresponds to IC(II) in [2, p.159]). But, they are not needed here.

8.3. Auxiliary computational results

As in [2], using the Matlab routine *eig.m*, one obtains

$$\begin{aligned}
\lambda_1(A) &= -0.050239361219464 + 0.516371450711010i,\\
\lambda_2(A) &= -0.050239361219464 - 0.516371450711010i.\\
\lambda_3(A) &= -0.187331625959257 + 0.994521686465592i,\\
\lambda_4(A) &= -0.187331625959257 - 0.994521686465592i,\\
\lambda_5(A) &= -0.375000000000000 + 1.363589014329465i,\\
\lambda_6(A) &= -0.375000000000000 - 1.363589014329465i,\\
\lambda_7(A) &= -0.562668374040742 + 1.616358701643860i,\\
\lambda_8(A) &= -0.562668374040742 - 1.616358701643860i,\\
\lambda_9(A) &= -0.699760638780536 + 1.795981478159753i,\\
\lambda_{10}(A) &= -0.699760638780536 - 1.795981478159753i.
\end{aligned}$$

Therefore, $\lambda_j(A),\ j = 1, \cdots, m = 2n = 10$ are distinct. Thus, matrix A is diagonalizable, regular, and asymptotically stable. The eigenvalues are ordered such that $Re\,\lambda_1(A) \geq \cdots \geq Re\,\lambda_{10}(A)$.
The weighted matrix R is computed as

$$R = \begin{bmatrix}
1.2501 & -0.2868 & -0.1297 & 0.0135 & -0.0988 & 0.1966 & -0.1314 & -0.3356 & -0.0196 & 0.2662\\
-0.2868 & 1.0887 & -0.3824 & -0.0842 & 0.0179 & -0.1567 & 0.2066 & 0.0440 & 0.0239 & 0.0319\\
-0.1297 & -0.3824 & 1.1899 & -0.3531 & -0.1196 & 0.2780 & 0.0018 & 0.2200 & -0.1271 & -0.3402\\
0.0135 & -0.0842 & -0.3531 & 1.0873 & -0.3227 & -0.0173 & -0.0525 & -0.1892 & 0.1947 & 0.0505\\
-0.0988 & 0.0179 & -0.1196 & -0.3227 & 1.2619 & -0.3017 & 0.0042 & 0.3092 & 0.0215 & 0.2699\\
0.1966 & -0.1567 & 0.2780 & -0.0173 & -0.3017 & 0.7620 & 0.2782 & 0.1039 & 0.0439 & -0.0256\\
-0.1314 & 0.2066 & 0.0018 & -0.0525 & 0.0042 & 0.2782 & 0.8373 & 0.3358 & 0.1512 & 0.0458\\
-0.3356 & 0.0440 & 0.2200 & -0.1892 & 0.3092 & 0.1039 & 0.3358 & 0.9171 & 0.3240 & 0.1085\\
-0.0196 & 0.0239 & -0.1271 & 0.1947 & 0.0215 & 0.0439 & 0.1512 & 0.3240 & 0.8373 & 0.2919\\
0.2662 & 0.0319 & -0.3402 & 0.0505 & 0.2699 & -0.0256 & 0.0458 & 0.1085 & 0.2919 & 0.7685
\end{bmatrix},$$

8.4. Numerical check of the validity of Corollary 21 (Application 1)

Here, we check the validity of

$$\frac{Re(Au,u)_R}{(u,u)_R} \in Re[W_{(\cdot,\cdot)_R}(A)] = [Re\,\lambda_{10}(A), Re\,\lambda_1(A)],\ 0 \neq u \in \mathbf{C}^{10}$$

and choose $u \in \{e, e_1, e_2, e_{1,2}\}$ where

$$\begin{aligned}
e &= [1,1,1,1,1,1,1,1,1,1]^T,\\
e_1 &= [1,0,0,0,0,0,0,0,0,0]^T,\\
e_2 &= [0,1,0,0,0,0,0,0,0,0]^T,\\
e_{1,2} &= [1,1,0,0,0,0,0,0,0,0]^T.
\end{aligned}$$

We obtain

$$[Re\,\lambda_{10}(A), Re\,\lambda_1(A)] = [-0.699760638780535, -0.050239361219464]$$

and further

$$\begin{aligned}
\frac{Re(Ae,e)_R}{(e,e)_R} &= -0.076392659033957 \in [Re\,\lambda_{10}(A), Re\,\lambda_1(A)],\\
\frac{Re(Ae_1,e_1)_R}{(e_1,e_1)_R} &= -0.419568056678684 \in [Re\,\lambda_{10}(A), Re\,\lambda_1(A)],\\
\frac{Re(Ae_2,e_2)_R}{(e_2,e_2)_R} &= -0.483140758290161 \in [Re\,\lambda_{10}(A), Re\,\lambda_1(A)],\\
\frac{Re(Ae_{1,2},e_{1,2})_R}{(e_{1,2},e_{1,2})_R} &= -0.230440140020361 \in [Re\,\lambda_{10}(A), Re\,\lambda_1(A)].
\end{aligned}$$

8.5. Numerical check of the validity of Theorem 6.1

Here, we obtain

$$\left(R^{-1}\,\tfrac{A^*R+RA}{2}\right)^2+\left(R^{-1}\,\tfrac{RA-A^*R}{2i}\right)^2 \doteq R^{-1}A^*RA \doteq$$

$$\begin{bmatrix}
2.0451 & -1.0850 & 0.0397 & -0.0038 & 0.0066 & -0.0013 & -0.1139 & -0.0054 & -0.0091 & 0.0044\\
-1.0900 & 1.9991 & -0.9022 & -0.0478 & -0.0070 & -0.1139 & 0.0060 & 0.1256 & -0.0031 & -0.0078\\
-0.0561 & -0.9022 & 2.0073 & -1.0978 & 0.0429 & -0.0054 & 0.1256 & 0.0104 & -0.1216 & -0.0090\\
-0.0038 & 0.0480 & -1.0970 & 2.0007 & -0.8984 & -0.0091 & -0.0031 & -0.1216 & 0.0060 & 0.1347\\
0.0082 & -0.0078 & -0.0529 & -0.8931 & 1.9473 & 0.0044 & -0.0078 & -0.0090 & 0.1347 & 0.0029\\
-0.1112 & 0.2210 & -0.1122 & 0.0172 & -0.0179 & 1.9892 & -1.0016 & 0.0107 & 0.0015 & 0.0010\\
0.2338 & -0.0003 & -0.2482 & 0.1239 & 0.0124 & -1.0016 & 1.9690 & -0.9964 & 0.0154 & -0.0020\\
0.1364 & -0.2461 & -0.0169 & 0.2447 & -0.1037 & 0.0107 & -0.9964 & 1.9701 & -1.0036 & 0.0192\\
0.0152 & -0.1246 & 0.2462 & 0.0010 & -0.2633 & 0.0015 & 0.0154 & -1.0036 & 1.9690 & -0.9979\\
-0.0166 & 0.0110 & 0.1448 & -0.2754 & 0.1288 & 0.0010 & -0.0020 & 0.0192 & -0.9979 & 1.9788
\end{bmatrix}.$$

and, for

$$D := \left(R^{-1}\,\tfrac{A^*R+RA}{2}\right)^2+\left(R^{-1}\,\tfrac{RA-A^*R}{2i}\right)^2 - R^{-1}A^*RA,$$

we get

$$|D|_\infty := \max_{j,k=1,\ldots,10}|D_{jk}| \doteq 3.0002\times 10^{-14}.$$

So, Theorem 6.1 is numerically confirmed.

8.6. Computational aspects

In this subsection, we say something about the used computer equipment and the computation times.

(i) As to the *computer equipment*, the following hardware was available: an Intel Core2 Duo Processor at 3166 GHz, a 500 GB mass storage facility, and two 2048 MB high-speed memories. As software package for the computations, we used MATLAB, Version 7.11.

(ii) The *computation time t* of an operation was determined by the command sequence *t1=clock; operation; t=etime(clock,t1)*. It is put out in seconds, rounded to four decimal places. For the computation of the eigenvalues of matrix A in Subsection 5.3, we used the command [XA,DA]=eig(A); the pertinent computation time was less than 0.0001 s.

9. Conclusion and outlook on to future work

It has been shown that there exist Rayleigh-quotient representations of the real parts, imaginary parts, and moduli of the eigenvalues of diagonalizable matrices that parallel those representations known for the eigenvalues of self-adjoint matrices. The key idea is to use a weighted scalar product defined by a positive definite matrix that is constructed by means of left eigenvectors of the considered matrix and the right eigenvectors of its adjoint. The results are of interest on their own in Linear Algebra. They are also of potential interest in applications. For example, in the theory of linear dynamical systems, in the study of stability of a vibration problem, the real parts of the eigenvalues of the system matrix are important. Moreover, in systems with conjugate-complex eigenvalues, the moduli of the imaginary parts of the eigenvalues are the circular damped eigenfrequencies of the system. A somewhat surprising point is also the derived relation $(R^{-1}\,\frac{A^*R+RA}{2})^2+(R^{-1}\,\frac{RA-A^*R}{2i})^2 = R^{-1}A^*RA$. On the whole, the results should be of interest to mathematicians as well as engineers.

The case of general matrices is more involved and will be dealt with in a subsequent paper.

References

[1] A. Czornik, P. Jurgaś, *Some properties of the spectral radius of a set of matrices*, Int. J. Appl. Math. Sci. **16**(2)(2006)183-188.

[2] L. Kohaupt, *Construction of a biorthogonal system of principal vectors of the matrices A and A^* with applications to the initial value problem $\dot{x} = Ax$, $x(t_0) = x_0$*, J. Comp. Math. Opt. **3**(3)(2007)163-192.

[3] L. Kohaupt, *Biorthogonalization of the principal vectors for the matrices A and A^* with application to the computation of the explicit representation of the solution $x(t)$ of $\dot{x} = Ax$, $x(t_0) = x_0$*, Appl. MAth. Sci. **2**(20)(2008)961-974.

[4] L. Kohaupt, *Solution of the vibration problem $M\ddot{y}+B\dot{y}+Ky = 0$, $y(t_0) = y_0$, $\dot{y}(t_0) = \dot{y}_0$* without *the hypothesis $BM^{-1}K = KM^{-1}B$ or $B = \alpha M+\beta K$*, Appl. MAth. Sci. **2**(41)(2008)1989-2024.

[5] L. Kohaupt, *Solution of the matrix eigenvalue problem $VA+A^*V = \mu V$ with applications to the study of free linear systems*, J. Comp. Appl. Math. **213**(1)(2008)142-165.

[6] L. Kohaupt, *Spectral properties of the matrix $C^{-1}B$ with positive definite matrix C and Hermitian B as well as applications*, J. Appl. Math. Comput., DOI 10.1007/s12190-015-0876-8, (2015) 28 pages.

[7] T.J. Laffey, H. Šmigoc, *Nonnegatively realizable spectra with two positive eigenvalues*, Linear Multilinear Algebra **58**(7-8)(2010)1053-1069.

[8] P. Lancaster, *Theory of Matrices*, Academic Press, New York and London, 1969.

[9] P.C. Müller, W.O. Schiehlen, *Linear Vibrations, Martinus Nijhoff Publishers*, Dordrecht Boston Lancaster, 1985.

[10] S.V. Savchenko, *On the change in the spectral properties of a matrix under perturbations of sufficiently low rank*, Funct. Anal. Appl. **38**(1)(2004)69-71.

[11] J. Stoer, R. Bulirsch, *Introduction to Numerical Analysis, Springer*, New York Heidelberg, Third Edition, 2010.

[12] F. Stummel, K. Hainer, *Introduction to Numerical Analysis*, Scottish Academic Press, Edinburgh, 1980.

Journal of Mathematical Sciences and Modelling, 2 (2) (2019) 99-111
Research Article

Journal of Mathematical Sciences and Modelling

Journal Homepage: www.dergipark.gov.tr/jmsm
ISSN 2636-8692
DOI: http://dx.doi.org/10.33187/jmsm.439873

The Bivariate Generalized Rayleigh Distribution

Ammar M. Sarhan[1]

[1]*Department of Mathematics & Statistica, Dalhouise University, Canada*

Article Info

Keywords: *Marshal-Olkin, Multivariate distribution, Reliability, Shock models.*
2010 AMS: *62H10*
Received: *2 July 2018*
Accepted: *17 January 2019*
Available online: *30 August 2019*

Abstract

This paper introduces a new bivariate distribution named the bivariate generalized Rayleigh distribution (BVGR). The proposed distribution is of type of Marshall-Olkin (MO) distribution. The BVGR distribution has generalized Rayleigh marginal distributions. The joint cumulative distribution function, the joint survival function, the joint probability density function and the joint hazard rate function of the proposed distribution are obtained in closed forms. Statistical properties of the BVGR distribution are investigated. The maximum likelihood and Bayes methods are applied to estimate the unknown parameters. Both maximum likelihood and Bayes estimates are not obtained analytically. Therefore, numerical algorithms are required to report on the model parameters and its reliability characteristics. Markov Chain Monte Carlo (MCMC) algorithm is applied for the Bayesian method. A real data set is analyzed using the proposed distribution and compared it with existing distributions. It is observed that the BVGR model fits this dataset better than the MO and the bivariate generalized exponential (BVGE) distributions.

1. Introduction

Surles and Padgett [15] introduced the two parameter Burr Type X distribution and also named as the generalized Rayleigh (GR) distribution. The GR distribution is a particular member of the exponentiated Weibull distribution, originally proposed by Mudholkar and Srivastava [11]. Surles and Padgett [16] and Al-khedhari et al. [1] discussed the parameters' estimations of this distribution using different techniques.
A new bivariate distribution is proposed by Sarhan and Balakrishnan [14], now known as Sarhan-Balakrishnan bivariate (SBBV) distribution, using the GE distribution and exponential distribution and they derived several interesting properties of this new distribution. Although the GE and exponential distributions are used to define the SBBV, the marginal distributions of SBBV distribution are not in known forms. Kundu et al. [5] modified the SBBV to include a scale parameter and discussed the parameters' estimation using maximum likelihood method. Kundu and Gupta [6] followed the same idea using the GE distribution to provide a new bivariate distribution called the bivariate generalized exponential (BVGE) distribution so that the marginal distributions are GE distributions. None of the marginal distributions of the SBBV and BVGE distributions accommodates a bathtub shaped of the hazard rate function. The lack of the bathtub shaped property limits the application of the SBBV and BVGE distributions. Kundu and Gupta [6] derived several interesting properties of the BVGE distribution and discussed the maximum likelihood estimates (MLEs) of the unknown parameters of the distribution. Kundu and Gupta [6] used the BVGE distribution to re-analyze a real data set that was originally analyzed by Meintanis [10] using the bivariate Marshal-Olkin (MO) distribution and concluded that the BVGE distribution provides a better fit than the MO distribution.
The main aim of this paper is to use the similar idea as of Sarhan and Balakrishnan [14] to introduce a new bivariate generalized Rayleigh (BVGR) distribution, using the GR distributions, so that the marginal distributions are GR distributions. The hazard rate functions of marginals of the BVGR distribution can be either increasing or decreasing or constant or of bathtub shaped. This property enriches the application of the BVGR distribution comparing to both the MO and the BVGE distributions. The proposed distribution has four parameters. The BVGR distribution can be interpreted as the joint distribution of the lifetimes of the two components of a reliability system that consists of two non-independent and non-identical components each follows a univariate GR lifetime distribution. The joint cumulative distribution function (jcdf), the joint survival function (jsf), the joint probability density function (jpdf) and the the joint hazard rate function (jhrf) of the BVGR distribution are derived in closed forms. The maximum likelihood and Bayesian methods are used to estimate the four unknown parameters of the BVGR distribution and some of its reliability measures. None of these estimates is derived in a closed form. Therefore, numerical methods are required to calculate them. For Bayesian method, we apply the Markov Chain Monte Carlo.

***Email addresses and ORCID numbers*: ammar.sarhan@dal, 0000-0002-7750-6910 (A. M. Sarhan)**

The article is organized as follows. The BVGR distribution and discusses some of its statistical properties are presented and discussed in Sections 2 and 3. Parameters' estimations of the BVGR distribution are discussed in Section 4. Section 5 analyses a real data set and compares the ability of the BVGR with the MO and BVGE distributions to fit that data set. Finally, Section 6 concludes the paper.

2. The bivariate generalized Rayleigh distribution

The cumulative distribution function of the univariate GR distribution is, Surles and Padgett [15],

$$F_{\mathrm{GR}}(x;\lambda,\alpha)=\left(1-e^{-(\lambda x)^2}\right)^{\alpha},\ x\geq 0;\ \alpha,\lambda>0. \tag{2.1}$$

The corresponding probability density function (pdf) is

$$f_{\mathrm{GR}}(x;\lambda,\alpha)=2\alpha\lambda^2 x e^{-(\lambda x)^2}\left(1-e^{-(\lambda x)^2}\right)^{\alpha-1},\ x\geq 0;\ \alpha,\lambda>0. \tag{2.2}$$

Here α and λ are the shape and scale parameters, respectively. We will use GR(α,λ) to denoted the GR distribution with parameters α and β. The GR(α,λ) generalizes the Rayleigh distribution.
Now, suppose that there three mutually independent random variables, say U_j, $j=1,2,3$. The random variable U_j follows GR(α_j,λ) distribution, $j=1,2,3$. Define $X_i=\max\{U_i,\ U_3\}$, $i=1,2$. The bivariate vector (X_1,X_2) follows the bivariate generalized Rayleigh distribution with the shape parameters α_1, α_2, α_3 and scale parameter λ. We will denote it by BVGR$(\lambda,\alpha_1,\alpha_2,\alpha_3)$. To simplify notation, we write $\alpha_{123}=\alpha_1+\alpha_2+\alpha_3$ and $\alpha_{i3}=\alpha_i+\alpha_3$ for $i=1,2$.
Before providing the details of the BVGR distribution, we first present some practical applications of this distribution to show how it may occur in practice.

Maintenance Model: Suppose a two-component system, each component has been maintained independently and there is an overall common maintenance for the system. Due to component maintenance, suppose the lifetime of the ith component is increased by a random amount U_j, $j=1,2$, and because of the overall common maintenance, the lifetime of each component is increased by a random amount U_3. Thus, the lifetimes of the component a and 2 are $X_1=\max\{U_1,U_3\}$ and $X_2=\max\{U_2,U_3\}$, respectively.

Stress Model: Suppose a system has two components. Component i is subject to individual independent stress say U_i, $i=1,2$. The system has an overall stress U_3 which has been transmitted to both the components equally, independent of their individual stresses. Therefore, the observed stress at component i is $X_i=\max\{U_i,U_3\}$, $i=1,2$.
The following results provide the joint cdf, joint pdf, joint sf, joint hazard rate function and conditional pdf.

Theorem 2.1. *If (X_1,X_2) follows BVGR$(\lambda,\alpha_1,\alpha_2,\alpha_3)$, then the joint cdf of (X_1,X_2) for $x_1>0,x_2>0$, takes the form*

$$F_{X_1,X_2}(x_1,x_2)=\prod_{i=1}^{3}\left\{1-e^{-(\lambda x_i)^2}\right\}^{\alpha_i} \tag{2.3}$$

where $x_3=\min\{x_1,x_2\}$.

Proof. This result is a direct consequence of the definition of X_1 and X_2.
The joint cdf of the BVGR$(\lambda,\alpha_1,\alpha_2,\alpha_3)$ can also be written as

$$\begin{aligned} F_{X_1,X_2}(x_1,x_2) &= \prod_{i=1}^{3}F_{\mathrm{GR}}(x_i;\lambda,\alpha_i) \\ &= \begin{cases} F_{\mathrm{GR}}(x_1;\lambda,\alpha_{13})F_{\mathrm{GR}}(x_2;\lambda,\alpha_2) & if \quad x_1<x_2 \\ F_{\mathrm{GR}}(x_1;\lambda,\alpha_1)F_{\mathrm{GR}}(x_2;\lambda,\alpha_{23}) & if \quad x_2<x_1 \\ F_{\mathrm{GR}}(x;\lambda,\alpha_{123}) & if \quad x_1=x_2=x. \end{cases} \end{aligned} \tag{2.4}$$

Theorem 2.2. *Let (X_1,X_2) follow the BVGR$(\lambda,\alpha_1,\alpha_2,\alpha_3)$, then the joint pdf of (X_1,X_2) is*

$$f_{X_1,X_2}(x_1,x_2)=\begin{cases} f_1(x_1,x_2) & if\ \infty>x_2>x_1>0, \\ f_2(x_1,x_2) & if\ \infty>x_1>x_2>0, \\ f_0(x) & if\ \infty>x_1=x_2=x>0, \end{cases} \tag{2.5}$$

where

$$\begin{aligned} f_1(x_1,x_2) &= f_{GR}(x_1;\lambda,\alpha_{13})\,f_{GR}(x_2;\lambda,\alpha_2) \\ &= 4\lambda^4\,\alpha_2\,\alpha_{13}\,x_1\,x_2 e^{-\lambda^2(x_1^2+x_2^2)}\left(1-e^{-\lambda^2x_1^2}\right)^{\alpha_{13}-1}\left(1-e^{-\lambda^2x_2^2}\right)^{\alpha_2-1} \\ f_2(x_1,x_2) &= f_{GR}(x_1;\lambda,\alpha_1)\,f_{GR}(x_2;\lambda,\alpha_{23}) \\ &= 4\lambda^4\,\alpha_1\,\alpha_{23}\,x_1\,x_2\,e^{-\lambda^2(x_1^2+x_2^2)}\left(1-e^{-\lambda^2x_1^2}\right)^{\alpha_1-1}\left(1-e^{-\lambda^2x_2^2}\right)^{\alpha_{23}-1} \\ f_0(x) &= \frac{\alpha_3}{\alpha_{123}}\,f_{GR}(x;\lambda,\alpha_{123}) \\ &= 2\lambda^2\,\alpha_3 x e^{-\lambda^2x^2}\left(1-e^{-\lambda^2x^2}\right)^{\alpha_{123}-1}. \end{aligned}$$

Proof. *The forms of $f_1(.,.)$ and $f_2(.,.)$ can be directly obtained by differentiating $F_{X_1,X_2}(x_1,x_2)$ in (2.4) with respect to x_1 and x_2 for $x_1>x_2$ and $x_2>x_1$. But, $f_0(.)$ can not be derived by using the following identity:*

$$\int_0^{\infty}\int_0^{x_2}f_1(x_1,x_2)dx_1dx_2+\int_0^{\infty}\int_0^{x_1}f_2(x_1,x_2)dx_2dx_1+\int_0^{\infty}f_0(x)dx=1 \tag{2.6}$$

from which we get $f_0(x)$ as given above, which completes the proof of the theorem. □

Comment 2.1: From Theorems 2.1 and 2.2, one can easily verify that if $\alpha_1+\alpha_3=\alpha_2+\alpha_3=1$, then both X_1 and X_2 are Rayleigh distributed. Let $\alpha_3=\alpha$ and $\alpha_1=1-\alpha>0$ and $\alpha_2=1-\alpha>0$, then the joint pdf of (X_1,X_2) takes the following form

$$f_{X_1,X_2}(x_1,x_2)=\begin{cases} f_{\mathrm{GR}}(x_1;\lambda,1)\,f_{\mathrm{GR}}(x_2;\lambda,1-\alpha) & \text{if } \infty>x_2>x_1>0,\\ f_{\mathrm{GR}}(x_1;\lambda,1-\alpha)\,f_{\mathrm{GR}}(x_2;\lambda,1) & \text{if } \infty>x_1>x_2>0,\\ \frac{\alpha}{2-\alpha}\,f_{\mathrm{GR}}(x;\lambda,2-\alpha) & \text{if } \infty>x_1=x_2=x>0. \end{cases} \tag{2.7}$$

Therefore, the joint pdf given in (2.7) has Rayleigh marginal distributions.
In the following we show that the BVGR distribution has both a singular part and an absolute continuous part similar to the Marshal-Olkin's bivariate exponential distribution, Sarhan and Balkrishnan bivariate distribution and the bivrariate generalized exponential distribution provided by Kundu and Gupta [6]. The function $f_{X_1,X_2}(.,.)$ may be considered to be a density function for the BVGR distribution if it is understood that the first two terms are densities with respect to two-dimensional Lebesgue measure and the third term is a density function with respect to one dimensional Lebesgue measure, see for example Bemis et al. [3]. It is well known that although in one dimension the practical use of a distribution with this property is usually pathological, but they do arise quite naturally in higher dimension. In case of BVGR distribution, the presence of a singular part means that if X_1 and X_2 are BVGR distribution, then $X_1=X_2$ has a positive probability. In many practical situations it may happen that X_1 and X_2 both are continuous random variables, but $X_1=X_2$ has a positive probability, see Marshall and Olkin [9], in this connection. In the following, we provide the explicit forms of the absolute continuous and the singular parts of the BVGR distribution.

Theorem 2.3. *If (X_1,X_2) follows the BVGR$(\lambda,\alpha_1,\alpha_2,\alpha_3)$, then*

$$F_{X_1,X_2}(x_1,x_2) \;=\; \frac{\alpha_3}{\alpha_{123}}\,F_s(x_1,x_2)+\frac{\alpha_{12}}{\alpha_{123}}\,F_a(x_1,x_2) \tag{2.8}$$

where the singular and the absolute continuous parts $F_s(.,.)$ and $F_a(.,.)$ are, for $x_3=\min\{x_1,x_2\}$,

$$F_s(x_1,x_2) \;=\; \left(1-e^{-\lambda^2x_3^2}\right)^{\alpha_{123}}, \tag{2.9}$$

and

$$F_a(x_1,x_2)=\frac{\alpha_{123}}{\alpha_{12}}\prod_{i=1}^{3}\left(1-e^{-\lambda^2x_i^2}\right)^{\alpha_i}-\frac{\alpha_3}{\alpha_{12}}\left(1-e^{-\lambda^2x_3^2}\right)^{\alpha_{123}}. \tag{2.10}$$

Proof. The joint cdf $F_{X_1,X_2}(x_1,x_2)$ can be written as

$$F_{X_1,X_2}(x_1,x_2)=P(X_1\le x_1,X_2\le x_2|A)\,P(A)+P(X_1\le x_1,X_2\le x_2|A')\,P(A')$$

Let $A=\{U_1<U_3\}\cap\{U_2<U_3\}\equiv\{X_1=X_2\}$, therefore,

$$P(A)=\int_0^\infty 2\alpha_3\lambda^2x\,e^{-\lambda^2x^2}\left(1-e^{-\lambda^2x^2}\right)^{\alpha_{123}-1}dx=\frac{\alpha_3}{\alpha_{123}},$$

and

$$\begin{aligned} F_s(x_1,x_2) &= P(X_1\le x_1,X_2\le x_2|A)\\ &= \alpha_{123}\int_0^{x_3}2\lambda^2x\,e^{-\lambda^2x^2}\left(1-e^{-\lambda^2x^2}\right)^{\alpha_{123}-1}dx\\ &= \left(1-e^{-\lambda^2x_3^2}\right)^{\alpha_{123}}. \end{aligned}$$

Once, $P(A)$ and $F_s(x_1,x_2)$ are obtained, the function $F_a(x_1,x_2)$ can be derived by subtraction as given in (2.10). It can be easily shown that F_s is the singular part as its mixed second partial derivatives is zero when $x_1\neq x_2$, and F_a is the absolute continuous part as its mixed second partial derivative gives a density function. □

Corollary 2.4. *If (X_1,X_2) follows the BVGR$(\lambda,\alpha_1,\alpha_2,\alpha_3)$, then the joint pdf of (X_1,X_2) can be expressed as a mixture of the singular and absolute parts as*

$$f_{X_1,X_2}(x_1,x_2)=\frac{\alpha_3}{\alpha_{123}}\,f_s(x_3)+\frac{\alpha_{12}}{\alpha_{123}}\,f_a(x_1,x_2) \tag{2.11}$$

where

$$f_s(x_3) \;=\; f_{GR}(x_3;\alpha_{123},\lambda)\;\; \textit{if } x_1=x_2=x_3=\min\{x_1,x_2\}$$

and

$$f_a(x_3)=\frac{\alpha_{123}}{\alpha_{12}}\begin{cases} f_{GR}(x_1,\alpha_{13},\lambda)\,f_{GR}(x_2;\alpha_2,\lambda) & \textit{if } x_1<x_2\\ f_{GR}(x_1,\alpha_1,\lambda)\,f_{GR}(x_2;\alpha_{23},\lambda) & \textit{if } x_1>x_2. \end{cases}$$

Here $f_s(.)$ and $f_a(.,.)$ are the singular and absolute continuous parts, respectively.

Figures 2.1 and 2.2 show different shapes of the joint pdf and the jhrf of the BVGR distribution along with their contours for different sets of values of parameters.

Set (1):$(\alpha_1, \alpha_2, \alpha_3, \lambda) = (1.2, 1.2, 0.2, 1)$

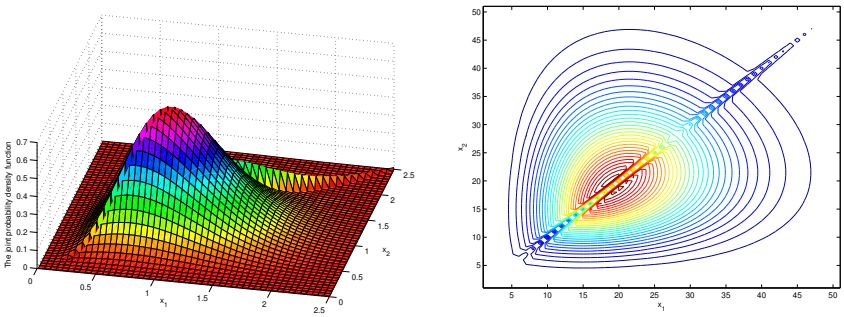

Set (2): $(\alpha_1, \alpha_2, \alpha_3, \lambda) = (1.2, 1.2, 2.1, 1)$

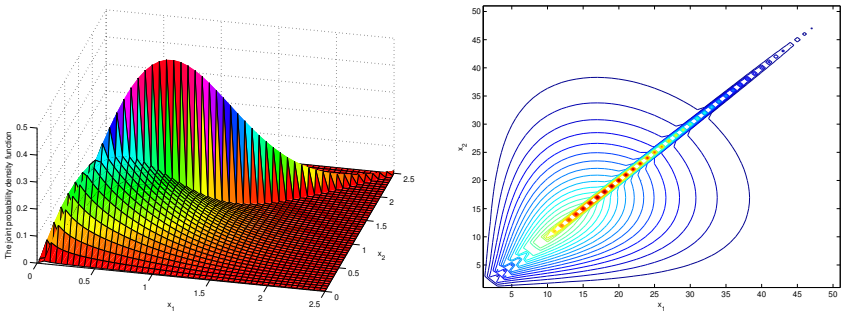

Set (3): $(\alpha_1, \alpha_2, \alpha_3, \lambda) = (1.2, 1.2, 1.0, 1)$

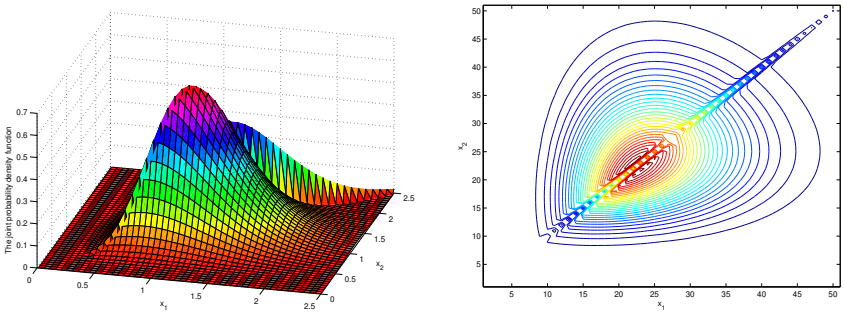

Set (4): $(\alpha_1, \alpha_2, \alpha_3, \lambda) = (1.2, 0.2, 2.1, 1)$

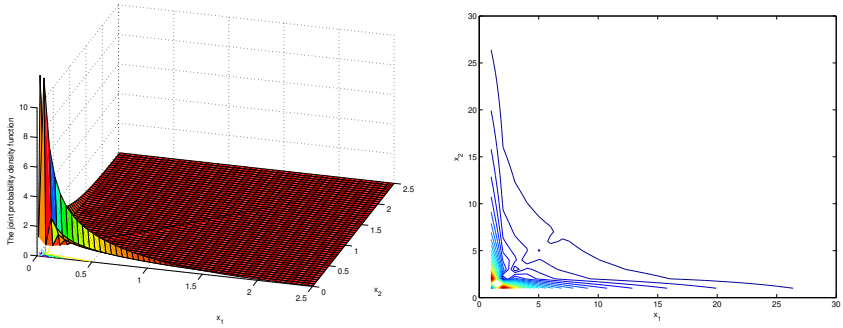

Figure 2.1: The joint probability density function of BVGR distribution.

Set (1):$(\alpha_1, \alpha_2, \alpha_3, \lambda) = (1.2, 1.2, 0.2, 1)$

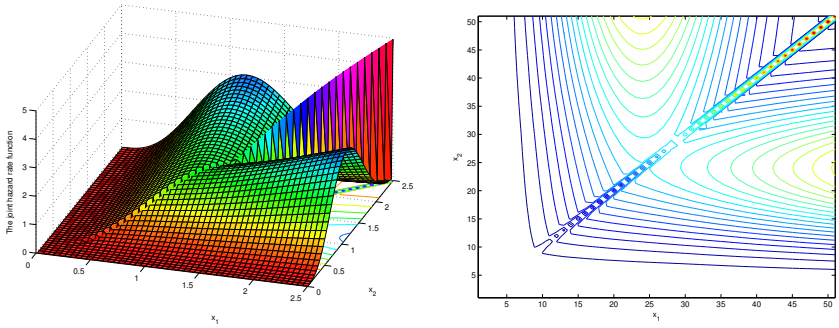

Set (2): $(\alpha_1, \alpha_2, \alpha_3, \lambda) = (1.2, 1.2, 2.1, 1)$

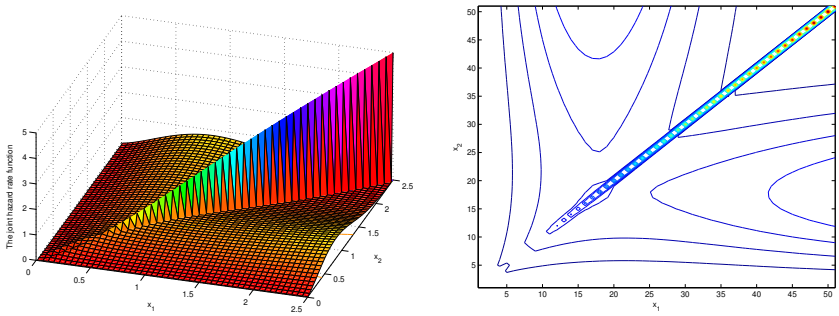

Set (3): $(\alpha_1, \alpha_2, \alpha_3, \lambda) = (1.2, 1.2, 1.0, 1)$

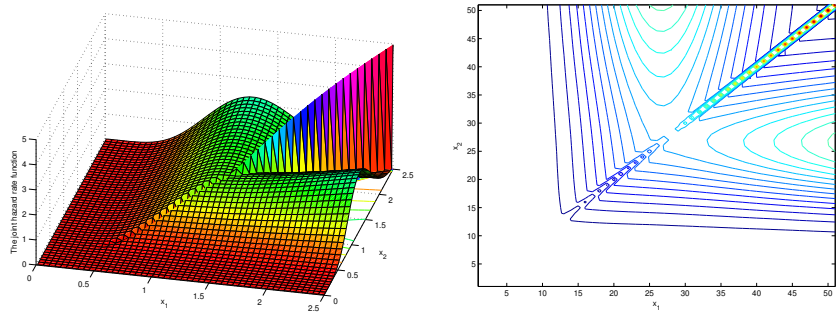

Set (4): $(\alpha_1, \alpha_2, \alpha_3, \lambda) = (1.2, 0.2, 2.1, 1)$

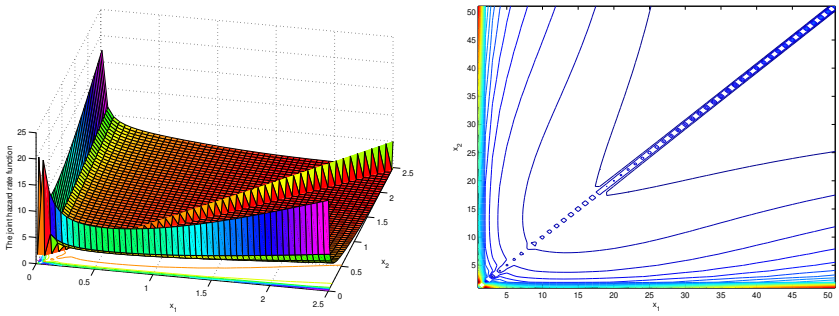

Figure 2.2: The joint hazard rate function of the BVGR distribution.

3. Statistical properties

3.1. Marginal distributions

We can easily verify that the marginal distribution of X_i, $i = 1,2$, follows GR(λ, α_{i3}). That is, the marginal cdf of X_i is

$$F_{X_i}(x_i) = \left(1 - e^{-(\lambda x_i)^2}\right)^{\alpha_{i3}}, \; x > 0. \tag{3.1}$$

Therefore, the marginal survival function of X_i is

$$S_{X_i}(x) = 1 - F_{X_i}(x) = 1 - \left(1 - e^{-(\lambda x)^2}\right)^{\alpha_{i3}}, \; x > 0. \tag{3.2}$$

The relation (3.2) gives the survival function of a parallel system with two independent units, say i and 3. The lifetime of unit i is U_i which follows GR(λ, α_i) and the lifetime of unit 3 is U_3 which follows GR(λ, α_3). Thus, the system lifetime $X_i = \max\{U_i, U_3\}$ follows GR$(\lambda, \alpha_i + \alpha_3)$.
Using (3.1), the marginal pdf of X_i is

$$f_{X_i}(x) = 2\lambda^2 \alpha_{i3} x e^{-(\lambda x)^2} \left(1 - e^{-(\lambda x)^2}\right)^{\alpha_{i3}-1}, \tag{3.3}$$

and the marginal hrf of X_i is

$$h_{X_i}(x) = \frac{2\lambda^2 \alpha_{i3} x e^{-(\lambda x)^2} \left(1 - e^{-(\lambda x)^2}\right)^{\alpha_{i3}-1}}{1 - \left(1 - e^{-(\lambda x)^2}\right)^{\alpha_{i3}}}. \tag{3.4}$$

It is observed by Raqab and Kundu (2006) that: (1) if $\alpha_{i3} \leq \frac{1}{2}$, the pdf is decreasing and the hrf takes a bathtub shape, (2) if $\alpha_{i3} > \frac{1}{2}$, the pdf is right-skewed and unimodal and the hrf is increasing. Shapes of the pdf and hrf of X_i for different values of λ and α_{i3} are provided in Figure 3.1. Surles and Padgett [15] showed that the GR distribution can be used quite effectively in modeling strength univariate data and also modeling general univariate lifetime data. Hence, we expect that the BVGR distribution can be used quite effectively in modeling strength bivariate data and also modeling general bivariate lifetime data comparing to the MO and the BVGE distributions.

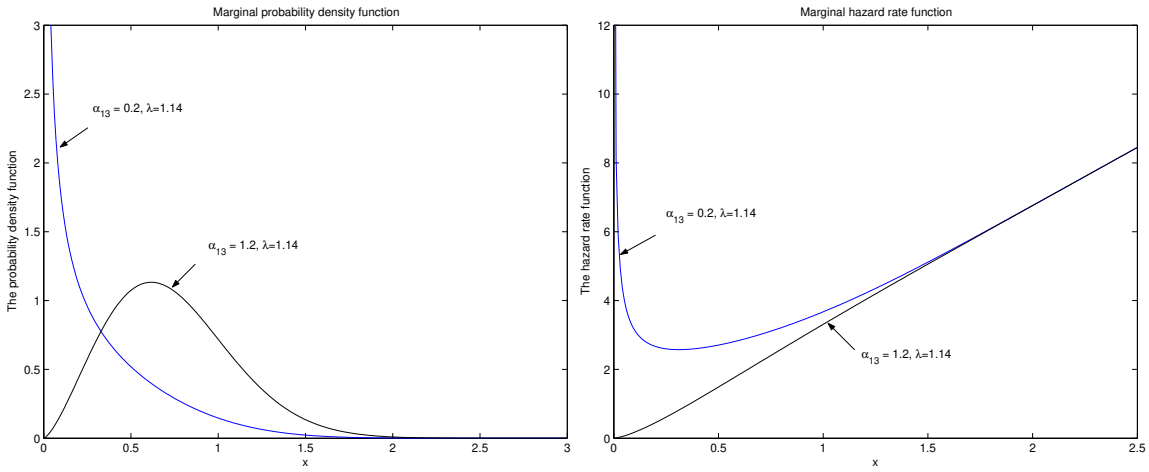

Figure 3.1: The probability density [left panel] and hazard rate [right panel] functions of the marginal distribution of X_1.

3.2. Conditional distributions

The following theorem provides the conditional pdf of X_1 given $X_2 = x_2$, say $f_{X_1|X_2}(x_1|x_2)$, which is not continuous at $X_1 = x_2$.

Theorem 3.1. *If $(X_1, X_2) \sim BVGR(\lambda, \alpha_1, \alpha_2, \alpha_3)$, then conditional pdf of X_1 given $X_2 = x_2$ is*

$$f_{X_1|X_2}(x_1|x_2) = \frac{\alpha_3}{\alpha_{123}} f^{(s)}_{1|2}(x_1|x_2) + \frac{\alpha_{12}}{\alpha_{123}} f^{(a)}_{1|2}(x_1|x_2) \tag{3.5}$$

where

$$f^{(s)}_{1|2}(x_1|x_2) \;=\; \frac{\alpha_{123}}{\alpha_{23}} F_{GR}(x_2; \lambda, \alpha_1) \;\; if \; x_1 = x_2$$

and

$$f^{(a)}_{1|2}(x_1|x_2) = \frac{\alpha_{123}}{\alpha_{12}} \begin{cases} \frac{\alpha_2}{\alpha_{23}} \frac{f_{GR}(x_1;\lambda,\alpha_{13})}{F_{GR}(x_2;\lambda,\alpha_3)} & if \; x_1 < x_2, \\ f_{GR}(x_1;\lambda,\alpha_1) & if \; x_1 > x_2. \end{cases}$$

Proof. *These results are obtained using the definition of conditional probability and the results of Corollary 2.4 and equation (3.3).*

The conditional pdf of X_1 given $X_2 = x_2$ can be rewritten as

$$\begin{aligned} f_{X_1|X_2}(x_1|x_2) &= \frac{\alpha_3}{\alpha_{23}} F_{GR}(x_1;\lambda,\alpha_1) I_{x_1=x_2} + f_{GR}(x_1;\lambda,\alpha_1) I_{x_1>x_2} \\ &\quad + \frac{\alpha_2}{\alpha_{23}} \frac{f_{GR}(x_1;\lambda,\alpha_{13})}{F_{GR}(x_2;\lambda,\alpha_3)} I_{x_1<x_2} \end{aligned}$$

where $I_A = 1$ if A is true and 0 otherwise.
Equivalently, $f_{X_1|X_2}(x_1|x_2)$ can be rewritten as in the following form

$$f_{X_1|X_2}(x_1|x_2) = \begin{cases} \frac{2\alpha_2\alpha_{13}\lambda^2 x_1 e^{-\lambda^2 x_1^2}\left(1-e^{-\lambda^2 x_1^2}\right)^{\alpha_{13}-1}}{\alpha_{23}\left(1-e^{-\lambda^2 x_2^2}\right)^{\alpha_3-1}} & x_1 < x_2\,, \\ 2\lambda^2\alpha_1 x_1 e^{-\lambda^2 x_1^2}\left(1-e^{-\lambda^2 x_1^2}\right)^{\alpha_1-1} & x_1 > x_2\,, \\ \frac{\alpha_3}{\alpha_{23}}\left(1-e^{-\lambda^2 x^2}\right)^{\alpha_1} & x_1 = x_2\,. \end{cases}$$

Obviously, the $f_{X_1|X_2}(x_1|x_2)$ is not continuous when $X_1 = x_2$. Plots in Figure 3.2 give different patterns of the conditional pdf's of X_1 given $X_2 = x_2$ plotted at different values of x_2 ($x_2 = 1.5, 0.5$) and different sets of parameters.
Similarly, the conditional pdf of X_2 given $X_1 = x_1$, which is not continuous at $X_2 = x_1$, can be derived in a similar form as above.

Theorem 3.2. *If $(X_1,X_2) \sim BVGR(\lambda,\alpha_1,\alpha_2,\alpha_3)$, then the conditional cumulative distribution function of X_1 given $X_2 \le x_2$, say $F_{X_1|X_2\le x_2}(x_1)$, is an absolute continuous function which is given by*

$$\begin{aligned} F_{X_1|X_2\le x_2}(x_1) &= P(X_1 \le x_1 | X_2 \le x_2) \\ &= \frac{F_{GR}(x_1;\alpha_1) F_{GR}(x_3;\alpha_3)}{F_{GR}(x_2;\alpha_3)} \\ &= \begin{cases} \left(1-e^{-\lambda^2 x_1^2}\right)^{\alpha_{13}} \left(1-e^{-\lambda^2 x_2^2}\right)^{-\alpha_3} & \text{if } x_1 \le x_2 \\ \left(1-e^{-\lambda^2 x_1^2}\right)^{\alpha_1} & \text{if } x_1 > x_2 \end{cases} \end{aligned}$$

Proof. *These results are obtained using the definition of conditional probability and the results of Theorems 2.3 and 3.1.*

Comment: Using Theorem 3.2, different moments of X_1, X_2, and conditional moments of $X_2|X_1 = x_1$ or $X_1|X_2 = x_2$ can be obtained in terms of infinite series.

Remarks If $(X_1,X_2) \sim \text{BVGR}(\lambda,\alpha_1,\alpha_2,\alpha_3)$ distribution, then

1. The cdf of $\max\{X_1,X_2\}$ is

$$P(\max\{X_1,X_2\} \le x) = \left(1-e^{-\lambda^2 x^2}\right)^{\alpha_1+\alpha_2+\alpha_3}. \tag{3.6}$$

That is, the $\max\{X_1,X_2\}$ has $\text{GR}(\lambda,\alpha_1+\alpha_2+\alpha_3)$. This result means that the reliability function of a parallel system with three independent units such that the lifetime of unit i follows $\text{GR}(\lambda,\alpha_i)$, $i = 1,2,3$, is

$$R(x) = 1 - \left(1-e^{-\lambda^2 x^2}\right)^{\alpha_1+\alpha_2+\alpha_3}. \tag{3.7}$$

2. For all $0 < x_1, x_2 < \infty$,

$$F_{X_1,X_2}(x_1,x_2) \ge F_{X_1}(x_1) F_{X_2}(x_2)\,. \tag{3.8}$$

One can easily prove (3.8), as follows. Since

$$F_{X_1,X_2}(x_1,x_2) = \bar{F}_{U_1}(x_1) F_{U_2}(x_2) F_{U_3}(x_3),\ x_3 = \min(x_1,x_2) \tag{3.9}$$

and

$$F_{X_1}(x_1) F_{X_2}(x_2) = F_{U_1}(x_1) F_{U_3}(x_1) F_{U_2}(x_2) F_{U_3}(x_2)\,. \tag{3.10}$$

From (3.9) and (3.10), we get

$$\begin{aligned} F_{X_1,X_2}(x_1,x_2) - F_{X_1}(x_1) F_{X_2}(x_2) &= F_{U_1}(x_1) F_{U_2}(x_2) \\ &\quad \times \begin{cases} F_{U_3}(x_1) \bar{F}_{U_3}(x_2) & if\ x_1 \le x_2 \\ \bar{F}_{U_3}(x_1) F_{U_3}(x_2) & if\ x_1 > x_2 \end{cases} \\ &\ge 0. \end{aligned}$$

which completes the proof of (3.8).

3. For all $0 < x_1, x_2 < \infty$,

$$\bar{F}_{X_1,X_2}(x_1,x_2) \ge \bar{F}_{X_1}(x_1) \bar{F}_{X_2}(x_2). \tag{3.11}$$

4. From (3.8), one can say that X_1 and X_2 are positive quadratic dependent. That is, for every pair of increasing functions $g_1(.)$ and $g_2(.)$,

$$Cov(g_1(X_1), g_2(X_2)) \ge 0.$$

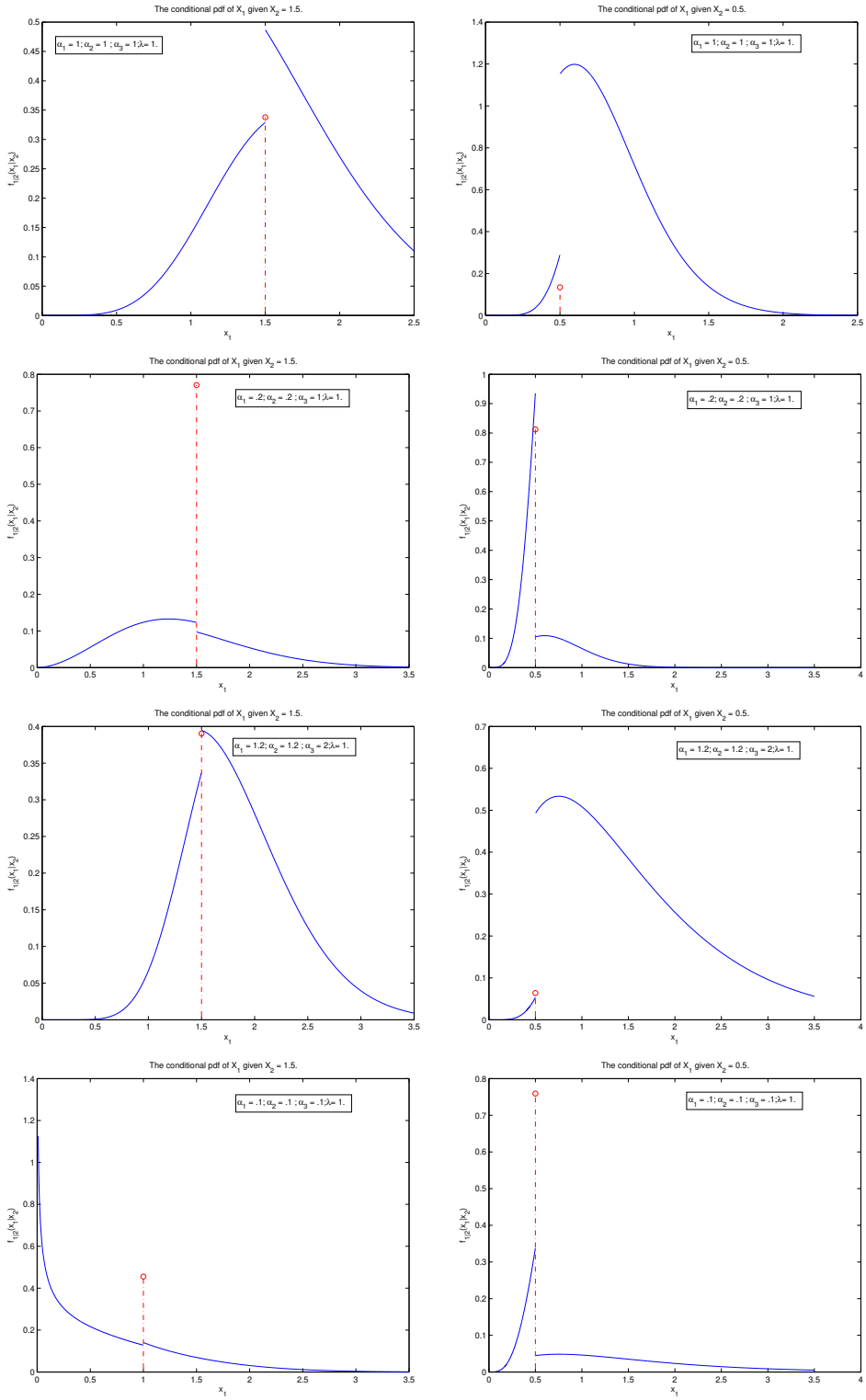

Figure 3.2: The conditional probability density function of X_1, given X_2 at different sets of the parameters.

3.3. Joint hazard rate function

Using the forms (2.3) and (3.1) together with the relations between the joint sf and the joint cdf of (X_1, X_2) given by

$$S_{X_1,X_2}(x_1,x_2) = 1 - F_{X_1}(x_1) - F_{X_2}(x_2) + F_{X_1,X_2}(x_1,x_2),$$

we can derive the joint sf of (X_1, X_2) as

$$S_{X_1,X_2}(x_1,x_2) = 1 - \sum_{j=1}^{2} \left\{1 - e^{-(\lambda x_j)^2}\right\}^{\alpha_{j3}} + \prod_{i=1}^{3} \left\{1 - e^{-(\lambda x_j)^2}\right\}^{\alpha_i}. \tag{3.12}$$

Using the relation between the joint pdf and the jsf of (X_1, X_2), one can derive the joint hazard rate function (jhrf) of (X_1, X_2) according to the following relation

$$h_{X_1,X_2}(x_1,x_2) = \frac{f_{X_1,X_2}(x_1,x_2)}{S_{X_1,X_2}(x_1,x_2)}.$$

Different shapes of the joint hrf and corresponding contour are provided in Figures 4 for different sets of values of the parameters.

4. Parameters' estimations

In this section we discuss the problem of computing the maximum likelihood estimates of the four unknown parameters of the BVRD. Let us assume that (x_{11}, x_{12}), (x_{21}, x_{22}), $\cdots$, (x_{n1}, x_{n2}) be a simple random sample "data" from the BVRD$(\alpha_1, \alpha_2, \alpha_3, \lambda)$. The likelihood function for this sample is

$$l(data;\theta) = \prod_{i=1}^{n} [f_1(x_{1i}, x_{2i})]^{I(x_{1i}<x_{2i})} [f_2(x_{1i}, x_{2i})]^{I(x_{2i}<x_{1i})} [f_0(x_{1i})]^{I(x_{1i}=x_{2i})}, \tag{4.1}$$

where $I(A)$ is an indicator function that is equal to 1 if A is true and 0 otherwise. Substituting (2.11) into (4.1) and take the natural logarithm, we get the log-likelihood function as

$$\begin{aligned}
\mathscr{L} \;=\; & \sum_{i=1}^{n} \Big\{ I(x_{1i} < x_{2i}) \Big[\ln\left(4\lambda^4 \alpha_2 \alpha_{13}\right) + \ln(x_{1i}x_{2i}) - \lambda^2 \left(x_{1i}^2 + x_{2i}^2\right) + \\
& \qquad (\alpha_{13} - 1) \ln\left(1 - e^{-\lambda^2 x_{1i}^2}\right) + (\alpha_2 - 1) \ln\left(1 - e^{-\lambda^2 x_{2i}^2}\right) \Big] \\
& + I(x_{2i} < x_{1i}) \Big[\ln\left(4\lambda^4 \alpha_1 \alpha_{23}\right) + \ln(x_{1i}x_{2i}) - \lambda^2 \left(x_{1i}^2 + x_{2i}^2\right) + \\
& \qquad (\alpha_{23} - 1) \ln\left(1 - e^{-\lambda^2 x_{2i}^2}\right) + (\alpha_1 - 1) \ln\left(1 - e^{-\lambda^2 x_{1i}^2}\right) \Big] \\
& + I(x_{2i} = x_{1i}) \Big[\ln\left(2\lambda^2 \alpha_3\right) + \ln(x_{1i}) - \lambda^2 x_{1i}^2 + (\alpha_{123} - 1) \ln\left(1 - e^{-\lambda^2 x_{1i}^2}\right) \Big\}.
\end{aligned} \tag{4.2}$$

4.1. Maximum likelihood method

Maximum likelihood point estimates (MLE) of the vector of the four unknown parameters is the value of that vector that maximizes the log-likelihood function (4.2). That is the MLE of $\theta = (\alpha_1, \alpha_2, \alpha_3, \lambda)$ is the solution of the following system of four non-linear equations with respect to $\alpha_1, \alpha_2, \alpha_3$, and λ.

$$\begin{aligned}
0 \;=\; & \frac{n_1}{\alpha_1 + \alpha_3} + \frac{n_2}{\alpha_1} + \sum_{i=1}^{n} \ln\left(1 - e^{-\lambda^2 x_{1i}^2}\right), \\
0 \;=\; & \frac{n_2}{\alpha_2 + \alpha_3} + \frac{n_1}{\alpha_2} + \sum_{i=1}^{n} \ln\left(1 - e^{-\lambda^2 x_{2i}^2}\right), \\
0 \;=\; & \frac{n_0}{\alpha_3} + \frac{n_1}{\alpha_1 + \alpha_3} + \frac{n_2}{\alpha_2 + \alpha_3} + \sum_{i=1}^{n} \Big[I(x_{1i} < x_{2i}) \ln\left(1 - e^{-\lambda^2 x_{1i}^2}\right) \\
& + \{I(x_{1i} > x_{2i}) + I(x_{1i} = x_{2i})\} \ln\left(1 - e^{-\lambda^2 x_{2i}^2}\right) \Big], \\
0 \;=\; & 2\lambda \sum_{i=1}^{n} \Bigg\{ I(x_{1i} < x_{2i}) \left[\frac{(\alpha_2 - 1)x_{2i}^2}{e^{\lambda^2 x_{2i}^2} - 1} + \frac{(\alpha_{13} - 1)x_{1i}^2}{e^{\lambda^2 x_{1i}^2} - 1} - x_{1i}^2 - x_{2i}^2 \right] + \\
& \qquad I(x_{1i} > x_{2i}) \left[\frac{(\alpha_1 - 1)x_{1i}^2}{e^{\lambda^2 x_{1i}^2} - 1} + \frac{(\alpha_{23} - 1)x_{2i}^2}{e^{\lambda^2 x_{2i}^2} - 1} - x_{1i}^2 - x_{2i}^2 \right] + \\
& \qquad I(x_{1i} = x_{2i}) \left[\frac{(\alpha_{123} - 1)x_{1i}^2}{e^{\lambda^2 x_{1i}^2} - 1} - x_{1i}^2 \right] \Bigg\} + \frac{4}{\lambda} \left(n_1 + n_2 + \frac{1}{2} n_0 \right),
\end{aligned} \tag{4.3}$$

where $n_1 = \sum_{i=1}^{n} I(x_{1i} < x_{2i})$, $n_2 = \sum_{i=1}^{n} I(x_{1i} > x_{2i})$, and $n_0 = \sum_{i=1}^{n} I(x_{1i} = x_{2i})$. The likelihood equations (4.3) do not have an explicit solution. Therefore, the distribution of the MLE of the parameters cannot be derived in an explicit form. Hence, we could not obtain the explicit confidence intervals for the parameters. We use R to get the MLEs and the corresponding Fisher information matrix. Using normality property of MLEs, we can construct the asymptotic confidence interval for each parameter.

4.2. Bayes estimation

Let us assume that the four parameters are independent random variables with gamma priori distributed. That is, the joint prior pdf of θ is

$$g_0(\theta) \propto \alpha_1^{a_{11}-1}\alpha_2^{a_{21}-1}\alpha_3^{a_{31}-1}\lambda^{a_{41}-1}e^{-a_{12}\alpha_1-a_{22}\alpha_2-a_{32}\alpha_3-a_{42}\lambda}\,,\ \alpha_1,\alpha_2,\alpha_3,\lambda>0\,, \tag{4.4}$$

where the hyperparameters a_{ij}, $i=1,2,3,4$ and $j=1,2$ are all positive and reflect the prior knowledge about the parameters. The log-prior density function is

$$\mathscr{G}_0(\theta) \propto (a_{41}-1)\ln(\lambda) - a_{42}\lambda + \sum_{i=1}^{3}\left[(a_{i1}-1)\ln(\alpha_i) - a_{i2}\alpha_i\right]. \tag{4.5}$$

Applying Bayes' theorem and using the likelihood function of the available data and the joint prior distribution of θ, the joint posterior probability density function of θ, given data, is

$$g(\theta|\text{data}) = \frac{1}{K}\exp\{\mathscr{L}+\mathscr{G}_0(\theta)\}\,, \tag{4.6}$$

where K is the normalizing constant. Obviously, the joint posterior distribution of θ is analytically intractable. Therefore, under the squared-error loss, Bayes estimators of the parameters and/or of any parametric function of θ, say $w(\theta)$, involve ratio of two multidimensional integrals as

$$\hat{w}(\text{data}) = \frac{\int_0^\infty\int_0^\infty\int_0^\infty\int_0^\infty w(\alpha_1,\alpha_2,\alpha_3,\lambda)\exp\{\mathscr{L}+\mathscr{G}_0(\theta)\}\,d\alpha_1\,d\alpha_2\,d\alpha_3\,d\lambda}{\int_0^\infty\int_0^\infty\int_0^\infty\int_0^\infty \exp\{\mathscr{L}+\mathscr{G}_0(\theta)\}\,d\alpha_1\,d\alpha_2\,d\alpha_3\,d\lambda}. \tag{4.7}$$

The integrals in (4.7) do not have analytical solution. Thus, some approximation methods should be used to solve these integrals an calculate the ratio of the integrals. Lindley [7] and Tierney and Kadane [13] discussed some methods of approximations that work well for low dimension. In this paper we will use Markov Chain Monte Carlo method that works well with higher dimensions cases, see Metropolis et al. [8] and Hastings [4]. One of the main advantages of the MCMC is it does not require to calculate the integrals that are needed for the normalizing constant K and/or included in the ratio that gives the Bayes estimators.
The MCMC method generates random draws from the joint posterior distribution by generating draws from an an arbitrary distribution that easy to simulate from then apply an accept-reject method. The arbitrary distribution is named a proposal distribution that satisfies two conditions: (1) it mimics the posterior distribution, (2) easy to simulate from. In this article, we use multivariate normal distribution as a proposal. We follow steps below to generate random draws from the joint posterior distribution (4.6) without computing the normalizing constant K:

1. Set the size of the random draws we wish to generate, say M.
2. Choose an initial guess of θ, say $\theta^{(0)}$.
3. $i=1,2,\cdots,M$, perform the following steps:
   (a) Generate θ^* from the multivariate normal with mean $\theta^{(i-1)}$ and variance-covariance Σ.
   (b) Compute the ratio $\kappa = \min\left\{1, \dfrac{g(\theta^*|\text{data})}{g(\theta^{(i-1)}|\text{data})}\right\}$.
   (c) Generate a random value u from uniform distribution on $(0,1)$.
   (d) If $\kappa \geq u$ set $\theta^{(i)}=\theta^*$, otherwise set $\theta^{(i)}=\theta^{(i-1)}$.

We discard the early M_0 number of burn-in draws and use the remaining $M-M_0$, "$\theta^{(M_0+1)}, \theta^{(M_0+2)}, \cdots, \theta^{(M)}$", as the desired draws from the joint posterior distribution. Thus Bayes estimate of θ_j is

$$\hat{\theta}_j = \frac{\sum_{i=M_0+1}^{M-M_0}\theta_j^{(i)}}{M-M_0}\,,\ j=1,2,3,4.$$

Furthermore, the lower and upper bounds of the $100(1-\vartheta)\%$, $0<\vartheta<1$, Bayesian probability interval (BPI) of θ_j are the $\frac{\vartheta}{2}$ 100th and $(1-\frac{\vartheta}{2})$ 100 th percentiles of the sequence of the $M-M_0$ draws $\theta_j^{(M_0+1)}, \theta_j^{(M_0+2)}, \cdots, \theta_j^{(M)}$, respectively.

5. Application

In order to discuss how the proposed distribution can be implemented in real life, we re-analyze the UEFA Champion's League Data. This data set was originally analyzed in Meintanis [10] using the Marshall-Olkin bivariate exponential model (MO) with three parameters $\lambda_1,\lambda_2,\lambda_3$, then by Kundu and Gupta [6] using the bivariate generalized exponential (BVGE) distribution with four parameters $\alpha_1,\alpha_2,\alpha_3$ and β. Kundu and Gupta [6] reported that the BVGE model fits the data better than MO model. In the following, we use the BVGR distribution to reanalyze this data and compare it with the MO and BVGE models.
Table 1 shows the MLEs of the unknown parameters of the proposed distribution along with the values of the log-likelihhod values and the Akaike information criterion (AIC; see [2]). The AIC suggests that the BVGR distribution provides a better fit than both the MO and BVGE distributions.
For Bayesian computations, we assumed that: (1) the four parameters follow gamma prior distributions with all hyperparameters equal and equal to 0,001, (2) the proposal distribution is multinormal with variance covariance matrix, which is the same as the Fisher information matrix,

$$\Sigma = \begin{pmatrix} 0.016461 & 9.574e-04 & 0.0011642 & -1.135e-04 \\ 0.000957 & 4.188e-03 & -0.0010077 & -2.663e-05 \\ 0.001164 & -1.008e-03 & 0.0086362 & -6.134e-05 \\ -0.000114 & -2.663e-05 & -0.0000613 & 3.688e-06 \end{pmatrix}.$$

Distribution	MLE	$\mathscr{L}$	AIC
MO	$\hat{\lambda}_1 = 0.012$, $\hat{\lambda}_2 = 0.014$, $\hat{\lambda}_3 = 0.022$	-339.006	684.012
MVGE	$\hat{\alpha}_1 = 1.351$, $\hat{\alpha}_2 = 0.465$, $\hat{\alpha}_3 = 1.153$, $\hat{\beta} = 0.039$	-296.935	601.870
MVGR	$\hat{\alpha}_1 = 0.492$, $\hat{\alpha}_2 = 0.166$, $\hat{\lambda}_3 = 0.410$, $\hat{\lambda} = 0.020$	-293.357	594.714

Table 1: The MLEs of the parameters, the log-likelihood values and AIC values.

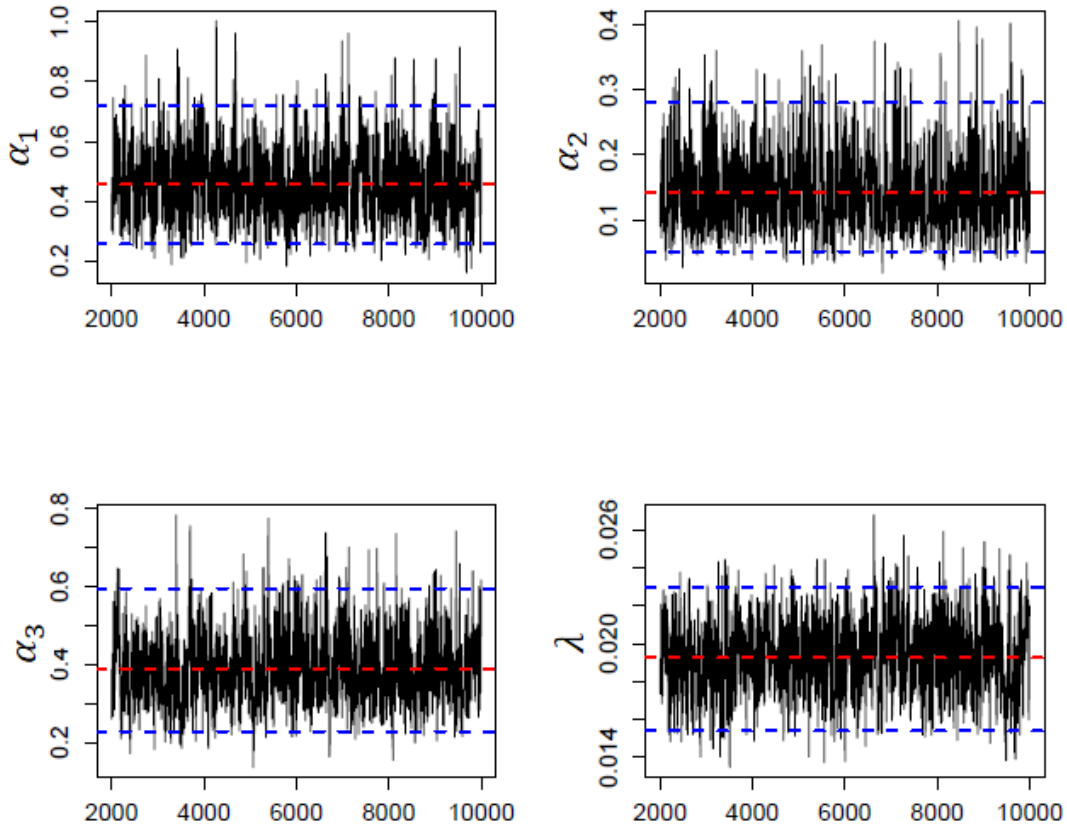

Figure 5.1: The trace plot of the random draws from the joint posterior distribution along with the posterior mean and the limits of the 95% BPI after discarding the early 2000 draws.

The acceptance rate is 37.07% which is very high for a four parameter case. The trace plots of the draws are plotted in Figure 5.1 after discarding the early 2000 draws (burn-in period). The trace plots show a good mix of the simulated draws. As a further diagnostic test for the draws, we provide the autocorrelations (ACFs) of the simulated draws from the joint posterior distribution of the four parameters after discarding the early 20% of the draws as shown in Figure 5.2. From the ACFs plot, we see that the Lag goes to zero very rapidly which indicates the draws converge to the actual distribution very fast.

Using the simulated draws, the posterior mean (Bayes estimates under squared error loss), median (Bayes estimate under absolute error loss) and the bounds of a 95% Bayesian probability intervals for the parameters are calculated as given in Table 2. Furthermore, the marginal posterior density functions are estimated as presented in Figure **??**.

6. Conclusions

A new bivariate lifetime distribution named bivariate generalized Rayleigh (BVGR) distribution function whose marginals are generalized Rayleigh distributions is proposed in this paper. The BVGR distribution is of Marshal-Olkin type. It is observed that the BVGR distribution is a singular distribution and has an absolute continuous part and a singular part. Since the joint distribution function and the joint density

			95% Bayesian Probability Interval	
Parameter	Mean	Median	Lower limit	upper limit
α_1	0.4569	0.4467	0.2568	0.7194
α_2	0.1423	0.1337	0.0507	0.2802
α_3	0.3895	0.3794	0.2288	0.5951
λ	0.0193	0.0192	0.0154	0.0230

Table 2: The basic posterior characteristics for the four parameters of the BVGR distribution.

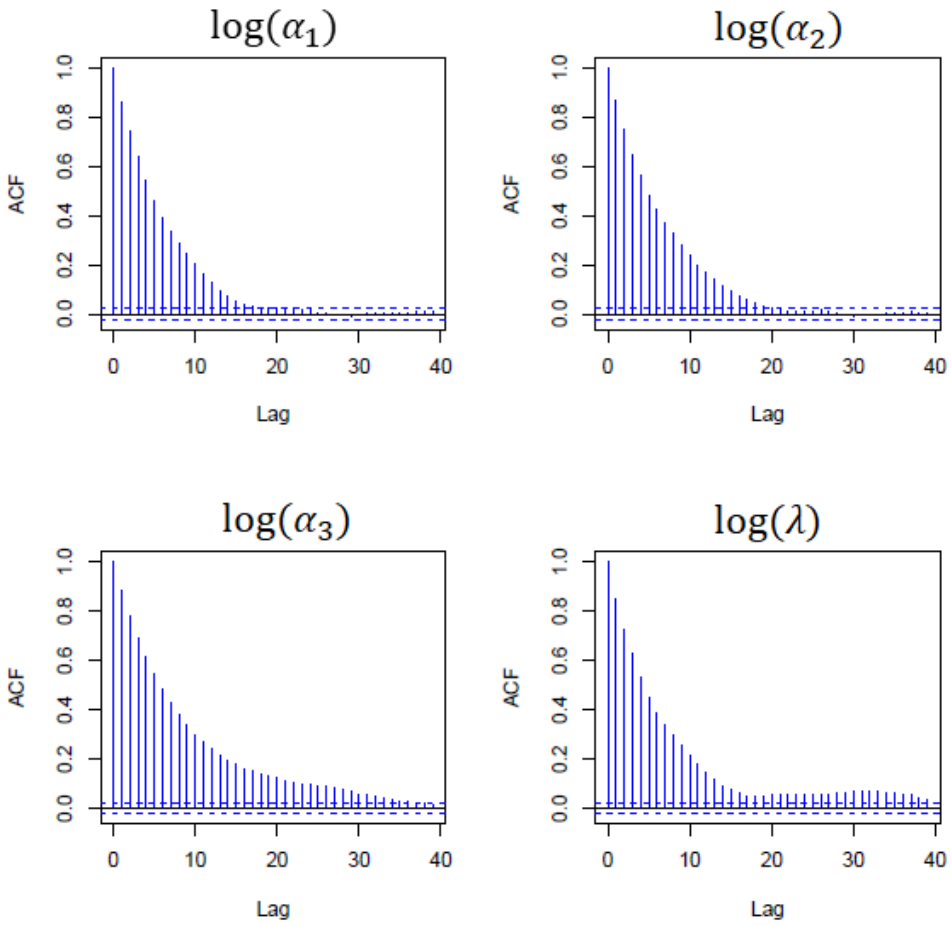

Figure 5.2: The autocorrelations of the simulated draws from the joint posterior distribution of the four parameters after discarding the early 20% of the draws.

function are in closed forms, this distribution can be used in practice for non-negative and positively correlated random variables. We investigated some statistical properties of the proposed distribution. Also, the marginal and conditional distribution of the BVGR distribution are derived in closed forms. The maximum likelihood and Bayesian methods are applied to estimate the four unknown parameters of the BVGR distribution. For Bayesian method, we used the Markov chain Monte Carlo (MCMC) method. One real data set is analyzed using the BVGR distribution which showed a better fit than the MO and BVGE distributions for this data set.

Acknowledgement

I would like to thank the reviewers for their comments.

References

[1] Al-khedhari A, Sarhan AM and Tadj L. Estimation of the generalized Rayleigh distribution parameters, *International Journal of Reliability and Applications*, (2008), **7**(1), *1-12*.
[2] Akaike H. Fitting autoregressive model for regression. *Annals of the Institute of Statistical Mathematics*, (1969), **21**, 243-247.
[3] Bemis B, Bain LJ and Higgins JJ. Estimation and hypothesis testing for the parameters of a bivariate exponential distribution, *Journal of the American Statistical Association,* (1972), **67**, 927-929.
[4] Hastings WK. Monte Carlo sampling methods using Markov chains and their applications. *Biometrika*, (1970), **57**, 97-109.
[5] Kundu D, Sarhan AM and Gupta RD. On Sarhan-Balakrishnan bivariate distribution. *Journal of Statistics and Probability*, (2012), **1**, no. 3, 163-170.
[6] Kundu D and Gupta RD. Bivariate Generalized Exponential Distribution, *Journal of Multivariate Analysis*, (2009), **100**, 581-593.
[7] Lindley DV. Approximate Bayesian methods. *Trabajos de Estadistica*, (1980), **31**, 223-245.
[8] Metropolis N, Rosenbluth AW, Rosenbluth MN, Teller AH, Teller E. Equation of state calculations by fast computing machines. *Journal of Chemical Physics*, (1953), **21**, 1087-1092.
[9] Marshall AW and Olkin IA. A multivariate exponential distribution, *Journal of American Statistical Association*, (1967), **62**, 30-44.
[10] Meintanis SG. Test of fit for Marshall-Olkin distributions with applications, *Journal of Statistical Planning and inference*, (2007), **137**, 3954-3963.
[11] Mudholkar GS and Srivastava DK. Exponentiated Weibull family for analyzing bathtub failure-rate data, *IEEE Transactions on Reliability*, (1993), **42**, 299-302.
[12] Raqab MZ, Kundu D. Burr Type X distribution; revisited, *Journal of Probability and Statistical Science,* (2006), **4**(2), 179-193.
[13] Tierney L, Kadane JB. Accurate approximations for posterior moments and marginal densities. *Journal of American Statistical Association*, (1986), **81**, 82-86.
[14] Sarhan AM and Balakrishnan N. A new class of bivariate distributions and its mixture. *Journal of Multivariate Analysis*, (2007), **98**, 1508-1527.
[15] Surles JG and Padgett WJ. Inference for reliability and stress-strength for a scaled Burr Type X distribution, *Lifetime Data Analysis*, (2001), **7**, 187-200.
[16] Surles JG and Padgett WJ. Some properties of a scaled Burr type X distribution, *Journal of Statistical Planning and Inference*, (2005), **128**, 271-280.

Journal of Mathematical Sciences and Modelling, 2 (2) (2019) 112-116
Research Article

Journal of Mathematical Sciences and Modelling

Journal Homepage: www.dergipark.gov.tr/jmsm
ISSN 2636-8692
DOI: http://dx.doi.org/10.33187/jmsm.435481

Conformable Fractional Cosine Families of Operators

M. Elomari[1*], S. Melliani[1] and L. S. Chadli[1]

[1] *Laboratory of Applied Mathematics and Scientific Calculus, Sultan Moulay Slimane University, BP 523, 23000, Beni Mellal, Morocco*
[*] *Corresponding author*

Article Info

Keywords: *α-cosine families, Conformable derivative, Mild solution.*
2010 AMS: *26A33*
Received: *21 June 2018*
Accepted: *21 January 2019*
Available online: *August 2019*

Abstract

In this paper we are concerned with the problem

$$\begin{cases} u^{(\alpha)}(t) = Au(t) + f(t,u(t)) \quad t \in [0,T] \\ u(0) = u_0, D^{\alpha}u(0) = u_1 \end{cases}$$

$$\begin{cases} u^{(\alpha)}(t) = Au(t) + f(t,u(t)) \quad t \in [0,T] \\ u(0) = u_0, D^{\alpha}u(0) = u_1 \end{cases}$$

Where $\alpha \in (1,2]$, and we use the conformable derivative. We give the notion of α-Cosine families and proveded the existence and uniqueness of the problem 0.1.

1. Introduction

Our primary objective is to investigate the abstract semi-linear α-order initial value problem

$$\begin{aligned} u^{(\alpha)}(t) &= Au(t) + f(t,u(t)) \quad t \in [0,T] \\ u(0) &= u_0, D^{\alpha}u(0) = u_1 \end{aligned}$$

Where $T \in \mathbb{R}_+^*$, $1 < \alpha < 2$, the linear operator $A : D(A) \subset X \to X$, $f : [0,T] \times X \to X$, $\mathscr{C} = \mathscr{C}([0,T],X)$ is the Banach space of all continuous functions equipped with the supnorm.
A is the (possibly unbounded) infinitesimal generator of a strongly continuous α-cosine family of linear operators in X and fis a nonlinear mapping from $f : [0,T] \times X \to X$. Our goal will be to give a systematic and general treatment of (1) from the standpoint of existence, uniqueness of solutions.
The pioneering work concerning the new definition of fractional derivative was done by [6]. This work open the door in front of sevral works in this sens. Thabet Abdeljawad and other authors feat this notion for introducing the basic definition of α-semigroup. But G. F. WEBB in [4] annonces the way to give an integral solution for one second problem, They precisely have considered the notion of cosine families. In this paper we will try to give the definition of α-cosine families, and provide the existence and uniqueness of the problem (1).
This paper is organised as follows. In section 2 we recall some notion concerning the new derivative. Section 3 deal with the Basic definition of α-Cosine families and some properties. The proof of mains results takes place in the last Section.

2. Preliminaries

In this section we will give some definition and properties concerning the new derevative important in the following.

Definition 2.1. *see[6] Let $\alpha \in (n,n+1]$ and $f : [0,\infty) \to \mathbb{R}$ be n-differentiable at $t > 0$, then the conformable fractional derivative of f of order α is defined by*

$$f^{(\alpha)}(t) = \lim_{\varepsilon \to 0} \frac{f^{(n)}(t + \varepsilon t^{n+1-\alpha}) - f^{(n)}(t)}{\varepsilon}$$
$$f^{(\alpha)}(0) = \lim_{t \to 0} f^{(\alpha)}(t)$$

Email addresses and ORCID numbers: m.elomari@usms.ma (M. Elomari), said.melliani@gmail.com (S. Melliani), sa.chadli@yahoo.fr (L. S. Chadli)

Remark 2.2. *see[6] As consequence of the previous definition, one can easily show that*

$$f^{(\alpha)}(t) = t^{n+1-\alpha} f^{(n+1)}(t)$$

where $\alpha \in (n, n+1]$, *and* f *is* $(n+1)$*-differentiable at* $t > 0$.

Definition 2.3. *see[6] Let* $\alpha \in (1,2]$, $(I^{\alpha} f)(t) = \int_0^t s^{\alpha-2} f(s) ds$.

Theorem 2.4. *see[6]*

$$\left(I^{\alpha} f\right)^{(\alpha)}(t) = f(t)$$

for $t \geq 0$

Example 2.5.

$$I^{\alpha}(\sin(t)) = \sum_{n=0}^{\infty} \frac{(-1)^n t^{2n+\alpha}}{(2n+\alpha)(2n+1)!}$$

where $\alpha \in (1,2)$

Definition 2.6. *see[5] Let* $\alpha > 0$. *For a Banach space* X, *A family* $\{T(t)\}_{t \geq 0} \subset \mathscr{L}(X,X)$ *is called a fractional* α*.semigroup if:*

1. $T(0) = I$
2. $T\left((s+t)^{\frac{1}{\alpha}}\right) = T\left(s^{\frac{1}{\alpha}}\right) T\left(t^{\frac{1}{\alpha}}\right)$, *for all* $s,t \in [0,\infty)$

Example 2.7. *Let* A *be a bounded linear operator on* X. *Define* $T(t) = e^{2\sqrt{t}A}$. *Then* $T(t)_{t \geq 0}$ *is a* $\frac{1}{2}$ *semigroup. Indeed:*

1. $T(0) = e^{0A} = I$
2. $\forall s,t \in [0,\infty)$, $T\left((s+t)^2\right) = e^{2(t+s)A} = e^{2tA} e^{2sA} = T(s)T(t)$

Definition 2.8. *see[5] An* α*-semigroup* $T(t)$ *is called a* c_0*-semigroup if, for each fixed* $x \in X$, $T(t)x \to x$ *as* $t \to 0^+$

The conformable α-derivative of $T(t)$ at $t = 0$ is called the α-infinitesimal generator of the fractional α-semigroup $T(t)$, with domain equals

$$\left\{ x \in X,\ \lim_{t \to 0} T(t)x \text{ exist} \right\}$$

3. α-Cosine families

We will give the following definition

Definition 3.1. *A one parameter family* $C^{\alpha}(t), t \in \mathbb{R}$ *of bounded linear operators mapping the Banach space* X *into itself is called a strongly continuous* α*-cosine family if and only if*

1. $C^{\alpha}(0) = I$
2. $C^{\alpha}\left((s+t)^{\frac{1}{\alpha}}\right) + C^{\alpha}\left((s-t)^{\frac{1}{\alpha}}\right) = 2C^{\alpha}\left(s^{\frac{1}{\alpha}}\right) C^{\alpha}\left(t^{\frac{1}{\alpha}}\right)$
3. *The mapping* $t \to C^{\alpha}(t)x$ *is a continuous mapping for each fixed* $x \in X$.

If $C^{\alpha}(t), t \in \mathbb{R}$ is a strongly continuous α-cosine family in X, then:$S^{\alpha}(t)$, $t \in \mathbb{R}$ is the one parameter family of operators in X defined by

$$S^{\alpha}(t) = (I^{\alpha} S^{\alpha})(t)$$

Example 3.2. *Let* A *be a bounded linear operator on* X. *Define* $C^{\alpha}(t) = \frac{e^{2\sqrt{t}A} + e^{-2\sqrt{t}A}}{2}$. *Then* $T(t)_{t \geq 0}$ *is a* $\frac{1}{2}$ *semigroup. Indeed:*

1. $C^{\alpha}(0) = e^{0A} = I$
2. $C^{\alpha}\left((t+s)^2\right) + C^{\alpha}\left((t-s)^2\right) = \frac{e^{2(t+s)A} + e^{-2(t+s)A}}{2} + \frac{e^{2(t-s)A} + e^{-2(t-s)A}}{2} = 2C^{\alpha}(t^2) C^{\alpha}(s^2)$
3. *The continuity is clear*

Proposition 3.3. *The family* $\{C^{\alpha}(t), t \in R\}$ *is a strongly cosine families if only if* $\{C(t) = C^{\alpha}(t)(t^{\frac{1}{\alpha}}), t \in R\}$ *is a strongly continuous cosine families*

Proof. Necessary condition: It is clear that $C(0) = I$. For all $s,t \in \mathbb{R}$, we have

$$\begin{aligned} C(t+s) + C(t-s) &= C^{\alpha}(t+s)(t^{\frac{1}{\alpha}}) + C^{\alpha}(t-s)(t^{\frac{1}{\alpha}}) \\ &= 2C^{\alpha}(t)(t^{\frac{1}{\alpha}}) C^{\alpha}(s)(t^{\frac{1}{\alpha}}) \\ &= 2C(t)C(s) \end{aligned}$$

Further the continuity of $t \to C_q^{\alpha}(t^{\frac{1}{\alpha}})x$ and the continuity of $t \to t^{\alpha}$ implies that $t \to C(t)x$ is continuous.
For the sufficient condition it suffice to note that $Ct^{\alpha} = C^{\alpha}(t)$ □

If $\{C^{\alpha}(t), t \in \mathbb{R}\}$ is a strongly continuous cosine family in X, then $\{S^{\alpha}(t), t \in \mathbb{R}\}$ is the one parameter family of operators in X defined by

$$S^{\alpha}(t)x = (IC^{\alpha})(t)x, \quad \forall t \in \mathbb{R},\ x \in X$$

Remark 3.4. *As the previous proposition* $\{S^{\alpha}(t), t \in \mathbb{R}\}$ *is a* α*-Sine family iff* $\{S(t) = S^{\alpha}(t^{\frac{1}{\alpha}}), t \in \mathbb{R}\}$ *is sine family.*

Proposition 3.5. *Let $C^\alpha(t), t\in\mathbb{R}\}$ be a strongly continuous cosine family in X.*
The following are true:

1. $C^\alpha(t)=C^\alpha(-t)\forall t\in\mathbb{R}$
2. $C^\alpha(s),S^\alpha(s),C^\alpha(t)$, *and* $S^\alpha(t)$ *commute for all* $s,t\in\mathbb{R}$
3. $S^\alpha(t)x$ *is continuous in* t *on* $\mathbb{R}$ *for each fixed* $x\in X$
4. $S^\alpha(s+t)+S^\alpha(s-t)=2S^\alpha(s)C^\alpha(t)$ *for all* $s,t\in\mathbb{R}$
5. $S^\alpha(s+t)=S^\alpha(s)C^\alpha(t)+S^\alpha(t)C^\alpha(s)$ *for all* $s,t\in\mathbb{R}$
6. $S^\alpha(t)=-S^\alpha(-t)$ *for all* $t\in\mathbb{R}$
7. *There exist constants* $M>1$ *and* $\omega\geq 0$ *such that* $C^\alpha(t)\leq Me^{\omega t^\alpha}$ *for all* $t\in\mathbb{R}$ *and*

$$\parallel S^\alpha(t_1)-S^\alpha(t_2)\parallel\leq\frac{M}{\omega}\left(e^{\omega t_1^\alpha}-e^{\omega t_2^\alpha}\right)$$

Proof. The proposition $1-6$ are consequence of the proposition 3.1. For 7, we have

$$\parallel S^\alpha(t_1)-S^\alpha(t_2)\parallel=\int_{t_2}^{t_1}\frac{C^\alpha(s)}{s^{1-\alpha}}ds$$

$$\leq M\int_{t_2}^{t_1}\frac{e^{\omega s^\alpha}}{s^{1-\alpha}}ds=[e^{\omega s}]_{t_2}^{t_1}$$

□

The α-infinitesimal generator of a strongly continuous α-cosine families $C^\alpha(t), t\in\mathbb{R}$ is the operator $A:X\to X$ defined by

$$Ax=\lim_{t\to 0}D^\alpha C^\alpha(t)$$

$$D(A)=\{x,t\to D^\alpha C^\alpha(t)x,\text{ is continuous of } t\}$$

$$E=\{x,t\to DC^\alpha(t)x,\text{ is continuous of } t\}$$

Lemma 3.6.

$$C(t)=\lim_{\alpha\to 1^+}C^\alpha(t)\textit{is a cosine families}$$

Proof. It suffice to note that $C^\alpha(t^{\frac{1}{\alpha}})$ is a cosine families, $t\to t^\alpha$ is continuous. □

Proposition 3.7. *Let $C^\alpha(t)$, $t\in\mathbb{R}$, be a strongly continuous α-cosine family in X with α-infinitesimal generator A. The following are true.*

1. $D(A)$ *is dense in* X *and* A *is a closed operator in* X.
2. *if* $x\in X$ *and* $r,s\in\mathbb{R}$, *then* $z=\int_r^s\frac{S^\alpha(u)}{u^{1-\alpha}}xdu\in D(A)$ *and* $Az=C^\alpha(s)x-C^\alpha(r)x$
3. *if* $x\in X$ *and* $r,s\in\mathbb{R}$, *then* $z=\int_0^s\int_0^r\frac{C^\alpha(u)}{u^{1-\alpha}}\frac{C^\alpha(v)}{v^{1-\alpha}}dvdux\in D(A)$ *and* $Az=2^{-1}(C^\alpha(s+r)x-C^\alpha(s-r)x)$
4. *if* $x\in X$, *then* $S^\alpha(t)x\in E$
5. *if* $x\in E$, *then* $S^\alpha(t)x\in D(A)$ *and* $(C^\alpha)^{(\alpha)}(t)x=AS^\alpha(t)x$
6. *if* $x\in D(A)$, *then* $C^\alpha(t)x\in D(A)$ *and* $D^\alpha C^\alpha(t)x=AC^\alpha(t)x=C^\alpha(t)Ax$
7. *if* $x\in E$, *then* $lim_{t\to 0}AS^\alpha(t)x=0$
8. *if* $x\in E$, *then* $S^\alpha(t)x\in D(A)$ *and* $D^\alpha S^\alpha(t)x=AS^\alpha(t)x$
9. *if* $x\in D(A)$, *then* $S^\alpha(t)x\in D(A)$ *and* $AS^\alpha(t)x=S^\alpha(t)Ax$
10. $C^\alpha(t+s)-C^\alpha(t-s)=2AS^\alpha(t)S^\alpha(s)$ *for all* $s,t\in\mathbb{R}$.

Proof. Use the previous lemma.
For 1 it suffuce to use the previous lemma and proposition 2.2 in [4].
For $2-10$ By change s by $s^{\frac{1}{\alpha}}$ and t by $t^{\frac{1}{\alpha}}$ and use proposition 2.2 in [4]. □

4. Mains results

In this section we consider the problem

$$\begin{array}{c}u^{(\alpha)}(t)=Au(t)+f(t,u(t))\quad t>0,\ \alpha\in(1,2)\\ u(0)=u_0,\ u^{(\alpha)}(0)=u_1\end{array}\qquad(1)$$

Where $A:D(A)\subset X\to X$ is a linear operator α infinitisimal generator of a $C^\alpha(t)$, $t\in\mathbb{R}$-Cosine families, and $u_0\in X$. We set $\mathscr{C}=\mathscr{C}([0,T],X)$.
$f:[0,T]\times X\to X$ is continuous and satisfies a Lipschitz condition $\parallel f(x,y)-f(x,y')\parallel\leq M_f\parallel y-y'\parallel$, $\forall x\in[0,T]$, $x,y\in X$.
T he folowing defiition is a extension of usual definition of mild see [4].

Definition 4.1. *A function $u:[0,\infty)\to X$ is a mild solution of (1) if*

1. u *is continuous differential on* $[0,\infty)$
2. u *is continuously* α*-differentiable on* $(0,\infty)$
3. $u(t)\in D(A)$ *for* $t>0$,
4. $u(t)=C^\alpha(t)u_0+S^\alpha(t)u_1+\int_0^t\frac{S^\alpha(t-s)f(s,u(s))}{s^{2-\alpha}}ds$

Theorem 4.2. *Suppose that $f:[0,T]\times X\to X$ is continuous and Lipschitzian with respect to the second argument, then for any $u_0,u_1\in X$ such that $C^\alpha(t)u_0, S^\alpha u_1\in D(A)$ for all $t>0$, the problem (1) has a unique mild solution*

Proof. Define the operator $P:\mathscr{C}\to\mathscr{C}$ By

$$(Pu)(t)=C^\alpha u_0+S^\alpha u_1+\int_0^t s^{\alpha-2}S^\alpha(t-s)f(s,u(s))$$

We give the proof in sevral step:
Step 1: Let $u_1,u_2\in\mathscr{C}$

$$|(Pu)(t+h)-(Pu)(t)|=\left|\int_0^{t+h}s^{\alpha-1}S^\alpha(t+h-s)f(s,u(s))ds-\int_0^t s^{\alpha-2}S^\alpha(t-s)f(s,u(s))ds\right|$$

$$\leq\left|\int_0^{t+h}s^{\alpha-1}\left(S^\alpha(t+h-s)-S^\alpha(t-s)\right)f(s,u(s))ds\right|+\left|\int_0^t s^{\alpha-2}S^\alpha(t+h-s)f(s,u(s))ds\right|$$

But

$$\left|s^{\alpha-1}\left(S^\alpha(t+h-s)-S^\alpha(t-s)\right)f(s,u(s))\right|\leq T^{\alpha-1}Mhe^{\omega T^\alpha}\sup_{s\in[0,T]}||f(s,u(s))||$$

By the dominated convergence theorem

$$\int_0^{t+h}s^{\alpha-2}\left(S^\alpha(t+h-s)-S^\alpha(t-s)\right)f(s,u(s))ds\to 0,\ \text{as } h\to 0$$

Also

$$\left|s^{\alpha-1}S^\alpha(t+h-s)f(s,u(s))\right|\leq T^{\alpha-2}Me^{\omega h}\sup_{s\in[0,T]}||f(s,u(s))||$$

By the dominated convergence theorem

$$\left|\int_0^t s^{\alpha-2}S^\alpha(t+h-s)f(s,u(s))ds\right|\to 0,\ \text{as } h\to 0$$

Hence $Pu\in\mathscr{C}$ i.e P maps $\mathscr{C}$ into itself.
Step 2: Let $u_1,u_2\in\mathscr{C}$, $t\in[0,T]$, with $u_1(0)=u_2(0)=u_0$

$$\begin{aligned}\|\,(Pu_1)(t)-(Pu_2)(t)\,\|&\leq\|\,C^\alpha(t)\left(u_1(0)-u_2(0)\right)\,\|+\|\,S^\alpha(t)\left(u_1(0)-u_2(0)\right)\,\|+\|\,s^{\alpha-2}S^\alpha(t-s)\left(f(s,u_1(s))-f(s,u_2(s))\right)\,\|\\&\leq MM_fe^{\omega T^\alpha}||u_1-u_2||\int_0^t s^{\alpha-1}ds\\&\leq t^\alpha\frac{MM_fe^{\omega T^\alpha}}{2}\end{aligned}$$

We set $\eta=\frac{MM_fe^{\omega T^\alpha}}{2}$ We can deduce that

$$\|\,(P^2u_1)(t)-(P^2u_2)(t)\,\|\leq\eta\int_0^t s^\alpha||u_1-u_2||ds$$

$$\leq\frac{\left(\eta t^{\frac{\alpha}{2}}\right)^2}{2}||u_1-u_2||$$

And by induction, we have for all $t\in[0,T]$

$$\|\,(P^2u_1)(t)-(P^2u_2)(t)\,\|\leq\frac{\left(\eta t^{\frac{\alpha}{2}}\right)^n}{n!}||u_1-u_2||$$

Since $\frac{\left(\eta t^{\frac{\alpha}{2}}\right)^n}{n!}\to 0,\ \text{as } n\to\infty$, then there exists $r\in\mathbb{N}$ such that follows that P^r is a contraction and there exists a unique $u\in\mathscr{C}$ such that $P^ru=x$. Furthermore, we have

$$P^r(Pu)=P(P^ru)=Pu$$

Hence Pu is a unique fixed point of P^r, so we conclude that u is the unique mild solution of (1). □

5. Conclusion

In this section you should present the conclusion of the paper. Conclusions must focus on the novelty and exceptional results you acquired. Allow a sufficient space in the article for conclusions. Do not repeat the contents of Introduction or the Abstract. Focus on the essential things of your article.

Acknowledgement

This is a text of acknowledgements. Do not forget people who have assisted you on your work. Do not exaggerate with thanks. If your work has been paid by a Grant, mention the Grant name and number here.

References

[1] Agarwal, RP, Zhou, H, He, Y: Existence of fractional neutral functional differential equations. Comput. Math. Appl. **59**(3), 1095-1100 (2010)
[2] Abdeljawad, T., On Conformable Fractional Calculus,Journal of Computational ad Applied Mathematics,Vol. 279, 1 May 2015, 57-66, arXiv: 1402.6892v1 [math D, S] 27 Feb 2014.
[3] Balakrishnan, A. V., Fractional Powers Of Closed Operators And The Semigroups Generated By Them, Pacific Journal of Mathematics 10, pp. 419-439, 1960.
[4] TRAVIS. C. C and WEBB. G. F. Cosine Families and abstract nonlinear second order differential equations. Acta Mathematica Academiae Seientiarum Hungaricae Tomus 32 (3–4), (1978), 75–96.
[5] Mohammed AL Horani. Roshdi Khalil and Thabet Abdeljawad. Conformable Fractional Semigroups of Operators. arXiv:1502.06014v1 [math.FA] 21 Nov 2014 Conformable.
[6] Khalil, R., Al Horani, M., Yousef. A. and Sababheh, M., A new Definition Of Fractional Derivative, J. Comput. Appl. Math. 264. pp. 65?0, 2014.
[7] Kilbas, AA, Srivastava, HH, Trujillo, JJ: Theory and Applications of Fractional Differential Equations. Elsevier, Amsterdam (2006)
[8] Pazy, A., Semigroups of Linear Operators and Applications to Partial Differntial Equations, Springer-Verlag, 1983.

Journal of Mathematical Sciences and Modelling, 2 (2) (2019) 117-124
Research Article

Journal of Mathematical Sciences and Modelling

Journal Homepage: www.dergipark.gov.tr/jmsm
ISSN 2636-8692
DOI: http://dx.doi.org/10.33187/jmsm.459653

A Design Entropy Based Hybrid Soft Classifier Algorithms for Improving Classification Performance of a Satellite Data

Ranjana Sharma[1*], P. K. Garg[1] and R. K. Dwivedi[2]

[1]*Professor, IIT Rorkee, India*
[2]*Prof & Principal, CCSIT, Teerthnakar Mahaveer University, Moradabad, India*
[*]*Corresponding author*

Article Info

Keywords: *Accuracy, Entropy, Fuzzy C-Means with entropy, Mixed classification/Soft classification, Pure classification.*
2010 AMS: *00A69*
Received: *13 September 2018*
Accepted: *28 January 2019*
Available online: *30 August 2019*

Abstract

Image classification of the satellite imagery interprets the thematic map to represent the spatial distribution of earth features. There are so many applications of Remote sensing image classification such as Resource utilization and environmental impact analysis etc. The overall process result depends on two main aspects Every object have distinctive signature and feature of interest The process can distinguish these features separately. Image classification is broadly classified in two ways Pure classification and Mixed classification. In the pure classification, the pixels are classified into class only and in the mixed classification, pixels can fit into one or more module according to their membership values. In hard classification, data may be lost because of the restriction being in a single class. However in the soft classification, this problem is resolved. After resolving the problem, there is a need of accuracy assessment. Accuracy parameter is very important factor in terms of classification. So, in this study, I am trying to design the algorithm for the hybridization classification with entropy to maintain the optimizing.

1. Introduction

Usually the pure classification is used to generate thematic maps and surface information. The pixels of the pure classification give particular land cover information. Conversely this defeat the real data of geographic surface, the covered data might be present in more than one land. The mixed pixel likelihood is higher for course resolution. The data in satellite is mixed and it gives numerous surface of earth information within pixel that is a big problem in terms of categorization or in accuracy. Accuracy assessment is again an issue in soft classification. Researchers and analyst have made great hard work in budding advanced classification approaches[26,28] for optimizing categorization appropriateness [13,8,26,29].Predictable methods of correctness measurement mandatory harden the surface of earth information. This once again leads to an inaccurate estimation. In remote sensing, both supervised and unsupervised classification techniques may be applied to perform soft classification [1]. It increases the classification accuracy and produces adequate land cover composition. Digital image categorization is typically depending upon to retrieve spectral information using a range of statistical classification techniques such as Maximum Likelihood Classifier (MLC), k-means clustering, Minimum Distance to mean classifier etc. The allocation of each pixel of the data from these classifiers in a single class thus produces pure or hard classification. However, often the pixels of the satellite do not represent a single class but contains more classes in single pixel area[30]. This situation is quite prevalent in developing country like India where the development has taken place in a haphazard manner. In a satellite image having coarse resolution, chances of class mixture within a single pixel are higher in the heterogeneous landscapes, and in interclass boundaries leading to higher proportion of mixed pixels in an image. Fine resolution satellite data, will be able to remove, by and large, the mixing of information within a pixel, yet the problem may still exist at inter-class boundary, where the number of such pixels may increase many folds. Whatever be the origin of mixed pixels, these may generate problem in image categorization. For instance, a miscellaneous pixel shows a combined spectral response that may be unlike to the spectral response of each of its component classes and, therefore, the pixel of satellite may not be allocated to any of its division classes [39]. Hence, error may occur in the classification of image [9] containing large number of mixed pixels. Hard classification approaches,

Email addresses and ORCID numbers: **sharmaranjana04@gmail.com, 0000-0002-0088-715 (R. Sharma), pkgiitr@gmail.com (P. K. Garg), principal.computers@tmu.ac.in (R. K. Dwivedi)**

can work only on single class but mixed pixels to be allocated more than one class. So information of pixel of image loss and we can say hard classification have only single class information. In case of hard classification methods mixed pixels may thus be treated as error or uncertainty, or uncertainty in class allocation. The land use land cover areal estimate obtain from hard classification, if used as an input to any Geographical Information System (GIS) based application, it may affect the accuracy of the end product. Thus, mixed pixels of image are not to be handed by hard classification. The problem of mixed pixels may be resolved by accommodating this in the classification process in some way to acquire the hidden information[14,24].The application of soft classification methods based on spectral mixture analysis[20],fuzzy set theory[21] may thus be adopted. The output from these methods is a set of class membership values for each[8], pixel, also named as soft or fuzzy classification outputs, which are represented as probability, fraction or proportion images [30]. The utilization of soft classification methods is an active area of research, which can be gauged from a number of research papers published during the last couple of years[11,23,25,30]. Hybrid soft classification methods are largely in their exploratory stage. The research needs to be conducted to examine these methods on different remote sensing data products acquired in complex and uncertain environments.

2. The Types of Entropy Based Hybrid Soft Classifiers

The measure of information, as per Shannon [32,33] states that it has an intimate relationship with entropy theory as in statistical thermodynamics. Therefore, information theory and thermodynamics must have some common points of interest. The increase in entropy has been regarded as the degradation of energy by Kelvin[16]. In statistical thermodynamics, entropy is defined as a measure of the disorder of a system. However, in information theory, entropy[10] is a measure of the lack of information about the actual structure of the system [19]. It is perceived that fuzzy based information can become complete by adding entropy to the standard one, since it can observe the nature of both methods more deeply by contrasting these two methods[4,7]. In this study, it has been observed that entropy based method is similar to a statistical model having Gaussian distribution, since both of them have error functions, while the standard method such as FCM[15], PCM[17], etc. are different from a statistical model. For this reason, standard method is purely fuzzy, while entropy based method connects a statistical model and a fuzzy model[3,4,7]. In this study, one of the primary motivations is to hybridize FCM and PCM with entropy. FUZZY C-MEAN WITH ENTROPY (FCMWE) CLASSIFIER Fuzzy c-Mean with Entropy (FCMWE) is the hybridization approach of classification where the emphasis is to integrate entropy based regularization method with FCM [12,15]. It is believed that the methods of Fuzzy c-Means become complete by adding entropy to the standard one as defined in Eq. (2.1)[7,19,22].

i) This hybridization has been proposed, to evaluate the Performance of algorithm which is entirely fuzzy, even as entropy based method is more similar to the statistical method.

ii) The principle of this process is based upon maximum entropy[31] which is further advance in various applications.

iii)[4][7] focus on comparison between methods and explain the entropy based algorithm more efficiently.

It is observed that the method of [3][7], also known as the standard method of FCM, is purely fuzzy, while entropy-based method is more similar to statistical models 34],[35]-[38]. The result which obtains the soft classifier gives result with higher uncertainty. But hybrid based classifier with optimum regularizing parameter generates classified output with lowest amount of uncertainty [18]. As nonlinearity, introduced by [7]and [4], smoothens the crisp solution into a differentiable one. Moreover, fuzzy solution approximates the crisp one i.e., the fuzzy solution converges to a crisp solution as m approaches to 1.

2.1. Fuzzy c-Mean with Entropy (fcmwe) Classifier

Fuzzy c-Mean introduces non-linearity using (u_{ki}) m. However, use of entropy is another type of nonlinearity. The process of regularization is completed by adding a new function which known as regularizing function. The basic objective function of FCM with entropy classifier and flowchart are given in Eq. (2.1) and Fig.(2.1)

$$J_{FCMWE}(U,V) = \sum_{i=1}^{c}\sum_{k=1}^{n} u_{ki} D(x_k, v_i) + v\sum_{i=1}^{c}\sum_{k=1}^{n} u_{ki}\log u_{ki}, (v>0) \tag{2.1}$$

Where v is regularizing parameter and has a value greater than 0. In the Eq. (2.1), the first term is the objective function of FCM classifier and second term is a nonlinear regularizing entropy function. It is observed that regularizing function is a strictly a convex function, and hence capable of fuzzifying the membership values.

2.2. Possibilstic c-Mean with Entropy (pcmwe) Classifiers

PCM c-Mean with Entropy (PCMWE) is a hybridization approach of classification where the emphasis is regularizing term. The working of algorithm gas defined in Fig. (2.2). The assigns pixel of image can vary some time its belong single cluster and some its belong more than one cluster. We know the membership of pixel does not follow the limit in FCM called hyper-line constraint. The entropy methods are support to rediscover repeatedly in fuzzy Clustering by different formulations. This hybridization has been proposed, to evaluate the Performance of algorithm which is purely fuzzy, while entropy based method is more similar to statistical method. The FCME and PCME clustering algorithm are nature in iterative where membership value are obtained by minimizing the generalized least- square error objective function[17], is obtained by minimizing objective function as,

$$j_m(U,V) = \sum_{i=1}^{N}\sum_{j=1}^{C}(\mu_{ij})^m ||x_i - v_j||_A^2 + \sum_{i=1}^{c}(1-\mu_{ij})^m + v(-\sum_{i=1}^{C}\mu_{ij}\log_2(\mu_{ij})) \tag{2.2}$$

Where v is regularizing parameter and has a value greater than 0 in Eq. (2.2).

3. The Study Area of Research

Study area of research Sitarganj Tehsil which is situated close to Pantnagar, Uttarakhand State,India which is shown in Fig. (3.1). The survey is based on remote sensing data from IRS P6, AWIFS, LISS-III and LISS-IV sensors. and the The on-board sensors on this satellite are

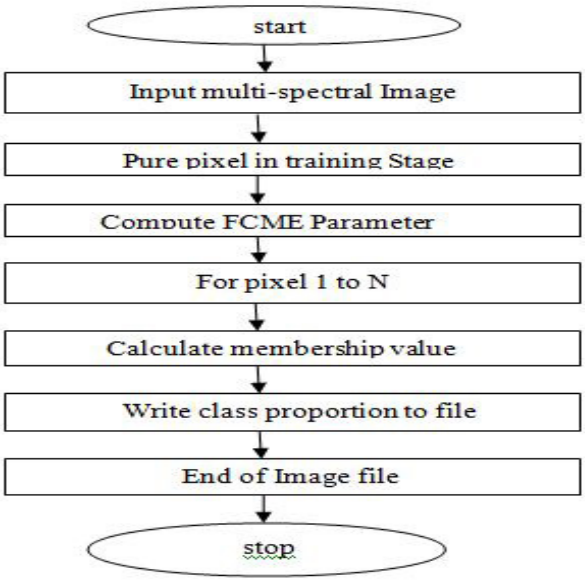

Figure 2.1: Flow chart of FCME classifier in supervised mode

LISS-IV (Linear Imaging Self Scanner), LISS-III and AWiFS.Fig. (3.1) describes these sensors characteristics in details.

Sensor	**Bands**	**Resolution [m]**	**Swath [km]**	**Quantization [bits]**
LISS-IV Mono mode	red	5.8	70.3	7
LISS-IV MX mode	green red NIR	5.8	70.3	7
LISS-III	green red NIR SWIR	23	141	10
AWifS	green red NIR SWIR	56 (nadir) . . . 70 (edge)	740	10

Table 1: Resourcesat-1 payload characteristics

4. Methodology of Research

Uncertainty reduction or noise process by[6] for soft classification required classified fraction images and reference classified fraction images (if available), perform sampling over classified data, apply accuracy assessment method on sampled data and finally produces accuracy [6] parameters. Accuracy assessment method[5][16]of sub-pixel categorization is also Conrad data, such as SCM, FERM, SCM, error matrix, RMSE and Entropy. It is known that these methods required reference data accept entropy. But Entropy is does not require any reference data , so it knows as absolute indicator. Accuracy assessment process for soft classification required classified fraction images and reference classified fraction images (if available), perform sampling over classified data, apply accuracy assessment method on sampled.

5. Result and analysis and discussion

In this study, Fuzzy C-means with Entropy(FCME)and PCM c-Mean with Entropy (PCMWE) have been used as a base soft classifier and entropy has been added to investigate the effect of this hybridized model known as FCMWE and PCMWE. The basic objective of this study is to identify the optimized value of regularizing parameter ν for FCMWE classifier and PCMWE classifier which generates classified output with minimum uncertainty. To obtain accurate information from this classifier, the optimization of regularizing parameter ν is required. To perform the FCMWE, PCMWE classification, fixed value of m=1 has been used for all varying values of ν (from 0 to 10^9). The class membership μ increases till ν=10, 10^2 and 10^3, the class membership is higher and lies between 0.91 to 0.99 for all the six classes. Regularizing parameter ν is the fixed parameter,$0 \leq \nu < \infty$ which regularizes the fuzzified solution to crisp solution. and thereafter it starts to decrease or becomes almost constant. {Fig.(5.1), Fig. (5.2) and Fig. (5.3)}
Thus, as per the analysis of class membership, the optimum value of ν for FCMWE classifier has been fixed as 105. However, this optimization would be further verified by entropy.

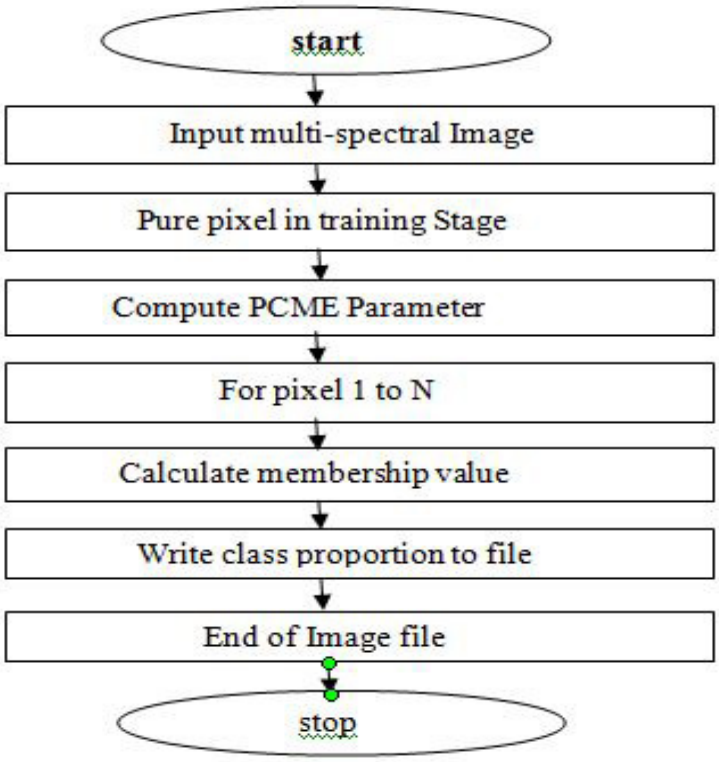

Figure 2.2: Flow chart of PCME classifier in supervised mode

5.1. Calculate Entropy of hybridize classifier (fcme)

The entropy of FCMWE classifier of classified fraction images can be computed by using Eq. (2.1) Fig. (5.1), Fig. (5.2) and Fig. (5.3) shows the computed entropy for AWiFS, LISS-III and LISS-IV fraction images of FCMWE classifier. It has been observed from Fig. (5.4), Fig. (5.5) and Fig. (5.6) that for v=10^2 and 10^3 the entropy values for all classes are low. For this optimized value of v, the membership is high i.e. up to 0.996 and the computed entropy is low 0.004.
This trend reflects that the uncertainty in results is low. In a nutshell, it can be concluded that whenever entropy has been used as an indirect accuracy measure and this shows the classification consistency with respect to a particular class.

Class	*Class membership*			*entropy*			*Optimized Mean value*
	AWiFS	*LISS-III*	*LISS-IV*	*AWiFS*	*LISS-III*	*LISS-IV*	
Agriculture	10^3	10^3	10^3	10^2	10^3	10^2	$7x10^2$
Bright Forest	10^3	10^3	10^3	10^3	10^2	10^2	$7x10^2$
Dense Forest	10^3	10^3	10^2	10^2	10^2	10^2	$4x10^2$
Agriculture Dry land	10^2	10^2	10^2	10^2	10^2	10^2	10^2
Agriculture Moist land	10^2	10^2	10^2	10^2	10^2	10^2	10^2
Water Body	10^2	10^2	10^2	10^2	10^2	10^2	10^2

Table 2: Class wise parameter optimization of(v) for FCME classifiers

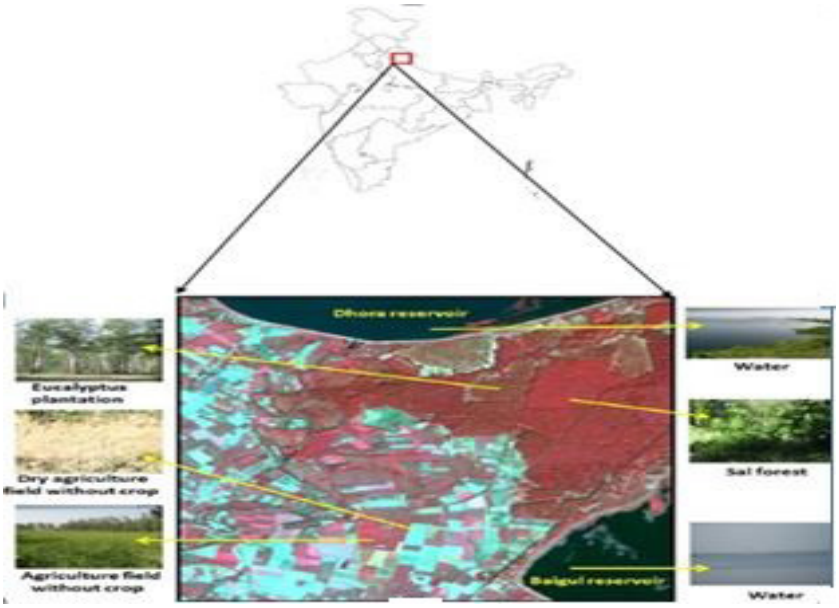

Figure 3.1: Location of study area

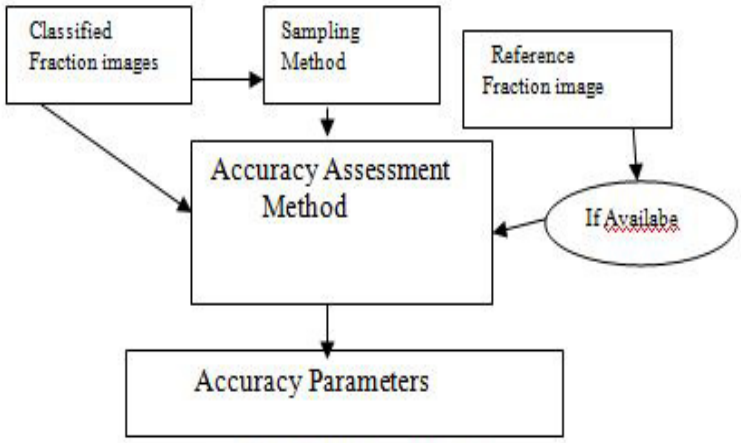

Fig.5: Methodology of research

Figure 4.1: Methodology of research

It has been recognized from the obtained results that irrespective of datasets $\nu = 7x10^2$ found more suitable to classify agriculture and Bright forest. However, for dry land, moist land and water body, $\nu = 10^2$ is found to be more suitable for the classification using FCMWE classification approach. For Dense forest $\nu = 4x10^2$ is found to be more appropriate for classification. To perform classification a constant value of weighting exponent m =1 has been used.

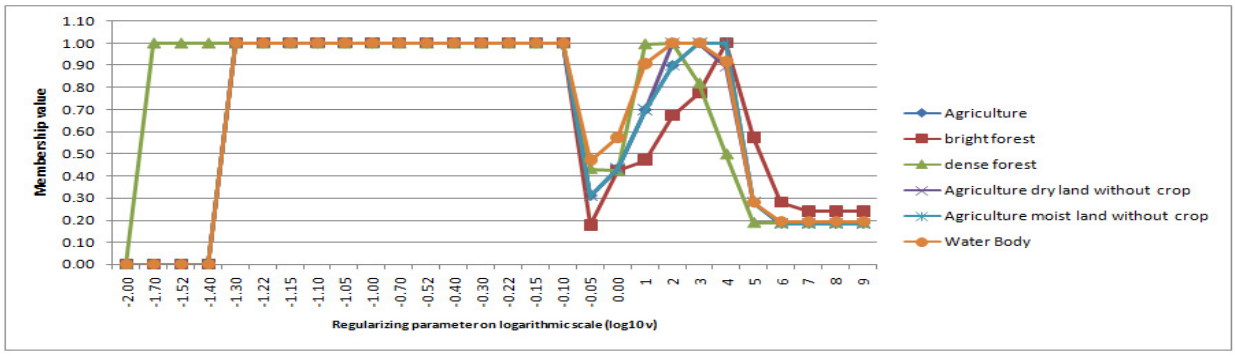

Figure 5.1: Class membership for FCMWE classifier using AWiFS datasets

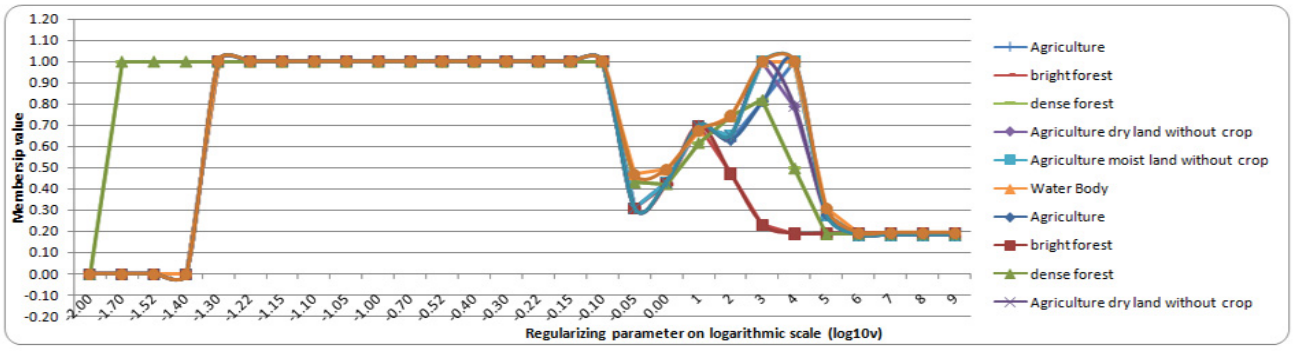

Figure 5.2: Class membership for FCMWE classifier using LISS- III datasets

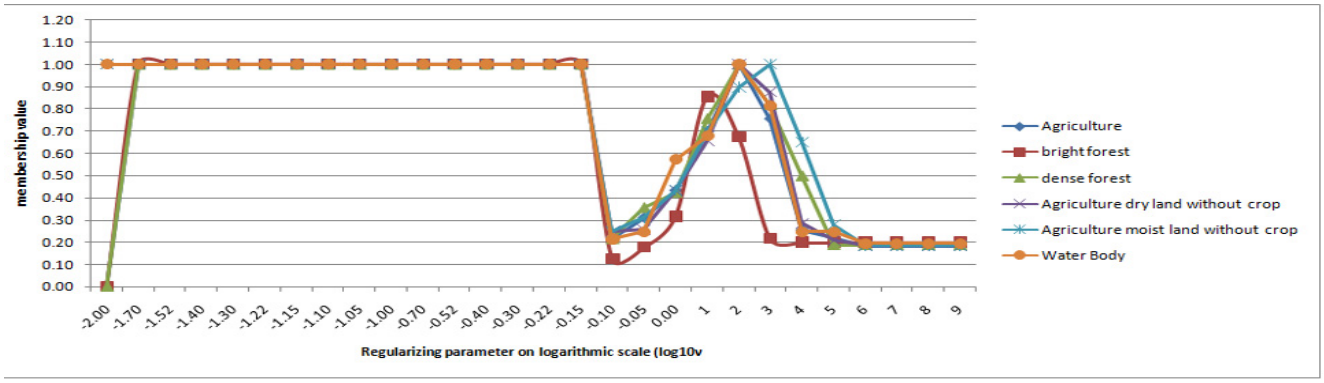

Figure 5.3: Class membership for FCMWE classifier using LISS- IV datasets

6. Conclusion

Fig. (6.1) shows the fraction images of AWiFS datasets for FCMWE classification. After examining the fraction images generated by FCMWE classifier, it has been observed that an intergrades phenomenon within pixel is more dominant in AWiFS imagery. It is shown in fraction images that regularizing parameter ν regularizes the output to remove inter-grade phenomena by using FCMWE classifier which removes uncertainty among classes. In FCMWE classifier the effect of regularizing parameter (ν) is dominant because of unity value of weighting exponent. This trend can be seen from fraction images {Fig. (6.1) } where actual class produces high membership and all remaining classes are reflecting very low membership i.e. almost zero.
In this research paper, I have designed two hybrid soft classification algorithms. Adding Regularization parameter ($0 < \nu < \infty$)in these algorithms we are getting better classification with low entropy.

References

[1] M. K. Arora, A. Peterson, (*Land cover classification from remote sensing data*, GIS development6, 2002,24-25, 30-31.
[2] M. A.Aziz, *Evaluation of soft classifiers for remote sensing data*, Abstr. Appl. Anal.,unpublished Ph.D thesis, Indian Institute of Technology Roorkee,Roorkee,India. (2004).
[3] J.C.Bezdek, *Pattern Recognition with Fuzzy Objective Function Algorithm*,Plenum, New York, USA,(1981), ISBN: 978-1-4757-0452-5.
[4] J.C.Bezdek,R.Ehrlich,W.Full, *The fuzzy c-means clustering algorithm, Computers and Geosciences,*,1984,10,191-203.
[5] R. G.Congalton, *A review of assessing the accuracy of classifications of remotely sensed data*, (1991),37,35-47.

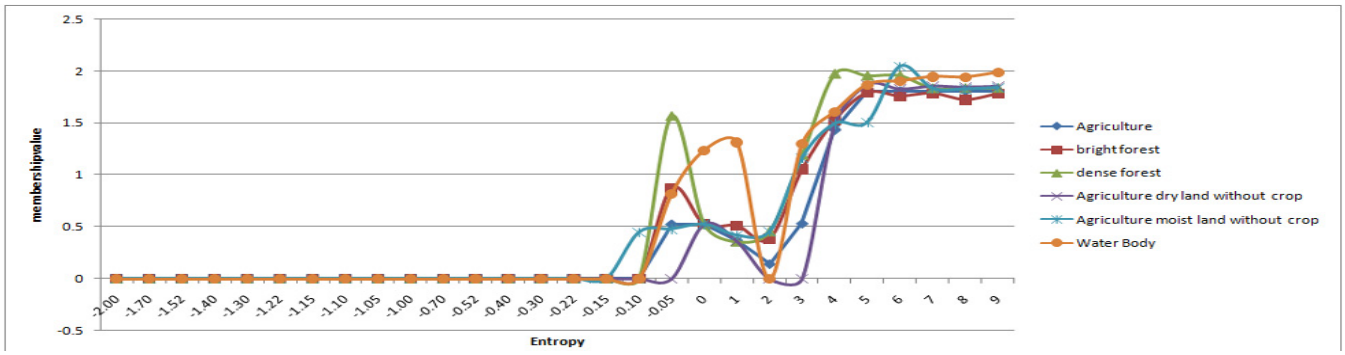

Figure 5.4: Entropy for FCMWE classifier using AWiFS dataset

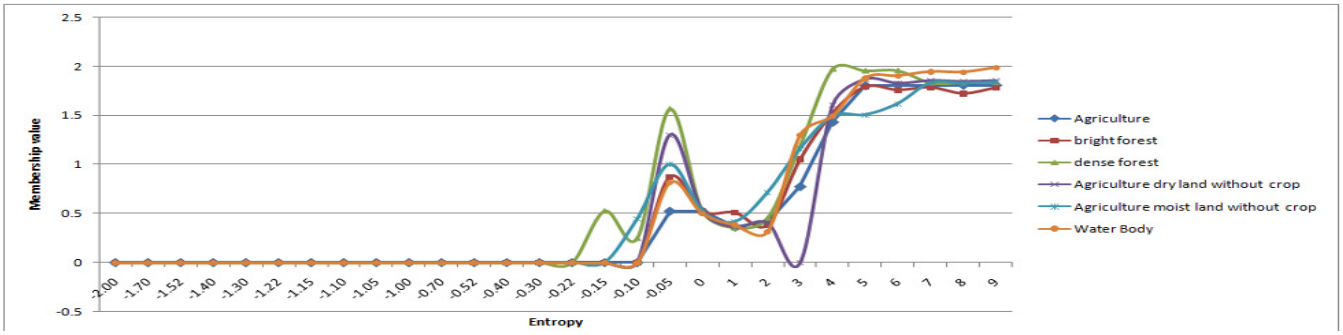

Figure 5.5: Entropy for FCMWE classifier using LISSIII dataset

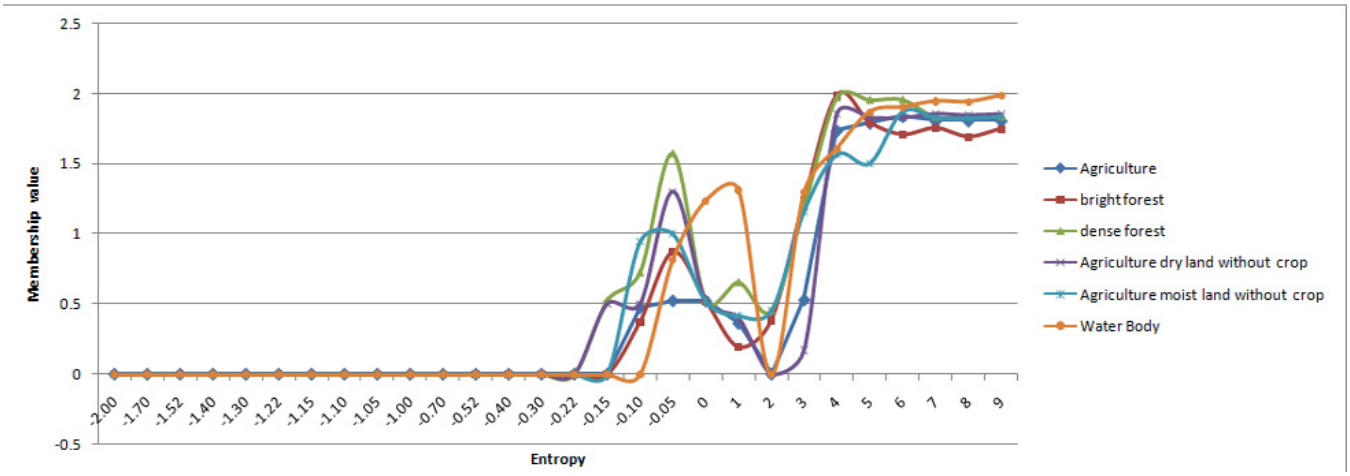

Figure 5.6: Entropy for FCMWE classifier using LISS-IV dataset

[6] H.Dehghan,H.Ghassemian, *Measurement of uncertainty by the entropy: application to the classification of MSS data, International journal of remote sensing*,(2006) vol.27, no. 18, 4005–4014.

[7] J.C.Dunn, *Well Separated Clusters and Optimal Fuzzy Partitions, Journal of Cybernetics*,(1981),4,95-104.

[8] R.k.Dwivedi,S. K.Ghosh, P.Roy, *Optimization of Fuzzy Based Soft Classifiers for Remote Sensing Data*,ISPRS-International Archives of the Photogrammetric, Remote Sensing and Spatial Information Sciences 1,(2012),385-390.

[9] R.k.Dwivedi,S. K.Ghosh, and Anil Kumar, *Investigation Of Image Classification Techniques For Performance Enhancement*,International Journal of Management and Technology, Volume 3, number 1, (2012),21-33.

[10] R.k.Dwivedi,S. K.Ghosh, *Visualization of Uncertainty usingentropy on Noise clustering with entropy classifier*, 3rd IEEE International Advance Computing Conference, (IACC-2013).(2013), ISBN:-978-1-4673-4528-6.

[11] J.R.Eastman, R.M.Laney, *Bayesian soft classification for sub-pixel analysis: critical evaluation*, Photogrammetric Engineering and Remote Sensing,68, (2002),1149-1154.

[12] D.Ferna.Ndez-Prieto, *An iterative approach to partially supervised classification problems*, International Journal of Remote Sensing, 23,(2002), 3887–3892.

[13] G.M.Foody,*Approaches for the production and evaluation of fuzzy land cover classifications from remotely-sensed data*, Journal of Remote Sensing, vol.17, no. 7,(1996),1317–1340.

[14] G.M.Foody,*Estimation of sub-pixel land cover composition in the presence of untrained classes*,Computers and Geosciences, vol. 26, no. 4, (2000),469–478.

[15] S. R.Kannan,R. Devi,S.Ramathilagam,K.Takezawa,*Effective FCM noise clustering algorithms in medical images*,Computers in Biology and Medicine,(2013), vol. 43, no.2, 73–83.

[16] J.Kivinen,M.Warmuth, *Boosting as Entropy Projection*,Proc. 12th Ann.Conf. Computational Learning Theory, (1999),134–144.

[17] R.Krishnapuram, J.M.Keller, *A possiblistic approach to clustering*,IEEE Transactions on Fuzzy Systems, 1,(1993), 98-108.

[18] A.Kumar, V. K.Dadhwal,*Entropy based fuzzy classification parameter optimization using uncertainty variation across spatial resolution*,Journal of Indian Society of Remote Sensing, (2010),Vol 38, No. 2,179-192.

[19] R.P.Li, M.Mukaidono, *Gaussian clustering method based on maximum-fuzzyentropy interpretation*,Fuzzy Sets and Systems 102,(1999) 253–258.

[20] D.Lu,Q. Weng, *A survey of image classification methods and techniques for improving classification performance*,International Journal of Remote Sensing, 28(5),(2007),823–870.

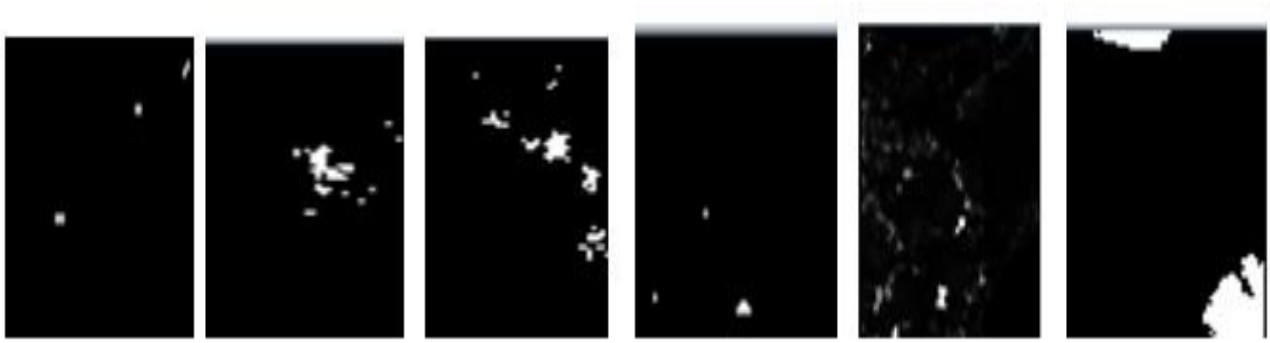

Figure 6.1: Entropy for FCMWE classifier using LISS-IV dataset

[21] A.M.Massone,F.Masulli,A.Petrosini, *Fuzzy clustering algorithms and Landsat images for detection of waste areas: A comparison*,In Advances in Fuzzy Systems and Intelligent Technologies,Proc. WILF '99, Italian Workshop on Fuzzy Logic,Shaker Publishing, Maastricht, The Netherlands,(2000), 165-175.

[22] S.Miyamoto,M.Mukaidono, *Fuzzy c-means as a regularization and maximumentropy approach*,In: Proc. of the 7th International Fuzzy Systems Association World Congress, Prague, Czech,(1997), June 25-30, 1997, vol. II, 86–92.

[23] K.Oki,T.M.Uenishi,K.Omasa, M.Tamura, *Accuracy of land cover area estimation from coarse spatial resolution images using an unmixing method*,International Journal of Remote Sensing, 25, (2004),1673-1683.

[24] I.Olthof, D.J.King, R.A.Lautenschlager, *Mapping deciduous forest ice storm damage using Landsat and environmental data*,Remote Sensing of Environment, 89, (2004),484–496.

[25] R.L.Powell,N.Matzke,C.De Souza JR,M.Clark,I.Numata,L.L.Hess, D.A.Roberts, *Sources of error in accuracy assessment of thematic land-cover maps in the Brazilian Amazon*,Remote Sensing of Environment, 90, (2004),221–234.

[26] Priyadarshi Upadhyay, S. K. Ghosh, and Anil Kumar, *A Brief Review of Fuzzy Soft Classification and Assessment of Accuracy Methods for Identification of Single Land Cover*,Studies in Surveying and Mapping Science (SSMS) American Society of Science and Engineering, Volume 2, (2014),ISSN 2328-6245.

[27] R.k.Dwivedi,S. K.Ghosh,A.Kumar, *Investigation Of Image Classification Techniques For Performance Enhancement*,Viewpoint "An International Journal of Management and Technology" ,(2012),ISSN-2229-3825.

[28] Ranjana Sharma,Achal Kumar Goyal,Achal Kumar Goyal, *A Review of Soft Classification Approaches on Satellite Image and Accuracy Assessment*, Proceedings of Fifth International Conference on Soft Computing for Problem Solving , Springer Singapore,(2016),vol.437,629-639.

[29] S. S.Sengar,A.Kumar,H. R.Wason,S. K.Ghosh,Krishna Murthy,sh, *Study of soft classification approaches for identification of earthquake-induced liquefied soil*,Geomatics, Natural Hazards and Risk(ahead-of-print), (2013),1-19.

[30] M.A.Shalan,M.K.Arora,S.K.Ghosh, *An evaluation of fuzzy classifications from IRS 1C LISS III imagery: a case study*, International Journal of Remote Sensing,24,(2003), 3179-3186.

[31] C. E.Shannon, *A Mathematical Theory of Communication*,Bell System Technical Journal 27(3), (1948),379–423.

[32] C. E.Shannon, *Prediction and Entropy of Printed English*,Bell System Technical Journal 30 (1), (1951),50–64.

[33] Xiao-Hong Wu,Jian-Jiang Zhou, *Alternative Noise Clustering Algorithm*,IEEE- ICSP Proceedings,(2006),0-7803-9737-1/06.

[34] A.N.Tihonov,V.Y.Arsenin, *Solutions of Ill-Posed Problems*,. Wiley, New York,(1977).

[35] V.Vapnik, *The Nature of Statistical Learning Theory*,Springer Verlag, New York,(1995).

[36] V.Vapnik, *IStatistical Learning Theory, John Wiley and Sons*,New York,(1998).

[37] V. N.Vapnik, *An overview of statistical learning theory*,IEEE Transactions of Neural Networks, 10, (1999),988-999.

[38] V. N.Vapnik , *The Nature of Statistical Learning Theory*,2nd Edition,(2000).

[39] J.Zhang,G.M.Foody, *A fuzzy classification of sub-urban land cover from remotely sensed imagery*,International Journal of Remote Sensing, 19,(2001), 2721-2738.

Journal of Mathematical Sciences and Modelling, 2 (2) (2019) 125-132
Research Article

Journal of Mathematical Sciences and Modelling

Journal Homepage: www.dergipark.gov.tr/jmsm
ISSN 2636-8692
DOI: http://dx.doi.org/10.33187/jmsm.437666

On the Probabilistic Characteristics of A Two Lane Slab-Type-Bridge Response Due to Traffic Flow

L. M. Anague Tabejieu[1*] and B. R. Nana Nbendjo[1]

[1] *Laboratory of Modelling and Simulation in Engineering, Biomimetics and Prototypes, Faculty of Science, University of Yaoundé I, P.O. Box 812, Yaoundé, Cameroon.*
[*] *Corresponding author*

Article Info

Keywords: *Bridge deflection, Thin rectangular plate, Traffic flow, Two lane slab-type-bridge.*
2010 AMS: *00A69*
Received: *27 June 2018*
Accepted: *21 March 2019*
Available online: *30 August 2019*

Abstract

In this study, an evaluation approach to obtain the two first probabilistic characteristics of a two lane slab-type-bridge response due to traffic flow is investigated. A two lane slab-type-bridge is modelled by a Simply Supported (SS) thin rectangular plate with two separate rectilinear paths. The modelling of the traffic flow is based on the assumption that two opposite series of vehicles of random weights arrive at the bridge at random times that constitute the Poisson stochastic process and with the stochastic velocities. The expected value and the standard deviation of the bridge deflection are obtained. We demonstrate that the bridge safety strongly depends to the mean value and to the standard deviation of the vehicles velocities.

1. Introduction

Vibration of a structure subjected to moving loads is of great theoretical and practical significance in civil engineering. Vibrations connected with this issue occur for example in the roadways loaded by traffic. [1] and [2] addressed a variety of engineering problems which are concerned with the dynamics of structures subjected to moving loads. Different types of structures and girders like beams, plates, shells, frames were considered and also different models of moving loads were assumed. For example, The dynamics response of the plate under moving load was considered by many authors but in most of their works the moving load was regarded as deterministic. A concise review of several related research studies is carried out in the following paragraph of this paper.
[3] proposed a classical closed-loop control algorithm to suppress the vibration of a simply-supported rectangular plate excited by a moving mass via a number of bonded active piezoelectric patches. [4] examined an inclined flat plate vibration due to traveling loads. [5] provided a semi-analytical simulation of a shear deformable plate vibration due to traveling inertial loads considering a general load distribution pattern and plate boundary condition. [6] analysed the dynamic behavior of an orthotropic plate simply supported on a pair of parallel edges and under a system of moving loads based on Lagrange equation and modal superposition. Preliminary results of the paper indicated that the multilane loading case is less critical than a single-lane loading case. [7] considered two series of moving inertial loads traversing the plate surface along parallel rectilinear trajectories with opposite directions and studied the resonance caused by this loads.
In real situation the load process has stochastic nature. So, the problem of vibrations of a plate subjected to this type of load was considered in some papers in stochastic approaches. [8] investigated the problem of a dynamic response of an infinite beam and a plate resting on a two-parametric foundation (Pasternak foundation) to the passage of a train of random forces. They developed an analytical technique to determine the two first probabilistic characteristics of the beam and plate responses. [9] investigated the dynamic response of a rectangular plate on a viscoelastic foundation under moving loads with varying velocity. The deflection distribution of the plate and the effects of the type of motion, initial speed of the load and foundation damping on the plate response are illustrated and analyzed.
In order to distinguish the present work from the above pertinent literature, we propose here to extend the work done by [7] by taking into account the more realistic model of moving loads (when it idealizes the vehicles on the bridge). In this model all the forces (vehicles) arrive at the plate at the random time instant, with stochastic velocities. So, a semi-analytical approach ([14]) to obtain the probabilistic characteristics of a two lane slab-type-bridge response due to two opposite series of stochastic moving loads is investigated. We call the attention of the reader about the fact that, the stochastic perturbation method proposed by [18] can be also used to achieve the same goal.

***Email addresses and ORCID numbers*: lmanaguetabejieu@gmail.com,0000-0002-7750-6910 (L. M. A. Tabejieu), nananbendjo@gmail.com, 0000-0002-7750-6910 (B. R. N. Nbendjo)**

Thus in this paper, the probabilistic characteristics of the plate response are sought in the form of the two first probabilistic moments, i.e. the expected value and the variance function.
The structure of this paper is as follows. After this Introduction in Section 1, the bridge model is presented and described in Section 2; the dynamic equations of motion for the vehicles-bridge are derived by using the Newton second law's; the Galerkin's method is used to discretize the equations. Section 3 presents a semi-analytical approach to obtain the probabilistic characteristics of the bridge plate response and some numerical results. Finally, conclusions are drawn in section 4.

2. The Bridge model and the mathematical formulation

Let us consider a model of a two lane slab-type-bridge (see Fig. 2.1(a)) modelled by a SS thin rectangular plate (of length a, width b and thickness h) with two separate rectilinear paths and subjected to two opposite series of moving forces with random values A_{ij} (vehicle weights) appearing at random times t_{ij}, as shown in Fig. 2.1(b). Such an excitation process is an appropriate model of vehicular traffic loads

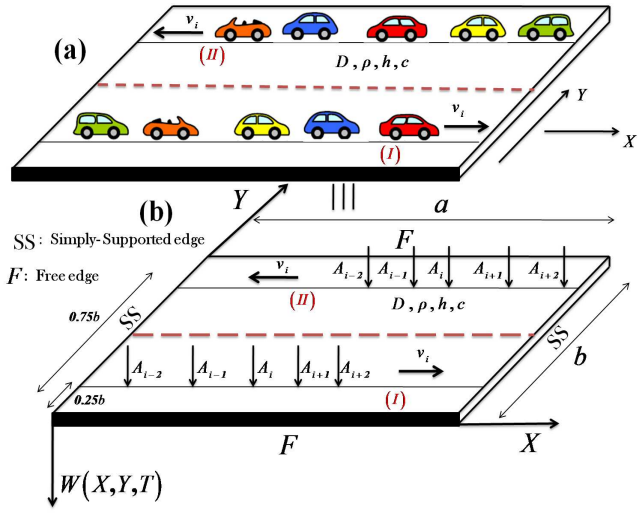

Figure 2.1: The general plan of the model of a two lane slab-type bridge and its loading (a). The simplified scheme of the model (b).

acting on the bridge. The plate is assumed to behave according to the Kirchhoff's hypothesis [10]. Thus, the vibrations of the plate due to these random forces are described by the following equation:

$$\rho h\frac{\partial^2 W}{\partial T^2}+c\frac{\partial W}{\partial T}+D\left[\frac{\partial^4 W}{\partial X^4}+\frac{\partial^4 W}{\partial X^2\partial Y^2}+\frac{\partial^4 W}{\partial Y^4}\right]=P(X,Y,T) \tag{2.1}$$

where $W(X,Y,T)$ denotes vertical deflection of the plate at point X, Y, and time T. $D=Eh^3/12\left(1-\upsilon^2\right)$ is the bending rigidity of the plate, with h, E, υ are the thickness, elastic modulus and Poisson's ratio of the plate, respectively. ρ represents the mass per unit of volume of the plate, c the damping coefficient of the plate and $P(X,Y,T)$ denotes the load process. In the case of a random train of forces (vehicles) moving in opposite directions in a two separate rectilinear paths $(n_l=2)$, the loading process has a form:

$$P(X,Y,T)=\sum_{j=1}^{n_l}\sum_{i=1}^{N_j(T)}A_{ij}\delta\left[X-X_{ij}\left(T-T_{ij}\right)\right]\delta\left[Y-Y_{0j}\right] \tag{2.2}$$

where $\delta[...]$ stands for the Dirac delta function, A_{ij} are the weights which are assumed to be random variables, mutually independent and also independent of the instants t_{ij} (arrival times of the moving forces), Y_{0j} is the deterministic y-coordinate that fixes the position of each traffic lane, n_l is the number of traffic lane considered and $N_j(T)$ is the number of forces that acted on the plate from the beginning of observation up to the time T and that describes the Poisson process. $X_{ij}\left(T-T_{ij}\right)$ is the distance covered by the $i-th$ force moving one by one to the time T on the $j-th$ traffic lane. It is assumed that one of a random train of forces traverses the plate on the following rectilinear trajectory ([14, 12]):

$$\begin{gathered}\frac{dX_{ij}(T-T_{ij})}{dT}=v_{ij}\left(T-T_{ij}\right)=\varepsilon_j v_{0j}+\sigma_{vj}\xi_{ij}\left(T-T_{ij}\right)\\ Y_{0j}=\begin{cases}0.25b & \text{For the trajectory (I)},\ \ \varepsilon_j=1\\ 0.75b & \text{For the trajectory (II)},\ \ \varepsilon_j=-1\end{cases}\\ 0\le X_{ij}\left(T-T_{ij}\right)\le a\end{gathered} \tag{2.3}$$

where $v_{ij}\left(T-T_{ij}\right)$ is the stochastic velocity of the $i-th$ force, that moving in the traffic lane j. v_{0j} presents the mean value of velocity, σ_{vj} its standard deviation and $\xi_{ij}\left(T-T_{ij}\right)$ the velocity disturbance. The function ε_j is introduced and defined as: $\varepsilon_j=1$ when the loads are crossing the plate in one of their rectilinear path (situation (I) of Fig. 2.1), and $\varepsilon_j=-1$ for the other line of the loads trajectory (situation (II)

of Fig. 2.1). It is assumed that, the force disturbances $\xi_{ij}\left(T-T_{ij}\right)$ are stationary random processes, here the mutually independent Gaussian white noise processes, i.e.

$$\begin{aligned}
&\mathrm{E}\left[v_{ij}\left(T-T_{ij}\right)\right]=v_{0j},\ \ \mathrm{E}\left[\xi_{ij}\left(T-T_{ij}\right)\right]=0\\
&\mathrm{E}\left[\xi_{ij}\left(T-T_{ij}\right)\xi_{kl}\left(T-T_{ij}\right)\right]=0\quad \text{for}\,(k,l)\neq(i,j)\,,\\
&\mathrm{E}\left[\xi_{ij}\left(T-T_{ij}\right)\xi_{ij}\left(T-T_{ij}+\varsigma\right)\right]=\Delta_j^2\delta\left(\varsigma\right)
\end{aligned}\tag{2.4}$$

where E[...] denotes the expected value of the quantity in brackets and $\Delta_j=v_{oj}\sigma_{vj}$.
In order to improve the accuracy of the numerical calculation, the following dimensionless variables are defined as follows:

$$w=\frac{W}{h},\ x=\frac{X}{a},\ y=\frac{Y}{b},\ t=\omega_0 T,\ x\in[0,\,1]\,,\ y\in[0,\,1]\tag{2.5}$$

Eq. (2.1) takes the form:

$$\frac{\partial^2 w}{\partial t^2}+\mu\frac{\partial w}{\partial t}+\frac{\partial^4 w}{\partial x^4}+2\left(\frac{a}{b}\right)^2\frac{\partial^4 w}{\partial x^2\partial y^2}+\left(\frac{a}{b}\right)^4\frac{\partial^4 w}{\partial y^4}=P\left(x,y,t\right)\tag{2.6}$$

with

$$\omega_0=\frac{1}{a^2}\sqrt{\frac{D}{\rho h}},\ \mu=\frac{ca^2}{\sqrt{\rho hD}},\ P\left(x,y,t\right)=\frac{a^4}{Dh}P\left(X,Y,T\right)\tag{2.7}$$

Eq. (2.3) takes the dimensionless form:

$$\begin{aligned}
&\tfrac{dx_{ij}(t-t_{ij})}{dt}=u_{ij}\left(t-t_{ij}\right)=\varepsilon_j u_{0j}+\sigma_{vj}\zeta_{ij}\left(t-t_{ij}\right)\\
&y_{0j}=\begin{cases}0.25 & \text{For the trajectory (I)},\ \ \varepsilon_j=1\\ 0.75 & \text{For the trajectory (II)},\ \ \varepsilon_j=-1\end{cases}\\
&0\leq x_{ij}\left(t-t_{ij}\right)\leq 1
\end{aligned}\tag{2.8}$$

where:

$$u_{0j}=\frac{v_{0j}}{a\omega_0},\ \ \zeta_{ij}=\frac{\xi_{ij}}{a\omega_0},\ x_{ij}=\frac{X_{ij}}{a},\ y_{0j}=\frac{Y_{0j}}{b}.\tag{2.9}$$

Since the parameters of the plate are deterministic, let the dynamic influence function $H_j\left(x,y,t-t_{ij}\right)$ denote the response of the plate at the time t to the moving force when the amplitude $A_{ij}=1$. This function satisfies the following equation:

$$\frac{\partial^2 H_j}{\partial t^2}+\mu\frac{\partial H_j}{\partial t}+\frac{\partial^4 H_j}{\partial x^4}+2\left(\tfrac{a}{b}\right)^2\frac{\partial^4 H_j}{\partial x^2\partial y^2}+\left(\tfrac{a}{b}\right)^4\frac{\partial^4 H_j}{\partial y^4}=\tfrac{a^3}{Dhb}1.\,\delta\left[x-x_{ij}\left(t-t_{ij}\right)\right]\delta\left[y-y_{0j}\right]\tag{2.10}$$

and the following boundary (Simply supported one) and initial conditions are considered

$$\begin{aligned}
&H_j\left(x,y,t-t_{ij}\right)|_{x=0}=H_j\left(x,y,t-t_{ij}\right)|_{x=1}=0\\
&H_j\left(x,y,t-t_{ij}\right)|_{y=0}=H_j\left(x,y,t-t_{ij}\right)|_{y=1}=0\,,\\
&\left.\tfrac{\partial^2 H_j(x,y,t-t_{ij})}{\partial x^2}\right|_{x=0}=\left.\tfrac{\partial^2 H_j(x,y,t-t_{ij})}{\partial x^2}\right|_{x=1}=0\,,\\
&\left.\tfrac{\partial^2 H_j(x,y,t-t_{ij})}{\partial x^2}\right|_{y=0}=\left.\tfrac{\partial^2 H_j(x,y,t-t_{ij})}{\partial x^2}\right|_{y=1}=0,\\
&H_j\left(x,y,t-t_{ij}\right)|_{t=t_{ij}}=0\,,\ \left.\tfrac{\partial H_j(x,y,t-t_{ij})}{\partial t}\right|_{t=t_{ij}}=0.
\end{aligned}\tag{2.11}$$

To investigate the probabilistic response of the system let us derive the modal equations. To do so, Galerkin's method is applied. According to this method and by taking into account the boundary conditions of the plate, the solution of the partial differential Eq. (2.10) is assumed to be in the form:

$$H_j\left(x,y,t-t_{ij}\right)=\sum_{n=1}^{\infty}\sum_{m=1}^{\infty}\chi_{n,m}^{(j)}\left(t-t_{ij}\right)\sin\left(n\pi x\right)\sin\left(m\pi y\right)\tag{2.12}$$

where $\chi_{n,m}^{(j)}\left(t-t_{ij}\right)$ is the generalized coordinates, $\sin\left(n\pi x\right)\sin\left(m\pi y\right)$ is the dimensionless solution of the eigenvalue problem which depends on the boundary conditions of the free oscillations of the plate and (n,m) is the natural mode with n and m nodal lines lying the $x-$ and $y-$directions, respectively. To apply the method, Eq. (2.12) is inserted into Eq. (2.10) and the resultant equation is multiplied by the corresponding eigenfunction and then integrated over the surface area of the plate. Thus, the dimensionless modal equation is obtained as:

$$\ddot{\chi}_{n,m}^{(j)}\left(t-t_{ij}\right)+\mu\dot{\chi}_{n,m}^{(j)}\left(t-t_{ij}\right)+\omega_{nm}^2\chi_{n,m}^{(j)}\left(t-t_{ij}\right)=\Gamma_m^{(j)}\sin\left[n\pi x_{ij}\left(t-t_{ij}\right)\right]\tag{2.13}$$

where:

$$\Gamma_m^{(j)}=1.\frac{4a^3\sin\left(m\pi y_{0j}\right)}{Dhb},\ \ \omega_{nm}^2=\left[\left(n\pi\right)^2+\left(\frac{m\pi a}{b}\right)^2\right]^2\tag{2.14}$$

3. Stochastic analysis

In this Section, an analytical approach for obtaining the probabilistic characteristics of the bridge plate response is developed (Subsect. 3.1) and some numerical results (Subsect. 3.2) are shown.

3.1. Effective solution of the problem

In order to directly evaluate the probabilistic characteristics of the system response under random train of moving loads, Eq. (2.13) needs to be transformed using the Itô integral and the Itô differentiation rule([13], [14]). By introducing the following state variables,

$$\begin{aligned} &z_1^{(j)}(n,m,t)=\chi_{n,m}^{(j)}(t)\,,\ z_2^{(j)}(n,m,t)=\dot{\chi}_{n,m}^{(j)}(t)\,,\\ &z_3^{(j)}(n,m,t)=\sin\left[n\pi x_{ij}(t)\right],\ z_4^{(j)}(n,m,t)=\cos\left[n\pi x_{ij}(t)\right]. \end{aligned} \tag{3.1}$$

In which for the simplicity $t-t_{ij}$ is replaced by t. In view of Eq. (2.13) and according to the Itô Lemma [13], the corresponding stochastic problem for the state variables $z_i^{(j)}$; $(i=1,2,3,4)$ may be written as a following set of Itô equations:

$$\begin{aligned} &\mathrm{d}z_1^{(j)}(n,m,t)=z_2^{(j)}(n,m,t)\,\mathrm{d}t\\ &\mathrm{d}z_2^{(j)}(n,m,t)=\left[-\omega_{nm}^2 z_1^{(j)}(n,m,t)-\mu z_2^{(j)}(n,m,t)\ +\Gamma_m^{(j)} z_3^{(j)}(n,m,t)\right]\mathrm{d}t\\ &\mathrm{d}z_3^{(j)}(n,m,t)=n\pi\sigma_{vj}z_4^{(j)}(n,m,t)\,\mathrm{d}W_{ij}(t)+\left[n\pi\varepsilon_j u_{0j}z_4^{(j)}(n,m,t)-0.5\left(n\pi\sigma_{vj}\right)^2 z_3^{(j)}(n,m,t)\right]\mathrm{d}t\\ &\mathrm{d}z_4^{(j)}(n,m,t)=n\pi\sigma_{vj}z_3^{(j)}(n,m,t)\,\mathrm{d}W_{ij}(t)+\left[-n\pi\varepsilon_j u_{0j}z_3^{(j)}(n,m,t)-0.5\left(n\pi\sigma_{vj}\right)^2 z_4^{(j)}(n,m,t)\right]\mathrm{d}t \end{aligned} \tag{3.2}$$

where $W_{ij}(t)$ is a unit Wiener stochastic process. By appropriately applying the mathematical expectation operator, the deterministic equations for various orders of the response moments can be derived. Thus, the dynamic response of the first order probabilistic moment is described by the following set of differential equations

$$\begin{aligned} &\frac{\mathrm{d}m_1^{(j)}(n,m,t)}{\mathrm{d}t}=m_2^{(j)}(n,m,t)\\ &\frac{\mathrm{d}m_2^{(j)}(n,m,t)}{\mathrm{d}t}=-\omega_{nm}^2 m_1^{(j)}(n,m,t)-\mu m_2^{(j)}(n,m,t)+\Gamma_m^{(j)}m_3^{(j)}(n,m,t)\\ &\frac{\mathrm{d}m_3^{(j)}(n,m,t)}{\mathrm{d}t}=n\pi\varepsilon_j u_{0j}m_4^{(j)}(n,m,t)-0.5\left(n\pi\sigma_{vj}\right)^2 m_3^{(j)}(n,m,t)\\ &\frac{\mathrm{d}m_4^{(j)}(n,m,t)}{\mathrm{d}t}=-n\pi\varepsilon_j u_{0j}m_3^{(j)}(n,m,t)-0.5\left(n\pi\sigma_{vj}\right)^2 m_4^{(j)}(n,m,t) \end{aligned} \tag{3.3}$$

where $m_i^{(j)}(n,m,t)=\mathrm{E}\left[z_i^{(j)}(n,m,t)\right]$ and the initial conditions (according to Eqs. (2.11), (2.12) and (3.1)) are: $m_1^{(j)}(n,m,0)=0$, $m_2^{(j)}(n,m,0)=0$, $m_3^{(j)}(n,m,0)=0$, $m_4^{(j)}(n,m,0)=1$. For the second order dynamic moment, let us introduce the following notations for the second order probabilistic moments of variables $z_i^{(j)}(n,m,t)$

$$\begin{aligned} &m_{2000}^{(j)}(k,l,n,m,t)=\mathrm{E}\left[z_1^{(j)}(k,l,t)\,z_1^{(j)}(n,m,t)\right]\\ &m_{1100}^{(j)}(k,l,n,m,t)=\mathrm{E}\left[z_1^{(j)}(k,l,t)\,z_2^{(j)}(n,m,t)\right]\\ &m_{1010}^{(j)}(k,l,n,m,t)=\mathrm{E}\left[z_1^{(j)}(k,l,t)\,z_3^{(j)}(n,m,t)\right]\\ &m_{1001}^{(j)}(k,l,n,m,t)=\mathrm{E}\left[z_1^{(j)}(k,l,t)\,z_4^{(j)}(n,m,t)\right]\\ &m_{0200}^{(j)}(k,l,n,m,t)=\mathrm{E}\left[z_2^{(j)}(k,l,t)\,z_2^{(j)}(n,m,t)\right]\\ &m_{0110}^{(j)}(k,l,n,m,t)=\mathrm{E}\left[z_2^{(j)}(k,l,t)\,z_3^{(j)}(n,m,t)\right]\\ &m_{0101}^{(j)}(k,l,n,m,t)=\mathrm{E}\left[z_2^{(j)}(k,l,t)\,z_4^{(j)}(n,m,t)\right]\\ &m_{0020}^{(j)}(k,l,n,m,t)=\mathrm{E}\left[z_3^{(j)}(k,l,t)\,z_3^{(j)}(n,m,t)\right]\\ &m_{0011}^{(j)}(k,l,n,m,t)=\mathrm{E}\left[z_3^{(j)}(k,l,t)\,z_4^{(j)}(n,m,t)\right]\\ &m_{0002}^{(j)}(k,l,n,m,t)=\mathrm{E}\left[z_4^{(j)}(k,l,t)\,z_4^{(j)}(n,m,t)\right] \end{aligned} \tag{3.4}$$

So, the differential equations for calculating the second order probabilistic moments of the variables $z_i^{(j)}$ are obtained as:

$$\begin{aligned}
\frac{\mathrm{d}m_{2000}^{(j)}(k,l,n,m,t)}{\mathrm{d}t} &= m_{1100}^{(j)}(k,l,n,m,t)+m_{1100}^{(j)}(n,m,k,l,t)\\
\frac{\mathrm{d}m_{1100}^{(j)}(k,l,n,m,t)}{\mathrm{d}t} &= m_{0200}^{(j)}(k,l,n,m,t)-\omega_{nm}^2 m_{2000}^{(j)}(k,l,n,m,t)-\mu m_{1100}^{(j)}(k,l,n,m,t)+\Gamma_m^{(j)} m_{1010}^{(j)}(k,l,n,m,t)\\
\frac{\mathrm{d}m_{1010}^{(j)}(k,l,n,m,t)}{\mathrm{d}t} &= m_{0110}^{(j)}(k,l,n,m,t)+n\pi\varepsilon_j u_{0j} m_{1001}^{(j)}(k,l,n,m,t)-0.5\left(n\pi\sigma_{vj}\right)^2 m_{1010}^{(j)}(k,l,n,m,t)\\
\frac{\mathrm{d}m_{1001}^{(j)}(k,l,n,m,t)}{\mathrm{d}t} &= m_{0101}^{(j)}(k,l,n,m,t)-n\pi\varepsilon_j u_{0j} m_{1010}^{(j)}(k,l,n,m,t)-0.5\left(n\pi\sigma_{vj}\right)^2 m_{1001}^{(j)}(k,l,n,m,t)\\
\frac{\mathrm{d}m_{0200}^{(j)}(k,l,n,m,t)}{\mathrm{d}t} &= -\omega_{kl}^2 m_{1100}^{(j)}(k,l,n,m,t)-\omega_{nm}^2 m_{1100}^{(j)}(n,m,k,l,t)-2\mu m_{0200}^{(j)}(k,l,n,m,t)+\Gamma_m^{(j)} m_{0110}^{(j)}(k,l,n,m,t)+\Gamma_l^{(j)} m_{0110}^{(j)}(n,m,k,l,t)\\
\frac{\mathrm{d}m_{0110}^{(j)}(k,l,n,m,t)}{\mathrm{d}t} &= -\omega_{kl}^2 m_{1010}^{(j)}(k,l,n,m,t)-\mu m_{0110}^{(j)}(k,l,n,m,t)+\Gamma_l^{(j)} m_{0020}^{(j)}(k,l,n,m,t)+n\pi\varepsilon_j u_{0j} m_{0101}^{(j)}(k,l,n,m,t)\\
&\quad -0.5\left(n\pi\sigma_{vj}\right)^2 m_{0110}^{(j)}(k,l,n,m,t)\\
\frac{\mathrm{d}m_{0101}^{(j)}(k,l,n,m,t)}{\mathrm{d}t} &= -\omega_{kl}^2 m_{1001}^{(j)}(k,l,n,m,t)-\mu m_{0101}^{(j)}(k,l,n,m,t)+\Gamma_l^{(j)} m_{0011}^{(j)}(k,l,n,m,t)-n\pi\varepsilon_j u_{0j} m_{0110}^{(j)}(k,l,n,m,t))\\
&\quad -0.5\left(n\pi\sigma_{vj}\right)^2 m_{0101}^{(j)}(k,l,n,m,t)\\
\frac{\mathrm{d}m_{0020}^{(j)}(k,l,n,m,t)}{\mathrm{d}t} &= \pi\varepsilon_j u_{0j}\left[n m_{0011}^{(j)}(k,l,n,m,t)+k m_{0011}^{(j)}(n,m,k,l,t)\right]-0.5\pi^2\sigma_{vj}^2\left[k^2+n^2\right] m_{0020}^{(j)}(k,l,n,m,t)+nk\pi^2\sigma_{vj}^2 m_{0002}^{(j)}(k,l,n,m,t)\\
\frac{\mathrm{d}m_{0011}^{(j)}(k,l,n,m,t)}{\mathrm{d}t} &= k\pi\varepsilon_j u_{0j} m_{0002}^{(j)}(k,l,n,m,t)-n\pi\varepsilon_j u_{0j} m_{0020}^{(j)}(k,l,n,m,t)-0.5\pi^2\sigma_{vj}^2\left[k^2+n^2\right] m_{0011}^{(j)}(k,l,n,m,t)+nk\pi^2\sigma_{vj}^2 m_{0011}^{(j)}(k,l,n,m,t)\\
\frac{\mathrm{d}m_{0002}^{(j)}(k,l,n,m,t)}{\mathrm{d}t} &= -\pi\varepsilon_j u_{0j}\left[k m_{0011}^{(j)}(k,l,n,m,t)+n m_{0011}^{(j)}(n,m,k,l,t)\right]-0.5\pi^2\sigma_{vj}^2\left[k^2+n^2\right] m_{0002}^{(j)}(k,l,n,m,t)+nk\pi^2\sigma_{vj}^2 m_{0020}^{(j)}(k,l,n,m,t)
\end{aligned} \tag{3.5}$$

For $(k,l)\neq(n,m)$, the above set of differential equations must be completed by adding a duplicate set of equations in which the parameters (k,l) should be replaced by (n,m) and vice versa. According to Eqs. ((2.11), (2.12), (3.1) and (3.3)), the initial conditions are:

$$\begin{aligned}
m_{2000}^{(j)}(k,l,n,m,0) &= m_{2000}^{(j)}(n,m,k,l,0)=0\\
m_{0200}^{(j)}(k,l,n,m,0) &= m_{0200}^{(j)}(n,m,k,l,0)=0\\
m_{0020}^{(j)}(k,l,n,m,0) &= m_{0020}^{(j)}(n,m,k,l,0)=0\\
m_{0002}^{(j)}(k,l,n,m,0) &= m_{0002}^{(j)}(n,m,k,l,0)=1\\
m_{1100}^{(j)}(k,l,n,m,0) &= m_{1100}^{(j)}(n,m,k,l,0)=0\\
m_{1010}^{(j)}(k,l,n,m,0) &= m_{1010}^{(j)}(n,m,k,l,0)=0\\
m_{1001}^{(j)}(k,l,n,m,0) &= m_{1001}^{(j)}(n,m,k,l,0)=0\\
m_{0110}^{(j)}(k,l,n,m,0) &= m_{0110}^{(j)}(n,m,k,l,0)=0\\
m_{0101}^{(j)}(k,l,n,m,0) &= m_{0101}^{(j)}(n,m,k,l,0)=0\\
m_{0011}^{(j)}(k,l,n,m,0) &= m_{0011}^{(j)}(n,m,k,l,0)=0
\end{aligned} \tag{3.6}$$

For the loading process, the solution of Eq. (2.6) is a superposition of individual response due to each train of forces moving to each lane. So the plate response may be expressed in the following form:

$$w(x,y,t)=\frac{a^3}{Dhb}\sum_{j=1}^{n_l}\sum_{i=1}^{N_j(t)}A_{ij}H_j\left(x,y,t-t_{ij}\right)=\frac{a^3}{Dhb}\sum_{j=1}^{n_l}\int_0^t A_j(\tau)H_j(x,y,t-\tau)\,\mathrm{d}N_j(\tau) \tag{3.7}$$

By taking into account the features of the Poisson process, we are looking for the expected value of the plate response in the form:

$$\begin{aligned}
\mathrm{E}[w(x,y,t)] &= \frac{a^3}{Dhb}\sum_{j=1}^{n_l}\mathrm{E}\left[A_j\right]\int_0^t \mathrm{E}\left[H_j\left(x,y,t-\tau_j\right)\right]\times\lambda_j(\tau)\wp\left\{x_j\left(t-\tau_j\right)<1\right\}\mathrm{d}\tau_j\\
&= \frac{a^3}{Dhb}\sum_{j=1}^{n_l}\mathrm{E}\left[A_j\right]\sum_{n=1}^{\infty}\sum_{m=1}^{\infty}\sin(n\pi x)\sin(m\pi y)\times\int_0^t m_1^{(j)}\left(n,m,t-\tau_j\right)\lambda_j(\tau)\wp\left\{x_j\left(t-\tau_j\right)<1\right\}\mathrm{d}\tau_j
\end{aligned} \tag{3.8}$$

and for the variance of the plate response in the form:

$$\sigma_w^2(x,y,t) = \left(\frac{a^3}{Dhb}\right)^2 \sum_{j=1}^{n_l} \mathrm{E}\left[A_j^2\right] \int_0^t \mathrm{E}\left[H_j^2\left(x,y,t-\tau_j\right)\right] \times \lambda_j(\tau)\, \wp\left\{x_j\left(t-\tau_j\right)<1\right\} \mathrm{d}\tau_j$$

$$= \sum_{j=1}^{n_l} \mathrm{E}\left[A_j^2\right] \sum_{k=1}^{\infty}\sum_{l=1}^{\infty}\sum_{n=1}^{\infty}\sum_{m=1}^{\infty} \sin(k\pi x)\sin(l\pi y)\sin(n\pi x)\sin(m\pi y) \times \left(\frac{a^3}{Dhb}\right)^2 \int_0^t m_{2000}^{(j)}\left(k,l,n,m,t-\tau_j\right)\lambda_j(\tau)\, \wp\left\{x_j\left(t-\tau_j\right)<1\right\} \mathrm{d}\tau_j \tag{3.9}$$

where $\lambda_j(\tau)$ is the arrival rate for the $j-th$ loads trajectory, $\wp\left\{x_j\left(t-\tau_j\right)<1\right\}$ is the unknown function which describing the fact that the probability that the forces occurring in time τ_j at the beginning of each rectilinear path j of the plate is still acting on to the structure in time t. This function can be evaluated by first looking for the transition probability density function $f\left(x_{ij},t-t_{ij}\right)$ for the process $x_{ij}\left(t-t_{ij}\right)$ (describes by Eq. (2.8)) which is governed by the following Fokker-Planck-Kolmogorov equation.

$$\frac{\partial f\left(x_{ij},t-t_{ij}\right)}{\partial t} + \varepsilon_j u_{0j} \frac{\partial f\left(x_{ij},t-t_{ij}\right)}{\partial x_{ij}} + \frac{1}{2}\sigma_{vj}^2 \frac{\partial^2 f\left(x_{ij},t-t_{ij}\right)}{\partial x_{ij}^2} = 0 \tag{3.10}$$

By using the Fourier transform, the normalization condition and the following formulas,

$$f\left(x_{ij},t-t_{ij}\right)\Big|_{\,t=t_{ij}} = \delta\left(x_{ij}\right),\ f\left(x_{ij},t-t_{ij}\right)\Big|_{\,x_{ij}=\infty} = 0 \tag{3.11}$$

the solution of Eq. (3.10) is given as:

$$f\left(x_{ij},t-t_{ij}\right) = \frac{1}{\mu_{ij}}\sqrt{\frac{2}{\pi(t-t_{ij})}}\exp\left[-\frac{(x_{ij}-\varepsilon_j u_{0j}(t-t_{ij}))^2}{2\sigma_{vj}^2(t-t_{ij})}\right]$$
$$\text{For } x_{ij}\geq 0\,,\quad j=1,2. \tag{3.12}$$

Thus, the probability $\wp\left\{x_{ij}\left(t-t_{ij}\right)<1\right\}$ that we are looking for takes a form:

$$\wp\left\{x_{ij}\left(t-t_{ij}\right)<1\right\} = \int_0^1 f\left(x_{ij},t-t_{ij}\right)\mathrm{d}x_{ij} = \frac{1}{\mu_{ij}\sqrt{2}}\left[\sigma_{vj}\mathrm{Erf}\left(\sqrt{\frac{1}{2\sigma_{vj}^2(t-t_{ij})}} - \varepsilon_j\frac{u_{0j}}{\sigma_{vj}}\sqrt{\frac{(t-t_{ij})}{2}}\right) + \mu_{ij} - \sigma_{vj}\right] \tag{3.13}$$

In which

$$\mu_{ij} = \sigma_{vj}\left[1-\mathrm{Erf}\left(-\varepsilon_j\frac{u_{0j}}{\sigma_{vj}}\sqrt{\frac{(t-t_{ij})}{2}}\right)\right] \tag{3.14}$$

$\mathrm{Erf}(...)$ is the error function.

Now, the explicit formulas for the expected value and for the variance function of a thin rectangular plate response due to a two opposite train of random forces (vehicles) were derived. In order to have a complete investigation of the dynamic behaviors of the studied system, the numerical analysis will be carried out in which the effects of some main parameters of the moving loads on the probabilistic bridge response will be analysed in the following section.

3.2. Numerical results and discussion

For the numerical purpose, the case of bridge plate having the following parameters are considered (see Table 1). It is assumed that the vehicles weight had a lognormal distribution with the expected value and the standard deviation equal to $\mathrm{E}[A] = 10^5$ N and $\mathrm{E}[A^2] = 1.2\times10^{10}\,\mathrm{N}^2$ ([16]), respectively. In this paper the problem will be confined to the homogeneous case. Therefore, the intensity of the load distribution is assumed to be constant for the simplicity: $\lambda_j(\tau) = \lambda = 0.33/\omega_0$ ([14]). Nevertheless, notice that, in traffic engineering [15], this intensity is related to the average passage speed of the vehicles and inversely. The mean value of the velocity v_{oj} varying from 10 to 50 m/s; the variation coefficient of velocity σ_{vj} varying from 0.01 to 0.3. We assume that $u_{01} = u_{02} = u_0$ and $\sigma_{v1} = \sigma_{v2} = \sigma_v$. The

Table 1: Properties of the model of plate studied ([7])

Item	Notation	Value
Length	a	24 m
Width	b	8 m
Thickness	h	1 m
Young's modulus	E	50 GPa
Poisson's ratio	υ	0.3
Mass density	ρ	2400 kg/m^3
damping coefficient	c	0.91 kg/s

presents numerical analysis is carried out by simulating first the deterministic Eqs. ((3.3) and (3.5)) through the fourth order Runge-Kutta algorithm. Therefore, the expected $\mathrm{E}[w(x,y,t)]$ and the standard deviation $\sigma_w^2(x,y,t)$ of the dimensionless plate displacement at the midspan $(x=1/2, y=1/2)$ are obtained for different range of the moving loads parameters.

In Fig. 3.1, the average plate deformation is shown when various numbers of modes are used to analyze the response of the structure. It is quite evident that moving from a single mode (mode (1, 1)) analysis to another one, mode (1,2) the accuracy of the solution drastically

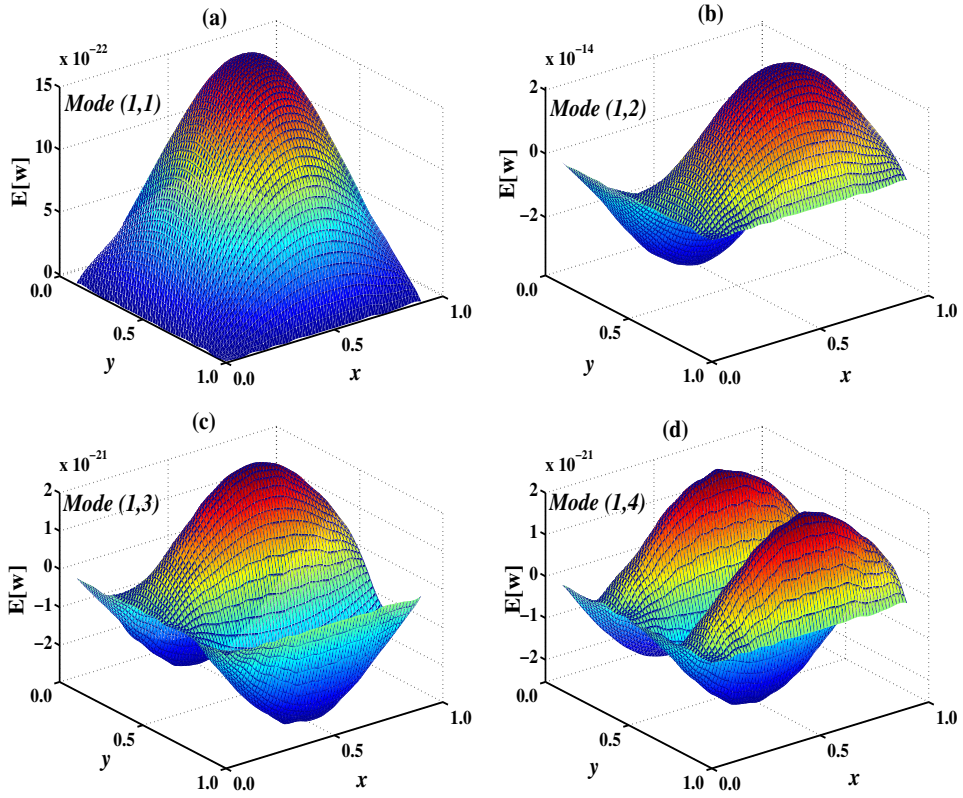

Figure 3.1: Average plate deformation when $\lambda_1 = \lambda_2 = 0.15, \sigma_{v1} = \sigma_{v2} = 0.3, u_{01} = u_{02} = 0.5$. (a) mode (1,1), (b) mode (1,2), (c) mode (1,3) and (d) mode (1,4). The parameters used are obtained according to Eqs. ((2.7),(2.14)) and Table 1

.

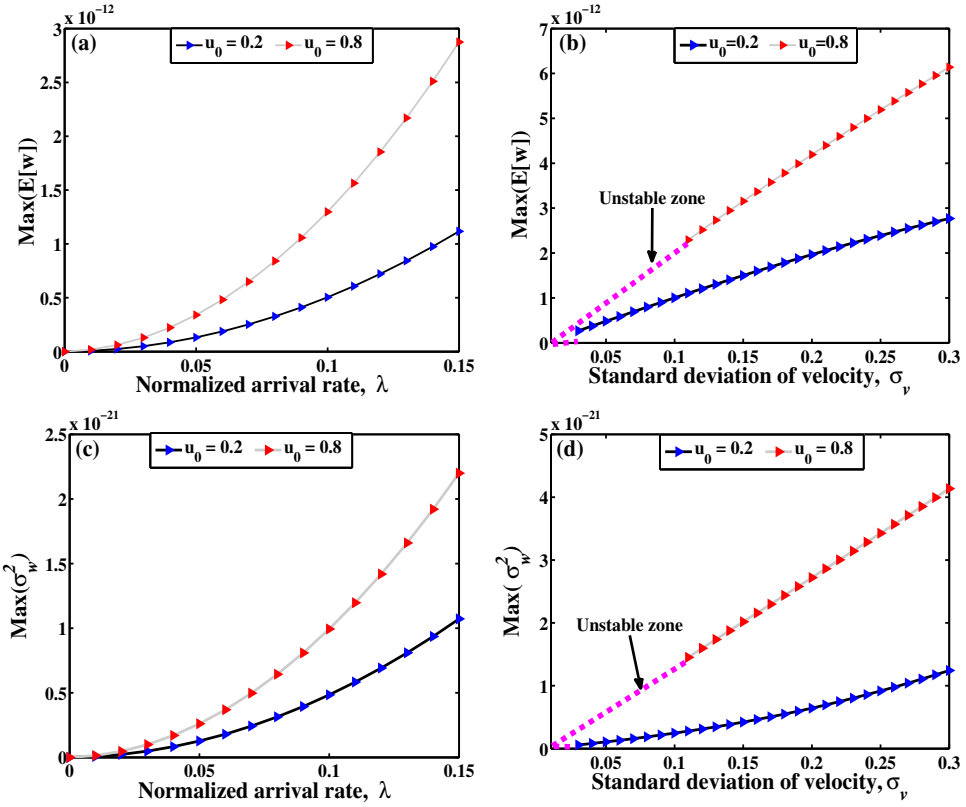

Figure 3.2: The maximum expected values and the variances of a plate displacement in relation to the normalized average flow intensity λ or the standard deviation of the stochastic velocity σ_v. (a), (b) expected value, (c), (d) variance. The other parameters used are obtained according to Eqs. ((2.7),(2.14)) and Table 1.

increases and an abrupt change in the shape of the plate is observed. This can be explain by the fact that, moving load is commonly expected to excite more modal shape, not only the first mode. Likewise, increasing the number of modes in the analysis to (1,4) apparently decreases the solution.
Fig. 3.2 illustrates the relations between the normalized average flow intensity λ or the standard deviation of the stochastic velocity and the expected values and variances of a stochastic maximal plate displacement $w(x,y,t)$. It is observed first that as the value of λ increases the expected $\mathrm{E}[w]$ and standard deviation σ_w^2 of a maximal plate deflection merely increase (see Figs. 3.2(a) and 3.2(c)). Since that the number of vehicles $N(t)$ is related to the arrival rate λ and inversely, this result confirms well the one obtains by [7] and by [17]. Secondly, the increase of the value of σ_v also increases the expected and the standard deviation of a maximal plate deflection (see Figs. 3.2(b) and 3.2(d)). The analysis leads us to the conclusion that it is necessary and more important to take into account the stochastic nature of the load velocity in such studies. The influence of the mean velocity on the same probabilistic features of the plate response is also investigated and it is observed that as the mean value of the velocities increases, the expected value and the variance of the plate response also increase. It is also observed that for a normalized average speed $u_0 = 0.8$ (about 50 m/s), an unstable zone is observed when the standard deviation of the velocity $\sigma_v \in [0.01, 0.11]$. This unstable zone decreases as the mean value velocity decreases.

4. Summary and conclusion

Summing up, an approach to analyse the stochastic vibrations of a two lane slab-type-bridge due to a set of random point forces, which idealise the traffic flow, moving with stochastic velocities has been presented. This approach has been built under the assumption that the force arrival times constitute a Poisson stochastic process and the velocity of each force is a special kind of stochastic process, which can be described by the sum of the mean value and a white noise disturbance. By using the Kirchhoff's hypothesis, a two lane slab-type-bridge has been modelled as a Simply Supported thin rectangular plate with two separate rectilinear paths. The results prove the strong influence of the variation coefficient of velocity on the plate response - both the expected value and the standard deviation of deflection. It has been observed that the bridge safety strongly depends to the mean value and to the standard deviation of the vehicles velocities. Thus, some bridges may last more than expected or prematurely destroy because of the effects of the moving load random velocities.
On the basis of the approach presented above the influence of different traffic load models parameters on the random response of a bridge can be studied. It enables us to select the optimum design solution from a reliability point of view.

References

[1] L. Frýba, *Vibration of Solids and Structures under Moving Load*, Thomas Telford, London, 1999.
[2] H. Ouyang, *Moving load dynamic problems: a tutorial (with a brief overview)*, Mechanical Systems and Signal Processing, **25** (2011), 2039-2060.
[3] A. Nikkhoo, F. R. Rofooei, *Parametric study of the dynamic response of thin rectangular plates traversed by a moving mass*, Acta Mechanica, **223** (2012), 15-27.
[4] J.-J. Wu, *Vibration analyses of an inclined flat plate subjected to moving loads*, Journal of Sound and Vibration, **299** (2007), 373-387.
[5] J. Vaseghi Amiri, A. Nikkhoo, M. R. Davoodi, M. Ebrahimzadeh Hassanabadi, *Vibration analysis of a Mindlin elastic plate under a moving mass excitation by eigenfunction expansion method*, Thin-Walled Structures, **62** (2012), 53-64.
[6] X. Q. Zhu, S. S. Law, *Dynamic Behavior of Orthotropic Rectangular Plates under Moving Loads*, Journal of Engineering Mechanics, **129** (2007), 79-87.
[7] A. Nikkhoo, M. Ebrahimzadeh Hassanabadi, S. Eftekhar Azamc, J. Vaseghi Amiri, *Vibration of a thin rectangular plate subjected to series of moving inertial loads*, Mechanics Research Communications, **55** (2014), 105-113.
[8] A. Rystwej, P. Śniady, *Dynamic response of an infinite beam and plate to a stochastic train of moving forces*, Journal of Sound and Vibration, **299** (2007), 1033-1048.
[9] M. Li, T. Qian, Y. Zhong, H. Zhong, *Dynamic Response of the Rectangular Plate Subjected to Moving Loads with Variable Velocity*, Journal of Engineering Mechanics, **140** (2013), 06014001.
[10] S. P. Timoshenko, *Theory of Plates and Shells*, Wiley, New York, 1959.
[11] P. Śniady, S. Biernat, R. Sieniawska, S. Zukowski, *Vibrations of the beam due to a load moving with stochastic velocity*, Probabilistic Engineering Mechanics, **16** (2001), 53-59.
[12] L. M. Anague Tabejieu, B. R. Nana Nbendjo, G. Filatrella, P. Woafo, *Amplitude stochastic response of Rayleigh beams to randomly moving loads*, Nonlinear Dynamics, **89** (2017), 925-937.
[13] W.-C. Xie, *Dynamic stability of structures*, Cambridge university press, New York, 2006.
[14] P. Śniady, S. Biernat, R. Sieniawska, S. Zukowski, *Vibrations of the beam due to a load moving with stochastic velocity*, Probabilistic Engineering Mechanics, **16** (2001), 53-59.
[15] R. J. Salter, *Highway Trafic Analysis and Design*, Macmillan, London, 1976.
[16] D. Bryja, P. Śniady, *Spatially coupled vibrations of a suspension bridge under random Highway traffic*, Earthquake Engineering and Structural Dynamics, **20** (1991), 995-1010.
[17] L. M. Anague Tabejieu, B. R. Nana Nbendjo, U. Dorka, *Identification of horseshoes chaos in a cable-stayed bridge subjected to randomly moving loads*, International Journal of Non-Linear Mechanics, **85** (2016), 62-69.
[18] M. Kamiński, *The Stochastic Perturbation Method for Computational Mechanics*, John Wiley & Sons Ltd, United Kingdom, 2013.

Journal of Mathematical Sciences and Modelling, 2 (2) (2019) 133-142
Research Article

Journal of Mathematical Sciences and Modelling

Journal Homepage: www.dergipark.gov.tr/jmsm
ISSN 2636-8692
DOI: http://dx.doi.org/10.33187/jmsm.458359

A Review on Hydrodynamical Stability of Thin Film Flowing Along an Inclined Plane

Souradip Chattopadhyay[1*], Anandamoy Mukhopadhyay[2] and Amlan K. Barua[1]

[1]*Department of Mathematics, Indian Institute of Technology Dharwad, Karnataka - 580011, India*
[2]*Department of Mathematics, Vivekananda Mahavidyalaya (The University of Burdwan), West Bengal - 713103, India*
[*]*Corresponding author*

Article Info

Keywords: *Hydrodynamical stability, Inclined plane, Thin film.*
2010 AMS: *35Q30, 35Q35, 35Q79, 76E07, 76E17, 76E25, 76E30.*
Received: *9 September 2018*
Accepted: *8 April 2019*
Available online: *30 August 2019*

Abstract

The dynamics and stability of thin liquid films have fascinated scientists over many decades. Thin film flows occur over a wide range of length scales and are central to numerous areas of engineering, geophysics and biophysics. These include nanofluidics and microfluidics, lava flows, coating flows, tear-film rupture, dynamics of continental ice sheets and surfactant replacement therapy. Study of falling film instability has its wide applications in the practical field of industry and engineering. Practical applications in industrial processing motivate the recent research to investigate the factors which may affect the formation of waves on the surface of the coating layers and/or to determine the ways to overcome or to minimize the unwanted factors within the desired limit of tolerance. The dynamics of a liquid film flowing down a plane under the action of gravity is a problem which appears in many technological and natural systems, namely large scale geophysical environments such as lava flows or spillways, daily life scenarios such as water flowing down a window pane or a slippery road on a rainy day, chemical engineering processes such as evaporators, heat exchanges and falling film reactors or surface coating. The aim of this paper is to throw light on the studies conducted on hydrodynamical stability.

1. Introduction

Hydrodynamical stability is an important branch of the fluid mechanics both from application and theoretical points of view. Stability is the measure of the ability of a system to resist the changes or in other words how a system reverts to its original state after suffering all possible modes of perturbation. An important criterion for a flow state to be physically stable is the ability of the system to withstand small disturbances which are present or may be transmitted from the surroundings to the flow. The theory of small oscillations is a useful tool for investigating the stability problems in hydrodynamics. If small disturbances superimposed on initial laminar flow, decay in time or with distance downstream, then the laminar flow is stable. If they increase, that is if the growth of the perturbation is unbounded, or if the real outcome is just another different state, or if it is a bounded but turbulent or chaotic state or accompanies the collapse of physical assumptions underlying the governing equations then the outcome is a different physical system. A very common example of instability is the formation of waves on surfaces of water owing to the action of wind. The "Taylor-Couette flow instability" is a well known instability, which arises due to centrifugal force, and Rayleigh-Benard convection, which arises due to difference of density are important instability phenomena occurring in laboratories and nature. A detailed description of the entire field is given by Schlichting [1], Lin [2], Hsieh and Ho [3] and Drazin and Reid [4]. It is very interesting that despite the effort of generations of applied mathematicians, beginning with Rayleigh, Kelvin and Reynolds, many simple understanding of phenomena related to hydrodynamic stability remain incomplete. Therefore it is an important task for the applied mathematics community to highlight different aspects of flow instability.
The instability of a thin film was first investigated in 1949 when Kapitza and Kapitza [5] took some elegant photographs with the help of some simple kitchen apparatus. After the publication of these photographs, the research community felt that these photographs represent a simple hydrodynamical instability phenomenon on a thin film flowing along an inclined plane. The beauty and simplicity of this phenomenon

Email addresses and ORCID numbers: **183111001@iitdh.ac.in, 0000-0002-4418-6201 (S. Chattopadhyay), ananda235@email.com (A. Mukhopadhyay), abarua@iitdh.ac.in (A. K. Barua)**

lie in the fact that although the movement of the film is due to inertia, the instability may occur at an extremely low Reynolds number under very common conditions. Their simplicity also lies in the fact that the wavy thin film flowing down an inclined plane can be parameterized by a single dimensionless parameter (Reynolds number) with mild approximation. For example, a simple tap water flow is sufficient to produce a wavy thin film. When the work of Kapitza and Kapitza [5] came to light, many top applied mathematicians became attracted to know the instability mechanism of the wavy thin film due to its added complexity of the involved free surface. The factors behind the origin of instability was first understood by Benjamin [6] in Cambridge through the use of long-wave expansion method. At Michigan, C. S. Yih [7] improved the theory of Benjamin by introducing the vital role of surface tension on a thin film. D. J. Benney [8] at MIT pioneered a lubrication approach to include nonlinear effects. Later Shkadov [9, 10] of Moscow State University introduced the averaging technique and then Sivashinsky [11] in Russia derived the famous Kuramoto-Sivashinsky equation for the falling film instability. Benjamin [6] and Yih [7] developed linear theories which were only able to describe the instability of the flat film in basic state. On the other hand the nonlinear theories developed by Benney [8], Shkadov [9, 10] and Sivashinsky [11] helped to describe only the wave dynamics of first 10 cm of the inclined plane but failed to demystify the rest 1m of the inclined plane. In the eighties, the theory of instability of falling film was improved significantly by the use of computational methods, which allows the simulation of wave dynamics within 1m channel to fully capture the entire sequence of the wave evolution. Pumir et al. [12] pointed out that the complex interfacial dynamics of a falling film often consist of quasi-stationary travelling waves which propagate long distances without changing their shape or speed. Theoretical as well as numerical investigations are still going on to explore the complex wave dynamics of a wavy thin film.

2. Review of Literature

Hydrodynamic mode of instability on a surface of an isothermal falling film was first shown by Kapitza and Kapitza [5] in their experimental work. After this experimental work, a thin viscous film flowing along a vertical/inclined wall became the topic of highest interest for many researchers. Benjamin [6] and Yih [7] studied the isothermal falling film by the way of linear stability analysis and predicted that when the Reynolds number Re, which is a flow parameter, exceeds some critical value $Re_c = \frac{5}{6}\cot\theta$ (where θ was the angle of inclination with the horizon), the uniform flow becomes unstable to long-wave disturbances. Benney's [8] long-wave model has considered the evolution of the finite-amplitude disturbances of the flat film. In this model the velocity components and pressure gradient are expanded in powers of ε, which is the ratio of the thickness of the flat film to the wave length of the disturbances in the direction of the flow. Under the assumption of long-wave length ($\varepsilon << 1$) the governing equations together with the boundary conditions reduced to a single nonlinear partial differential equation, that describes the evolution of the free surface. Later, a nonlinear analysis was performed by Gjevik [13], Lin [14], Nakaya [15] and others. Lin [16] and Gjevik [13] found that the supercritical stability was possible in the region near the upper branch of the neutral stability curve. Nakaya [15] showed that in the presence of surface tension, an initially growing monochromatic wave reaches an equilibrium state of finite amplitude. Lin and Krishna [17] extended the analysis of Lin [16] for investigating the nonlinear stability of a liquid film with respect to the three dimensional side-band disturbances. They showed that the finite amplitude, supercritical stable, long monochromatic wave is stable to three-dimensional side-band disturbances under the modal interaction if the bandwidth is less in magnitude than ε, which is proportional to the ratio of the amplitude to the film thickness. The equations derived by Gjevik [13] was solved numerically by Pumir et al. [12] and they obtained its solitary wave solutions, which were earlier observed by Kapitza, Paul, Liu and Gullub [18]. Further, Liu and Gullub [19, 20] studied the flow development down a plane inclined at small angles ($4^\circ \leq \theta \leq 10^\circ$) for moderate Reynolds ($6 < Re < 26$) and Weber numbers ($3 < We < 33$), by introducing artificial perturbations of varying amplitudes and frequencies at the entrance, so that the two-dimensional regular waves appeared slightly downstream. They confirmed with careful measurements the theoretical predictions for the critical Reynolds number that was earlier proposed by Benjamin [6] and Yih [7]. Alekseenko et al. [21], Chang [22], Fulford [23], Lin and Wang [24], Hanratty [25, 26], Hewitt and Hall-Taylor [27] and Nakaroyakov et al. [28] studied the instability mechanism of thin film and their observations were documented in books/monographs. In our careful observation we have noticed that most of the studies dealt with the flow of a thin liquid film on an inclined plane assuming that the fluid is isothermal but in practical field it is sometimes necessary to consider the thin film to be non-isothermal.

Heat is the energy transferred between one system and its environment because of the temperature difference which exists between them. In fluid medium, a bulk amount of heat is transferred by means of convection, from the higher temperature region to the lower temperature region. The temperature of the part of the fluid increases which is in contact with the hot object and that fluid expands and naturally becomes less dense. Since the expanded fluid is lighter than the surrounding cooler fluid and more dense, buoyant force causes it to rise. From the surrounding region some of the cooler fluid then flows to take the place of the rising warmer fluid and the process continues. In the case of the thin heated films, buoyancy effects are so small that it can be treated as negligible. Uniform or non-uniform heating of the thin layers may cause considerable temperature difference at the interface and thus the thermocapillary force will draw liquid from the warmer region to the cooler region. Thermocapillary or Marangoni instability is known to be one of the most ubiquitous types of instability of the heated liquid films. This arises due to the variation of the interfacial temperature along the film interface leading thus to the non-uniformity of the surface tension, which generates an interfacial shear stress. Such a stress entails, by means of viscosity, the liquid into motion, while even hotter liquid reaches the film surface and accelerates the film flow.

Pearson [29] first investigated the thermocapillary or Marangoni instability in the liquid layers. He discussed the short wave thermocapillary instability considering a horizontal liquid layer with non-deformable free surface. He found that the surface tension variation in the absence of buoyancy can lead to convection in the thin film. Later Scriven and Sternling [30] concluded that disturbances with zero wave number are always unstable by considering the surface deformation, without taking into account the force of gravity. Further the long wave thermocapillary instability was studied by Smith [31], where the force of gravity was taken into account. The combined effect of the thermocapillary instability and a number of physical factors such as condensation/evaporation, vapor recoil and rupture due to long-range attractive Van der Waals interactions have been considered by a number of authors, such as Bankoff [32] and Burelbach et al. [33] and others. Flow of a viscous film down a heated inclined/vertical plane is an interesting problem, since the presence of the thermocapilarity, couples the hydrodynamic and the thermal boundary layer equations. Goussis and Kelly [34] first studied the thermocapillary instability in a liquid film falling down an inclined uniformly heated plane based on Orr-Sommerfeld model and the linearized energy equations. They found that a heated wall has a destabilizing effect on the free surface but a cooled wall stabilizes the flow. The long wave instability of a uniform film of volatile viscous liquid falling down a uniformly heated inclined plane was investigated by Joo et al. [35] for two-dimensional disturbances.

They took into account the thermocapillary, surface tension and evaporation effects. Actually that work was an effective extension of the Benny's [8] long wave expansion for non-isothermal film flow. For this reason the evolution equation in terms of $h(x,t)$ is known as 'Benny equation with Marangoni effect' in the literature. The terms depending on the Marangoni number are of second order in comparison with those due to gravity and mean flow. They applied the linear and nonlinear stability theory to analyse the comparison among the different types of instabilities and finally obtained similar results as that of Goussis and Kelley [34]. Later the steady-state profile for a thin, non-isothermal coating film down an inclined plane of constant temperature, was discussed by Lopez et al. [36]. They studied the linear stability of the film to spanwise disturbances and then numerically solved the steady-state and the linear disturbance equation. They found that the small heating causes a destabilizing effect in the leading front of a coating film and also found that increasing the Biot number and allowing more heat to dissipate at the liquid-gas interface inhibit the effect of the heating.

Kabov et al. [37], Kabov [38] and Scheid et al. [39] reported various experimental works on the thermocapillary/ Marangoni instability of a thin liquid film heated from below with a local heat source. In these experiments a vertically falling thin liquid film is heated from the wall side by a device. The transverse dimension of the heater is much longer than its width in the streamwise direction. The heater generates a temperature distribution at the film surface which in turn sets up surface tension gradients which drive the fluid away from the heated region. This thermocapillary flow results in the formation of a bump in the streamwise direction, the height of which increases as the heat flux supplied by the heater increases. For a certain critical value of the heat flux, an instability in the transverse direction develops. Here this instability takes the form of rivulets at the downstream edge of the bump.

Motivated by these experimental works, Kalliadasis et al. [40] studied the thermocapillary instability of a falling liquid film heated from below by a heating device on the substrate, where the transverse dimension of the heater is much longer than width in the streamwise direction as considered by Kabov [38], Kabov et al. [37] and Scheid et al. [39] in their experimental works. They found that in the region where the wall temperature gradient is positive, the free surface develops a bump and the height of this bump was found to be an increasing function of the Marangoni number. Further, they also showed that the temperature distribution on the free surface and demonstrated that for the finite Peclet number, the temperature field is distributed downstream resulting in a free-surface temperature distribution with a maximum in the region where the wall temperature gradient is negative. Later Kalliadasis et al. [41] studied the thermocapillary instability of a viscous liquid film flowing down a uniform heated plane by using integral boundary layer approach, which was introduced by Shkadov [9, 10] in two dimensions and Demekhin and Shkadov [42] in three dimensions for non-isothermal flows. It combines the boundary-layer approximation of Navier-Stokes equation assuming a self-similar velocity profile on the interface with the Karman-Pohlhausen averaging method in the boundary-layer theory. Kalliadasis et al. [41] assumed a parabolic velocity profile and a linear temperature profile for the transient and non-uniform flow to apply this method. Ruyer-Quil et al. [43] studied the problem by higher order weighted residual approach with polynomial expansions for both velocity and temperature field to overcome these limitations, which introduce the second order dissipative effects that are known to determine the amplitude of the front-running capillary waves. Consequently this model is fully compatible with the Benny's expansion method up to the second order. In the study above they have shown clearly that the transport of the heat by the flow plays a double role and for the small amplitude waves it stabilizes the flow but for the large amplitude waves it promotes the instability. Trevelyan et al. [44] determined an expression of the critical Reynolds number for a thin liquid film falling down a uniformly heated wall. For that purpose they have derived a free surface evolution equation under the assumption of the small Reynolds and Marangoni numbers $[O(1)]$, to include the convective heat transport effect at a lower relevant order. They assumed that the Peclet number is large $\left(O\left(\varepsilon^{-n}\right)\right)$ for $0 < n < 1$), but in that case in the cross-stream direction, the assumption of small temperature gradient is violated. On the other hand, the experimental findings by Kabov [38], Kabov et al. [37] and Scheid et al. [39] prominently indicate that there is a certain critical value of the heat flux for the onset of instability. To achieve such a critical value, a large temperature difference (large Marangoni number) would be required as pointed out by Kalliadasis et al. [41] and the agreement becomes much better for a large temperature difference.

The long-wave theory was used by Miladinova et al. [45] to conduct a weakly nonlinear and a fully nonlinear analysis of the evolution equation governing the film thickness in the presence of thermocapillarity arising from a linear base temperature profile. They discovered that a positive base temperature gradient destabilizes the flow and exerts an influence on the amplitude and the phase speed of the finite-amplitude waves. By using a long-wave evolution equation, Miladinova et al. [46] studied the three-dimensional instabilities of nearly sinusoidal waves on vertically falling and nonuniformly heated films. Further the linear stability of finite-amplitude two-dimensional waves was analysed using the Floquet theory. Mukhopadhyay and Mukhopadhyay [47] studied the nonlinear stabilities of viscous film flows down an inclined plane with linear temperature variation. They found that the unconditional stable zone vanishes after a cut off Marangoni number whereas subcritical, supercritical and explosive zones increase with the increase in Marangoni number.

Long-wave thermocapillary instability for the case of a horizontal thin liquid layer lying upon a solid substrate for both uniform and non-uniform base temperatures was studied by Yeo et al. [48]. They found that for a non-uniform base temperature, the film height thickens near the region where temperature gradients are negligible and severely thins upstream. Demekhin et al. [49] later investigated the linear stability of a thin liquid layer falling down an inclined wall heated by a downstream, linearly increasing temperature distribution. They saw that, in the case of linearly increasing temperature distribution, thermocapillary forces can either destabilize or stabilize the flow which are in contrast to the case of uniform heating, where the thermocapillary forces have only a destabilizing effect on all instability modes.

The Benney equation with Marangoni effect has been extensively studied by many authors. Scheid et al. [50] examined the validity domain of the Benney equation with Marangoni effect and they found that thermocapillary can strongly reduce the validity domain of the Benney equation. They also ensured that the Benney equation still remains very helpful to study the thin film flows with various physical effects since it allows to describe the film evolution by one single equation with various relevant parameters. The linear and nonlinear regimes of the two long-wave instability modes for a film flowing down a uniformly heated plane by using the regularized reduced model was analyzed by Scheid et al. [51] and there they also scrutinized the influence of Prandtl, Reynolds and Marangoni numbers on the speed, shape, flow patterns and temperature distributions for solitary waves obtained from the regularized model. They also found that for small amplitude waves, the transport of heat by the flow has a stabilizing effect but promotes the instability of the large-amplitude waves when a recirculation zone is present. The bifurcation analysis of the first and second-order Benney equation for isothermal film flow was further carried out by Oron and Gottlieb [52]. The main result of their study is that, for smaller values of Reynolds number, the primary bifurcation of the first order Benney equation is supercritical and subcritical for larger values, while for the second order Benney equation, for any Reynolds number, the bifurcation is supercritical only. Later Samanta and Dandapat [53] studied the bifurcation analysis of first and second order Benney equation for viscoelastic fluid flowing down a vertical plane by using the method of multiple scales and they have found that the

first order Benney equation gives both supercritical stable and subcritical unstable zones depending on the Reynolds number being smaller or greater than its critical value. They also obtained that the second order Benney equation exhibits only supercritical bifurcation and the supercritical stable region increases with increasing of Reynolds number.

Extensive review of the literature on the falling film instability down a heated vertical/inclined plane are found in Oron et al. [54], Velarde and Zeytounian [57], Nepomnyashchy et al. [56] and Colinet et al. [55].

Due to the technological applications, the effect of electric field on a thin liquid film produces a class of problems, which have got the attention of several researchers. Presence of the electric field introduces additional physical effects on the flow dynamics such as body force due to a current in conducting fluids and the Maxwell stress at the free interface. The electric field produces dispersion and hence linear stabilization of short wave modes. Schwarz and Melcher [58] examined the effects of an electric field on the linear stability of a sharp interface separating two non-conducting dielectric fluids of infinite extent. They also pointed out that the electric field introduces a polarization force which tends to deflect the interface from its initial flat position. The interaction of an electrostatic field on the film flowing in an inclined plane was studied by Kim et al. [59]. They obtained that, in the thin film limit, the effect of the electric field occurred in the wave evolution as an external pressure distribution that causes the destabilizing effect on the film. It is very interesting to note that, they provide a discussion on the application of their results to a proposed electrostatic liquid film space radiator. Further Gonzalez and Castellanos [60] investigated the nonlinear stability of a perfectly conducting film flowing down an inclined plane with linear temperature variation in the presence of a normal electric field. They derived a nonlinear evolution equation with a Hilbert transform type of term within the limit of small Reynolds number and predicted the destabilizing effect of the electric field in the finite amplitude regime. Later Dandapat and Mukhopadhyay [61] extended the study of Gonzalez and Castellanos within the regime of large Reynolds number and confirmed the existence of supercritical stable and subcritical unstable zones and also determined a critical value of the electric parameters below which the flow remains stable always.

Mukhopadhyay and Mukhopadhyay [62] investigated the stability of conducting viscous film flowing down an inclined plane with linear temperature variation in the presence of a uniform normal electric field. They found that both the Marangoni and electric Weber numbers have a qualitatively same influence on the stability characteristics but the effect of magnetic number is much stronger as compared to the effects of the electric Weber number.

The flow of the electrically conducting liquid film has several practical applications in different cooling systems, nuclear energy equipment and in other technological applications, e.g. in laser cutting process, where the surface waves are undesirable at the molten interface. Applying a magnetic field to counteract the inertia force, the instability could be prevented to maintain the smooth flow. This is more desirable since the electromagnetic field has no mechanical contact with the fluid flow.

The literature of MHD film flow down an inclined/vertical plane is sparse. In presence of a transverse uniform magnetic field, linear stability analysis for the electrically conducting liquid film flowing down an inclined plane was first investigated by Hsieh [63] and later followed by Ladikov [64], Sarma and Lu [65], Rai and Gupta [66]. It was found that the MHD coupling increases the stability of liquid film and can serve as a powerful remedy in suppressing instability of the flow. Gordeev and Murzenko [67] investigated wave flows of a conducting viscous fluid film over a horizontal plane in transverse constant magnetic and electric fields. They have considered an induction-free approximation to derive the evolution equation and discovered that the flow suffers from instability at a critical (sufficiently large) value of external electric field without any connection to the Reynolds number. The propagation of weakly nonlinear waves over a flow of an electrically conducting viscous film flowing down an inclined plane under the electromagnetic field by the long-wave expansion method was studied by Korsunsky [68]. He mainly performed the linear stability analysis of the evolution equation. He found that the magnetic field provides a stabilizing effect on the film flow, while, the electrical field destabilizes it. Further Dandapat and Mukhopadhyay [69] have studied the same problem as Korsunsky [68] and they performed both the linear and nonlinear stability analysis within the regime of small Reynolds number. Mukhopadhyay and Mukhopadhyay [70] investigated the stability of conducting liquid film flowing down an inclined plane at moderate Reynolds number in the presence of a constant electromagnetic field. They found that the magnetic field stabilizes the flow but the electric field stabilizes a disturbance of the flow depending on its orientation with the flow.

Another set of problems concern the effect of rotation on the thin liquid falling film. The hydrodynamic instability of a thin film flowing down a rotating inclined plane was first investigated by Ruiz-Chavarria and Davalos-Orozco [71]. They considered that the fluid is flowing down a rotating inclined plane close to the axis of rotation in order to neglect the centrifugal force. A stabilizing effect of the Coriolis force was found in their study and the linear instability of the thin film was described in the limit of small wave numbers and small Reynolds numbers. Later, Busse and Davalos-Orozco [72] studied the same problem by considering small wave number and small rotation approximation in such a way that both the forces, centrifugal and the Coriolis, have equal importance in the instability phenomena in the investigated region. They incorporated the effects of the centrifugal force together with the effects of the gravity and the Coriolis force in their study. They found a critical rate of rotation below which the film flowing down a rotating inclined plane is more stable than the flow in the horizontal rotating plane, while above this rate of rotation the situation is reversed.

Mukhopadhyay and Mukhopadhyay [73] studied the stability of a thin viscous liquid film flowing down a rotating nonuniform heated inclined plane and found that the Coriolis force is dominant for very small rotation while for relatively large rotation the centrifugal force is dominant.

Mukhopadhyay et al. [74] showed the impact of Biot number (Bi) which describes heat transfer at the free surface on instability mechanism. Using the long-wave expansion method, a generalized nonlinear evolution equation of Benney type was derived for the development of the free surface. They used a normal mode approach and the method of multiple scales to obtain the linear and weakly nonlinear stability solution for the film flow. The linear stability analysis of the evolution equation shows that the Biot number plays a double role; for $Bi < 1$, it gives destabilizing effect but for $Bi > 1$, it produces stabilization. At $Bi = 1$, the instability is maximum. The weakly nonlinear study reveals that the impact of Marangoni number Mr is very strong on the bifurcation scenario even for a slight variation. Recently Mukhopadhyay and Chattopadhyay [75] investigated interfacial instability of a thin liquid film flowing down an inclined plane where they considered the linear variation of fluid properties such as density, dynamical viscosity, surface tension, and thermal diffusivity, for the small variation of temperature. Using long-wave expansion method and considering order analysis especially for very small Biot number, they obtained a single surface equation in terms of the free surface $h(x,t)$. They discussed different stability zones and threshold amplitude in the subcritical as well as supercritical zones for the variation of the parameters for density, viscosity and surface tension, measuring the rate of change with respect to temperature and also showed the variation of nonlinear wave speed for the same variation.

Study of the falling film instability draws the attention of several researchers for mainly two reasons. First, for its complexity of involving a free surface, which appealed to the applied mathematics community to formulate the classical flow instabilities, such as Tollmein-Schlicting, Kelvin-Helmholtz, Couette, Rayleigh, Poiseuille etc. Second, and the most important reason is its wide application in the practical field of industry and engineering. Experimental results have shown that presence of the waves on a liquid film surface makes a massive change on the coating surface because waves substantially enhance the heat and mass transfer rates. It is important in the other coating processes to suppress the surface waves on the fluid interface because the surface wave on a coating layer is highly undesirable as it decreases the glossy texture of the finished product. In many industrial and technological applications like microfabrication processes, coating or microelectromechanical systems etc., the temperature gradients are applied to control the flow of the liquid in order to impose uniform thickness of the liquid layers upon the solid surface. As surface tension is a temperature dependent property of the liquid, in the presence of the temperature gradient the free surface experiences the surface tension gradient or Marangoni stress and such stresses can generate the thermocapillary flows and interfacial instabilities. Thus any small variation in the temperature could lead to the growth of the instabilities that can disrupt the entire coating layer.

3. Hydrodynamic Stability

In fluid dynamics, hydrodynamic stability is the field which analyses the stability and the onset of the instability in fluid flows. The study of hydrodynamic stability aims to find out if a given flow is stable or unstable: if a physical state withstands a disturbance and it still returns to its original state after suffering all possible modes of disturbances, then it is in a stable state; otherwise, we can say that it is in unstable state. The foundations of hydrodynamic stability, both theoretical and experimental, were laid notably by Kelvin, Helmholtz, Rayleigh, and Reynolds during the nineteenth century. These foundations gave many useful tools to study hydrodynamic stability. The principle of the hydrodynamical stability considers a hydrodynamic system, in accordance with the equations governing it, is in a stationary state in which none of the variables describing the flow are dependent of time. Let $X_1, X_2, \ldots, X_j$ be a set of parameters which defines the system. These parameters will be geometrical parameters, that is parameters characterizing the velocity field, the angle of inclination for a flow on an inclined plane or the magnitudes of the different forces acting on the system, such as gravitational force, pressure gradients, temperature gradients, Coriolis force, magnetic fields, centrifugal force etc.

While considering the stability of such a system with the given set of parameters $X_1, X_2, \ldots, X_j$ we essentially try to determine the reaction of the system to small disturbances. Then the question arises whether the system which is disturbed will come back to its original state or whether moving further from the steady state away will never return to its original configuration. In the former case, the system is said to be in a stable state and in the latter case, it is said to be in an unstable state. More rigorously, a system is said to be in an unstable state if it is unstable with respect to a special mode of disturbances. On the other hand, a system is in a stable state if it is stable in every possible mode of disturbances. Marginal stability or Neutral stability is the locus in the parameter space $X_1, X_2, \ldots, X_j$ which separates the stable/unstable states. The locus of the marginal/neutral states in the $\left(X_1, X_2, \ldots, X_j\right)$ space can be defined by an equation of the form

$$\sum \left(X_1, X_2, \ldots, X_j\right) = 0. \tag{3.1}$$

The determination of this locus is one of the prime objects of the hydrodynamic stability.

In determining the stability of the hydrodynamical system, one particular parameter is chosen as a variable, keeping all the other parameters as constant. Now continuously varying that parameter, when the system changes from stable to unstable state for a certain critical value, we may say that, instability sets in for that critical value of the parameter when all the other parameters have their preassigned values.

States of neutral stability generally may be of two kinds; first the amplitude of the small disturbance may dampen/grow periodically; second, it may dampen/grow non-periodically. The core concern of the researcher is not the latter but the former case, where the transition from the stable to unstable state occurs via a marginal state exhibiting oscillatory motions with a certain definite characteristic frequency. Linearly unstable solutions cannot be realized. Linear theory predicts that flows diverge exponentially from unstable solutions. But as the difference becomes finite, the nonlinear effects can no longer be neglected. Nonlinearities usually cause a saturation of the exponential divergence and the flow evolves to a new steady, periodic or non-periodic flow. Typically, the resulting flow is spatially and/or temporally more complicated than the unstable solution. Nonlinear techniques have to be used to describe the resulting flows. One such simplification is provided by a weakly nonlinear analysis, which goes one step beyond linear stability analysis. In this analysis, the nonlinear terms are neglected assuming the perturbations to be small up to compared the leading order terms in an asymptotic expansion. Nonlinearities make their appearance at higher orders and may cause saturation of the exponential growth predicted by linear analysis for unstable flows. This analysis is only valid near the linear stability boundary and when the new flow is not very different from the unstable solution. Nevertheless, it addresses the question of what happens to an unstable flow.

3.1. Linear stability analysis in terms of normal modes

The starting point of investigation of hydrodynamic stability is the eigenvalue analysis, which proceeds in two stages:

1. Linearization about the laminar solution and
2. Search for unstable eigenvalues of the linearized problem.

An unstable eigenvalue is an eigenvalue in the complex upper half plane, corresponding to an eigenmode of the linearized problem which grows exponentially as a function of time t. A flow will be unstable if there exists such a growing eigenmode. Such modes of instability depend on the geometry (inclination angle of the inclined plane along which the film flows), the Reynolds number and other parameters. If the amplitude of the disturbance grows exponentially then at some point the nonlinear processes will become very important.

A widely used technique in the Hydrodynamic Stability Theory is the Linear Stability Analysis. In this analysis, at first, the evolution equations for perturbations about a steady solution are derived. The perturbation evolution equations are nonlinear, which makes them difficult to solve. Based on the assumption that the perturbations are infinitesimally small nonlinearity is neglected in this analysis. The means of infinitesimal disturbance is a disturbance in which its amplitude is small compared to any length scale such as its wave length. This makes the evolution equation linear and is much easier to solve by superposition of the evolution operator. If all the modes of the

linear operator eventually decay, any small perturbation will also degenerate and then the flow will return to the known steady solution. But stability will be lost when a single mode keeps growing with time. Thus the main task of this analysis is to determine whether any mode of the evolution operator shows persistent growth. In linear stability analysis, in order to investigate the reaction of the system to every possible mode of disturbances, we assume a very simple form for the disturbances, namely, Normal modes or Travelling waves $\eta = \eta_0 \exp i\left(k_x x + k_y y - \omega t\right) + \text{c.c.}$ where, η_0 is the amplitude of the disturbance which is arbitrary but small, $k = \sqrt{k_x^2 + k_y^2} = \dfrac{2\pi}{\lambda}$ (where λ is the wave length of the disturbance) is the wave number, which is real and $\omega = \omega_r + i\omega_i$ is the complex frequency and c.c. stands for complex conjugate. Here the growth is assumed to be exponential, which is the strongest possible disturbance and is observed in nature. Since $\exp(-i\omega t) = \exp(-i\omega_r t)\exp(\omega_i t)$, the disturbance will be unstable as time grows, if its imaginary part $\omega_i > 0$ and will be stable if $\omega_i < 0$. The equation $\omega_i = 0$ gives the neutral stability curve in the (Re, k) plane (where Re represents the Reynolds number), which separates the stable and unstable region.

The intersection of the two neutral curves determines the minimum Re at which the instability sets in. This value is known as the critical Reynolds number Re_c, below of which the flow is always stable to infinitesimal disturbances. The flow may become unstable for $Re < Re_c$ under finite amplitude disturbances. This type of instability is known as subcritical instability. On the other hand, flow may become stable for $Re > Re_c$ under finite amplitude disturbances, known as supercritical stability. Also $c_r = \dfrac{\omega_r}{k}$ gives the linear phase speed of the wave propagation.

An important thing now arises from the above discussion is that, we can use a complex representation for a real disturbance, because of the fact that, although the disturbance is taken complex, to make it a real number we use the c.c. part. If $\eta = \eta_0 \exp i\left(k_x x + k_y y - \omega t\right) + \eta_0 \exp -i\left(k_x x + k_y y - \omega t\right)$ is substituted in the evolution equation, we get twice as many terms. One set has $\eta_0 \exp i\left(k_x x + k_y y - \omega t\right)$ as a factor and other set have $\eta_0 \exp -i\left(k_x x + k_y y - \omega t\right)$ as a factor. For the expression to be always true for any x, y and t each of these sets separately must be equal to 0.

3.2. Weakly nonlinear stability analysis by the method of multiple scales

Multiple scales, or more precisely, scales of different orders arise in many of the physical problems as different physical effects usually manifest themselves over a different length and time scales. So, it has wide applicability to the nonlinear wave propagation that involves physical phenomena, which occur in relation to various scales. Sturrock [76] first introduced the method of multiple scales for an investigation of nonlinear effects in the electron plasmas. The weakly nonlinear theory of hydrodynamic stability, first proposed by J. T. Stuart [77], became popular in the seventies when Benney [8] successfully developed this method for the nonlinear wave propagation of a thin film flowing down an inclined plane. A deep description of this method has been given by L. Debnath [78]. Excerpts of this are as follows. Let

$$L\left(\frac{\partial}{\partial t}, \frac{\partial}{\partial x}, \lambda\right) u(x,t) = N\left(\frac{\partial}{\partial t}, \frac{\partial}{\partial x}, \mu\right) u^2(x,t) \quad x \in R,\ t > 0 \tag{3.2}$$

is a nonlinear partial differential equation, where L and N are the differential operators and λ, μ are the fixed parameters. We introduce the sets of independent variables $x_0, x_1, \ldots, x_m$ and $t_0, t_1, \ldots, t_m$ defined by $x_n = \varepsilon^n x$ and $t_n = \varepsilon^n t$, where ε is a small parameter characterizing the smallness of the associated terms. Consequently, the dependent variable $u(x,t)$ can be regarded as a function of these new variables, so that $u(x,t) = u(x_0, x_1, \ldots, x_m, t_0, t_1, \ldots, t_m)$.

Since the method is called the derivative expansion method, it is appropriate to introduce the expansions of the derivative operators

$$\frac{\partial}{\partial x} = \sum_{n=0}^{m} \varepsilon^n \frac{\partial}{\partial x_n} \tag{3.3}$$

and

$$\frac{\partial}{\partial t} = \sum_{n=0}^{m} \varepsilon^n \frac{\partial}{\partial t_n}. \tag{3.4}$$

Using these expansions in (3.2) leads to the following results

$$L\left(\frac{\partial}{\partial t}, \frac{\partial}{\partial x}, \lambda\right) = \sum_{n=0}^{m} \varepsilon^n L_n\left(\frac{\partial}{\partial t_0}, \frac{\partial}{\partial t_1}, \ldots, \frac{\partial}{\partial t_m}, \frac{\partial}{\partial x_0}, \frac{\partial}{\partial x_1}, \ldots, \frac{\partial}{\partial x_m}, \lambda\right) + O\left(\varepsilon^{m+1}\right), \tag{3.5}$$

$$N\left(\frac{\partial}{\partial t}, \frac{\partial}{\partial x}, \mu\right) = \sum_{n=0}^{m} \varepsilon^n N_n\left(\frac{\partial}{\partial t_0}, \frac{\partial}{\partial t_1}, \ldots, \frac{\partial}{\partial t_m}, \frac{\partial}{\partial x_0}, \frac{\partial}{\partial x_1}, \ldots, \frac{\partial}{\partial x_m}, \mu\right) + O\left(\varepsilon^{m+1}\right). \tag{3.6}$$

We also assume that $u(x,t)$ has the asymptotic representation

$$u(x_0, x_1, \ldots, x_m, t_0, t_1, \ldots, t_m) = \sum_{n=0}^{m} \varepsilon^n u_n(x_0, x_1, \ldots, x_m, t_0, t_1, \ldots, t_m) + O\left(\varepsilon^{m+1}\right). \tag{3.7}$$

In general, $u(x,t)$ can be expanded in terms of another small parameter δ which measures the degree of nonlinearity of the wave field. It is assumed that the new parameter is related to ε. However, to keep it simple, $u(x,t)$ has been expanded in powers of ε.

We substitute (3.5)-(3.7) in the equation (3.2) and then equate the coefficients of the like powers of ε to obtain a system of perturbation equations from which it is possible to determine the functions u_n successively. The underlying assumption is that each perturbed quantity u_n must be nonsecular (bounded) at each stage of the perturbation process and thus, the method of the multiple scales can be applied effectively to a general dispersive wave system with or without small dissipation.

4. Formulation of the problem

Consider a viscous, two-dimensional incompressible thin film flowing under the action of gravity along an inclined plane of inclination $\theta\left(0 \leq \theta \leq \frac{\pi}{2}\right)$ with the horizon. If the plane is vertical then $\theta = \frac{\pi}{2}$. Through θ, the geometry of the flow is incorporated as a parameter. In the problem formulation, the liquid flowing has constant dynamical viscosity and density denoted by μ and ρ respectively. The free surface of the liquid is bounded by an ambient air of constant atmospheric pressure p_a. The frame of reference is to be chosen in such a way that the x-axis is along the plane and z-axis perpendicular to the plane, and their intersection is the origin, which is a fixed point on the inclined/vertical plane. The dynamics of a falling liquid film is fairly well described as a free surface problem of two-dimensional single phase Navier-Stokes equation (momentum conservation) supplemented by continuity equation (mass conservation) and pertinent boundary conditions.

I. Governing equations

With respect to the chosen frame of reference, the governing equations in vector form are represented by

$$\rho\left[\frac{\partial \mathbf{V}}{\partial t} + (\mathbf{V}.\nabla)\mathbf{V}\right] = \rho\mathbf{g} - \nabla p + \mu\nabla^2\mathbf{V}, \tag{4.1}$$

$$\nabla.\mathbf{V} = 0 \tag{4.2}$$

where $\nabla = \left(\frac{\partial}{\partial x}, 0, \frac{\partial}{\partial z}\right)$ is the del operator, $\mathbf{V} = (u, 0, v)$ is the velocity vector, $\mathbf{g} = (g\sin\theta, 0, -g\cos\theta)$ is the gravitational acceleration and p denotes the pressure of the liquid. To derive the above equation it is assumed that there is no influence of the air above the free surface.

II. Boundary conditions

The boundary conditions along the plane $z = 0$ is the no-slip condition (i.e. fluid particles adhere to the plane do not move) which gives

$$\mathbf{V} = 0. \tag{4.3}$$

Also the free surface $z = h(x,t)$ which is in contact with the surrounding air, experiences two types of boundary conditions:

(i) Kinematic condition

It states that the liquid particles on the free surface must remain attached, which gives,

$$\partial_t h + \mathbf{V}.\nabla(h - z) = 0. \tag{4.4}$$

(ii) Balance of normal and tangential stresses

The normal stress undergoes a jump across the interface with curvature of the free surface due to capillary force, which gives,

$$[[\mathbf{n}.\tau.\mathbf{n}]] - [[p]] = -\sigma_0\nabla.\mathbf{n} \tag{4.5}$$

also the continuity of the shear stress gives,

$$[[\mathbf{n}.\tau.\mathbf{t}]] = 0 \tag{4.6}$$

where, [[#]] denotes a jump in the quantity as one moves across the interface from the liquid to vacuum region. Here $\mathbf{n}$ and $\mathbf{t}$ are the normal (outward pointing) and tangent vectors to the interface respectively, σ_0 is the constant surface tension of the liquid and the viscous stress tensor τ is given by $\tau = \left(\frac{\partial u_i}{\partial xj} + \frac{\partial u_j}{\partial xi}\right)$.

III. Methodology

The problem described above is well posed but it is almost difficult to find a unique solution by the use of existing mathematical tools. A steady state basic solution for the uniform parallel flow of the above problem can be obtained, which is popularly known as Nusselt's solution. However it is quite difficult to find a non-trivial solution of the problem. There are several reasons behind this. These are:

1. the governing mass and momentum conservation equations are coupled and the conservation equations are highly nonlinear,
2. the complexity of setting boundary conditions on the curvilinear interface,
3. presence of the different body force/forces, such as electromagnetic force, gravity, Coriolis force, centrifugal force etc.

Therefore, instead of finding the direct solution it would be wise to simplify the problem using certain type of approximations. There are two types of approximations available in the literature, which are widely used for the study of thin film flows. One approach is initiated by Benney [8] and Mei [79], and is known as 'long-wave expansion or perturbation expansion' technique The other approach, initiated by Kaptiza [5, 80] and Shkadov [9, 10], and is called 'integral-boundary layer or boundary-layer lubrication' method. Both the methods are discussed below.

(i) Long wave expansion method

In this method the underlying assumption is that the average thickness of the fluid layer is much smaller in comparison with its characteristic length scale, whose order may be considered as the same of its wave length. Therefore the spatial gradients along the interface will be small. Now by expanding the dependent variables such as velocity, pressure etc. asymptotically in powers of the long-wave parameter ε (the ratio of the average film thickness to the characteristic length scale) and substituting these in the governing equations together with the boundary conditions and then solving the leading order equations, we get the zeroth order solutions of the dependent variables. Considering the first order approximation of the governing equations and boundary conditions and using the solution of the zeroth order equations, we get the first order solutions of the dependent variables. Repeating this process, other leading order corrections of the dependent variables can be obtained. Finally substituting these corrected solutions in the kinematic equation we get a surface equation of the form

$$\partial_t h = f\left(h^n, \partial_{x^m} h\right) \tag{4.7}$$

which involves different algebraic powers n and differentiation of orders m of the film height $h(x,t)$. It is to be noted here that the long-wave expansion method becomes invalid when the asymptotic expansion of at least one dependent variable in terms of ε diverges. In deriving long-wave equation it is assumed that the Reynolds number is very small and is of order unity $[O(1)]$. In this method the surface equation is valid only at a small vicinity of the critical Reynolds number, which is a serious limitation in the range of validity of the long-wave equation.

(ii) Integral-boundary-layer method

This method is a direct extension of the Karman-Polhausen integral-boundary layer theory. In this method initially the full Navier-Stokes equation is simplified by using the boundary-layer approximation and the pressure term is eliminated but the inertia term is left intact. Though the boundary layer approximation simplifies the Navier-Stokes equation considerably by dropping several terms, the resulting equation is still difficult to handle as this does not represent the so called surface equation. In the second phase, integrating the boundary layer equations across the film thickness by assuming a specific shape (parabolic or semi-parabolic) of the velocity profile for the transient and non-uniform flow, one obtains a coupled set of two equations in terms of two measurable quantities the flow rate $q(x,t) = \int_0^{h(x,t)} u(x,t,z)\, dz$ and film thickness $h(x,t)$ of the form

$$h_t + q_x = 0, \tag{4.8}$$

$$q_t + f\left(h^m, q^n, \partial_{t^i x^j} f(h,q)\right) = 0 \tag{4.9}$$

with some additional approximations, such as quasi-stationary approximation. The above coupled equations can be combined into a single, second order surface equation for the film thickness $h(x,t)$. The results of the integral-boundary layer method is in good agreement with the available experimental/numerical solutions in the range of moderate Reynolds number. Thus the range of validity is extended by this method.

5. Conclusion

In this work we tried to include the important findings of several researchers on the topic of thin film flow instability. Our study reveals the following:

1. Thin film flow instability has wide range of applications. The study of thin film helps to solve the problems in the practical field of industry and engineering as well as to develop the theoretical knowledge about many types of flow instability.
2. Several authors investigated the thermocapillary or Marangoni instability in the thin liquid film which is extensively used in coating industry for uniform thickness of the liquid layers on the solid surface.
3. The presence of electric field in the thin film flow along inclined plane introduces additional physical effects on the flow dynamics such as body force due to a current in conducting fluids and the Maxwell stress at the free interfaces. This type of study is important due to its technological applications.
4. Studies of several researchers on the thin film flow in the presence of constant electromagnetic field are important as this is used to solve the problems of magnetic film coating.
5. Stability of film flowing down a rotating inclined plane with or without heating effect is another important class of problems useful to solve in the paper industry.
6. There is ample scope of research for the hydrodynamical study of thin film flow along an inclined/vertical plane with a view to solving the problems of different industrial and technological issues, especially in coating industry.

Acknowledgement

The authors are grateful to Prof. Sukriti Ghosal, Principal, M.U.C. Women's College, Burdwan, India for proof reading and to enhance the quality of text of the paper. The First author acknowledges his sincerest gratitude to his parents Dr. Kusal Chattopadhyay and Mandira Chattopadhyay for their constant inspiration and encouragement throughout this research.

References

[1] H. Schlichting, Boundary Layer Theory, McGraw-Hill Book Company Inc, New York., (1955), 308-337
[2] C.C. Lin, Hydrodynamic Stability, Cambridge University Press, New York (1955)
[3] D.Y. Hsieh, S.P. Ho, Wave and stability in fluids., World Scientific, Singapore (1994)
[4] P.G. Drazin, W.H. Reid, Hydrodynamic Stability, Cambridge University Press, Cambridge(1981)
[5] P.L. Kapitza, S.P. Kapitza, Wave flow of thin layers of a viscous fluid: III. Experimental study of undulatory flow conditions. Sov. Phys. J. Exp. Theor.Phys.,19 (1949), 105-120

[6] T.B. Benjamin, Wave formation in laminar flow down an inclined plane. J. Fluid Mech. 2 (1957),554-574
[7] C.S. Yih, Stability of liquid flow down an inclined plane. Phys. of Fluids 6(3) (1963), 321-334
[8] D.J. Benny, Long waves on liquid films. J. Math. Phys. 45 (1966), 150-155
[9] V.Ya. Shkadov, Wave models in the flow of a thin layer of a viscous liquid under the action of gravity. Izv. Akad. Nauk SSSR, Mekh. Zhidk. Gaza 1 (1967), 43-50
[10] V.Ya. Shkadov, Theory of wave flow of a thin layer of a viscous liquid. Izv. Akad. NaukSSSR, Mekh. Zhidk. Gaza 2 (1968), 20-25
[11] G.I. Sivashinsky, Nonlinear analysis of hydrodynamic instability in laminar flame, I. - Derivation of the basic equation, Acta Astronautica 4 (1977), 1177-1206
[12] A. Pumir, P. Manneville, Y. Pomeau, On solitary waves running down an inclined plane. J. Fluid Mech. 135 (1983), 27-50
[13] B. Gjevik, Occurrence of finite-amplitude surface waves on falling liquid films. Phys. Fluids. 13 (1970), 1918-1925
[14] S.P. Lin, Finite-amplitude stability of a parallel flow with a free surface. J. Fluid Mech. 36 (1969), 113-126
[15] C. Nakaya, Long waves on a thin fluid layer flowing down an inclined plane. Phys. Fluids. 18 (1975), 1407-1412
[16] S.P. Lin, Finite amplitude side-band stability of a viscous film. J. Fluid Mech. 63 (1974), 417- 429
[17] M.V.G. Krishna, S.P. Lin, Nonlinear stability of a viscous film with respect to three-dimensional side-band disturbances. Phys. Fluids 20 (1977), 1039-1044
[18] J. Liu, J.D. Paul, J.P. Gollub, Measurements of the primary instabilities of film flows. J.Fluid Mech. 250 (1993), 69-101
[19] J. Liu, J.P. Gollub, Onset of spatially chaotic waves on flowing films. Phys. Rev. Lett. 70(15) (1993), 2289-2292
[20] J. Liu, J.P. Gollub, Solitary wave dynamics of film flows. Phys. Fluids 6 (1994), 1702-1712
[21] S.V. Alekseenko, V.E. Nakoryakov, B.G. Pokusaev, Wave formation on a vertical falling liquid film. AIChE J. 31 (1985), 1446-1460
[22] H.C. Chang, Wave evolution on a falling film. Annu. Rev. Fluid Mech. 26 (1994), 103-136
[23] G.D. Fulford, The flow of liquid in thin films. Adv. Chem. Engg. 5 (1964), 151-236
[24] S.P. Lin, C.Y. Wang, Modeling Wavy film flows. In: Encyclopedia of Fluid Mechanics (ed. Cheremisinoff, N. P.) (1985), 931-951
[25] T.J. Hanratty, Interfacial instabilities caused by airflow over a thin liquid layer. In waves on Fluid Interfaces, Academic Press, London (1983), 221-259
[26] T.J. Hanratty, Separated flow modeling and interfacial transport phenomena. Appl. Sci.Res. 48 (1991), 353-390
[27] G.F. Hewitt, M.S. Hall-Taylor, Annular Two-Phase Flow. Pergamon Press, Oxford (1970)
[28] V.E. Nakaroyakov, B.G. Pokusaev, I.R. Schreiber, Wave Propagation in Gas-Liquid Media.Begell, New York (1992)
[29] J.R.A. Pearson, On convection cells induced by surface tension. J. Fluid Mech 4 (1958), 489- 500
[30] L.E. Scriven, C.V. Sternling, On cellular convection driven by surface tension gradients: effects of mean surface-tension and surface viscosity. J. Fluid Mech. 19 (1964), 321-340
[31] K.A. Smith, On convective instability induced by surface-tension gradients. J. Fluid Mech.14 (1966), 401-414
[32] S.G. Bankoff, Significant questions in thin liquid-film heat-transfer. ASME J. Heat Transfer 116 (1994), 10-16
[33] J.B. Burelbach, S.G. Bankoff, S.H. Davis, Nonlinear stability of evaporating/condensing liquid films. J. Fluid Mech. 195 (1988), 463-494
[34] D.A. Goussis, R.E. Kelly, Surface waves and thermocapillary instabilities in a liquid film flow. J. Fluid Mech. 223 (1991), 24-45
[35] S.W. Joo, S.H. Davis, S.G. Bankoff, Long-wave instabilities of heated falling films: two-dimensional theory of uniform layers. J. Fluid Mech. 230 (1991), 117-146
[36] P.G. Lopez, S.G. Bankoff, M.J. Miksis, Non-isothermal spreading of a thin liquid film on an inclined plane. J. Fluid Mech. 324 (1996), 261-286
[37] O.A. Kabov, I.V. Marchuk, V. Chupin, Thermal imaging study of the liquid film flowing on a vertical surface with local heat source. Russ. J. Engng. Thermophys. 6 (1996), 105-138
[38] O.A. Kabov, Formation of regular structures in a falling liquid film upon local heating. Thermophys. Aeromech. 5 (1998), 547-551
[39] B. Scheid, O.A. Kabov, C. Minetti, P. Colinet, J.C. Legros, Measurement of free surface deformation by the reflectance-Schlieren method. In Proc. 3rd. European Thermal Sciences conference, (ed. E. W. P. Hahne et al.), Heidelberg (2000)
[40] S. Kalliadasis, A. Kiyashko, E.A. Demekhin, Marangoni instability of a thin liquid film heated from below by a local heat source. J. Fluid Mech. 475 (2003), 377-408
[41] S. Kalliadasis, E.A. Demekhin, C. Ruyer-Quil, M.G. Velarde, Thermocapillary instability and wave formation on a film falling down a uniformly heated plane. J. Fluid Mech. 492 (2003),303-338
[42] E.A. Demekhin, V.Ya. Shkadov, Three-dimensional waves in a liquid flowing down a wall.Izv. Akad. Nauk SSSR, Mekh. Zhidk. Gaza 5 (1984), 21-27
[43] C. Ruyer-Quil, B. Scheid, S. Kalliadasis, M.G. Velarde, R.Kh. Zeytounian, Thermocapillary long waves in a liquid film flow. Part 1 Low-dimensional formulation. J . FluidMech. 538 (2005), 199-222
[44] P.M.J. Trevelyan, S. Kalliadasis, Wave dynamics on a thin-liquid film falling down a heated wall. J. Engineering Mathematics 50 (2004), 177-208
[45] S. Miladinova, S. Slavtchev, G. Lebon, J.C. Legros, Long-wave instabilities of non- uniform heated falling films. J. Fluid Mech. 453 (2002), 153-175
[46] S. Miladinova, D. Staykova, G. Lebon, B. Scheid, Effect of nonuniform wall heating on the three-dimensional secondary instability of falling films. Acta Mechanica 30 (2002), 1-13
[47] A. Mukhopadhyay, A. Mukhopadhyay, Nonlinear stability of viscous film flowing down an inclined plane with linear temperature variation. Journal of Physics D Applied Physics. 40(18) (2007), 5683-5690
[48] L.Y. Yeo, R.V. Craster, O.K. Matar, Marangoni instability of a thin liquid film resting on a locally heated horizontal wall. Physical Review E 67 (2003), 056315.1-056315.14
[49] E.A. Demekhin, S. Kalliadasis, M.G. Velarde, Suppressing falling film instabilities by Marangoni forces. Phys. Fluids 18 (2006), 042111-1-16
[50] B. Scheid, C. Ruyer-Quil, U. Thiele, O.A. Kabov, J.C. Legros, P. Colinet, Validity domain of the Benney equation including Marangoni effect for closed and open flows. J. Fluid Mech. 527 (2004), 303-335
[51] B. Scheid, C. Ruyer-Quil, S. Kalliadasis, M.G. Velarde, R.Kh. Zeytounian, Thermocapillary long waves in a liquid film flow. Part 2. Linear stability and nonlinear waves. J.Fluid Mech. 538 (2005), 223-244
[52] A. Oron, O. Gottlieb, Subcritical and supercritical bifurcations of the first and second- order Benney equations. J. Engineering Mathematics 50 (2004), 121-140
[53] B.S. Dandapat, A. Samanta, Bifurcation analysis of first and second order Benney equations for viscoelastic fluid flowing down a vertical plane. J.Phys. D: Appl. Phys. 41 (2008), 095501
[54] A. Oron, Nonlinear dynamics of thin evaporating liquid films subject to internal heat generation. In Fluid Dynamics at Interfaces, (ed. W. Shyy and R. Narayanan), Cambridge University Press (1999)
[55] P. Colinet, J.C. Legros, M.G. Velarde, Nonlinear dynamics of surface-tension-driven instabilities, Wiley VCH (2001)
[56] A.A. Nepomnyashchy, M.G. Velarde, P. Colinet, Interfacial phenomena and convection.Chapman and Hall (2002)
[57] M.G. Velarde, R.Kh. Zeytounian, Interfacial Phenomena and the Marangoni effect. Springer (2002)
[58] J.R. Melcher, W.J. Schwartz, Interfacial relaxation over stability in a tangential electric field. Phys. Fluids 11 (1968), 2604-2616
[59] H. Kim, S.G. Bankoff, M.J. Misksis, The effect of an electrostatic field on film flowing down an inclined plane. Phys. Fluids 4 (1992), 2117-2130
[60] A. Gonzalez, A. Castellanos, Nonlinear electrodynamic waves on film falling down an inclined plane. Phys. Rev. E 53 (1996), 3573-3578
[61] A. Mukhopadhyay, B.S. Dandapat, Nonlinear stability of conducting viscous film flowing down an inclined plane at moderate Reynolds number in the presence of a uniform normal electric field. J. Phys. D: Appl. Phys. 38 (2005), 138-143
[62] A. Mukhopadhyay, A. Mukhopadhyay, Stability of conducting viscous film flowing down an inclined plane with linear temperature variation in the presence of a uniform normal electric field. Int. J. Heat and Mass Transfer. 52 (2009), 709-715
[63] D.Y. Hsieh, Stability of a conducting fluid flowing down an inclined plane in a magnetic field. Phys. Fluids 8 (1965), 1785-1791
[64] Yu.P. Ladikov, Flow stability of a conducting liquid flowing down an inclined plane in the presence of a magnetic field. Fluid Dynamics 8 (1966), 1-4
[65] P.C. Lu, G.S.R. Sarma, Magnetohydrodynamic gravity-capillary waves in a liquid film.Phys. Fluids 10 (1967), 2339-2344
[66] A.S. Gupta, L. Rai, Hydrodynamic stability of a liquid film flowing down an inclined conducting plane. J. Phys. Soc. Japan 24 (1968), 626-632
[67] Yu.N. Gordeev, V.V. Murzenko, Wave film flows of a conducting viscous fluid in the tangential magnetic field. Appl. Math. Theor.Phys. 3 (1990), 96-100
[68] S. Korsunsky, Long waves on a thin layer of conducting fluid flowing down an inclined plane in an electromagnetic field. Eur. J. Mech. B/Fluids 18 (1999), 295-313
[69] B.S. Dandapat, A. Mukhopadhyay, Finite amplitude long wave instability of a film of conducting fluid flowing down an inclined plane in presence of an electromagnetic field. Int. J.Appl. Mech. Engg. 8 (2003), 379-383
[70] A. Mukhopadhyay, A. Mukhopadhyay, Stability of conducting liquid film flowing down an inclined plane at moderate Reynolds number in the presence of a constant electromagnetic field. Int. J. Non-Linear Mechanics. 43(7) (2008), 632-642
[71] L.A. Davalos-Orozco, G. Ruiz-Chavarria, Hydrodynamic stability of a fluid layer flowing down a rotating inclined plane. Phys. Fluids A 4 (1992), 1651-1665

[72] L.A. Davalos-Orozco, F.H. Busse, Instability of a thin film on a rotating horizontal or inclined plane. Physical Review E 65 (2002), 026312.1-026312.10
[73] A. Mukhopadhyay, A. Mukhopadhyay, Stability of a thin viscous fluid film flowing down a rotating non-uniformly heated inclined plane. Acta Mechanica 216(1) (2011), 225-242
[74] A. Mukhopadhyay, A. Mukhopadhyay, S. Mukhopadhyay, Instabilities of thin viscous film flowing down a uniformly heated inclined plane. J. of heat and mass transfer research 3 (2015), 1-22
[75] A. Mukhopadhyay, S. Chattopadhyay, Long wave instability of thin film flowing down an inclined plane with the linear variation of thermophysical properties for very small Biot number. Int J. of Non-Linear Mechanics 100 (2018), 20-29
[76] P.A. Sturrock, Non-linear effects in electron plasmas. A Royal Society journal 242 (1957), issue 1230
[77] J.T. Stuart, On the non-linear mechanics of wave disturbances in stable and unstable parallel flows Part 1. The basic behavior in plane Poiseuille flow. J. Fluid Mech. 9 (1960), 353-370
[78] L. Debnath, Nonlinear partial differential equations for scientists and engineers. Springer (2005)
[79] C.C. Mei, Nonlinear gravity waves in a thin sheet of viscous fluid. J. Math. Phys. 45 (1966), 266-288
[80] P.L. Kapitza, Wave flow of thin layers of a viscous fluid. Sov. Phys. J. Exp. Theor. Phys. 18 (1948), 3-28